On the fate of chiral anomalous effects in AMPT model

Guo-Liang Ma

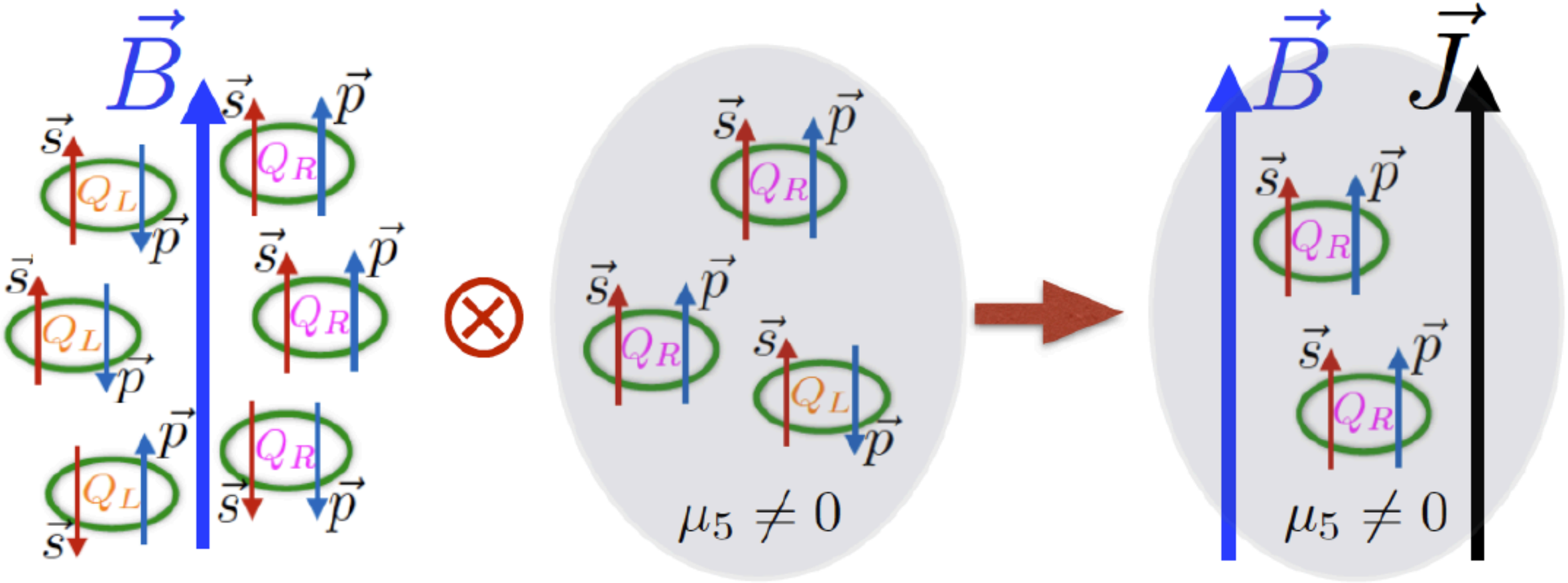
Fudan University



Outline

- **Introduction**
- **Why & How to study CME using AMPT**
- **Why & How to study CMW using AMPT**
- **Summary**

Chiral Magnetic Effect (CME)



- Initial fluctuations of topological charge in QCD vacuum → P and CP odd metastable domains → Charge separation in the direction of magnetic field

Chiral Magnetic Effect: $\mathbf{J} = \frac{Qe}{2\pi^2}\mu_5\mathbf{B}$

nature physics

LETTERS

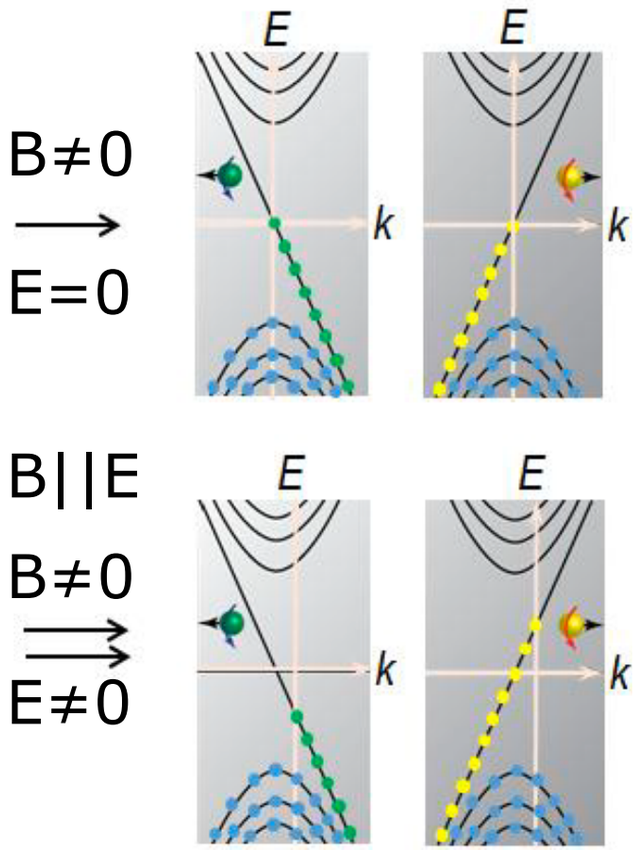
PUBLISHED ONLINE: 8 FEBRUARY 2016 | DOI: 10.1038/NPHYS3648

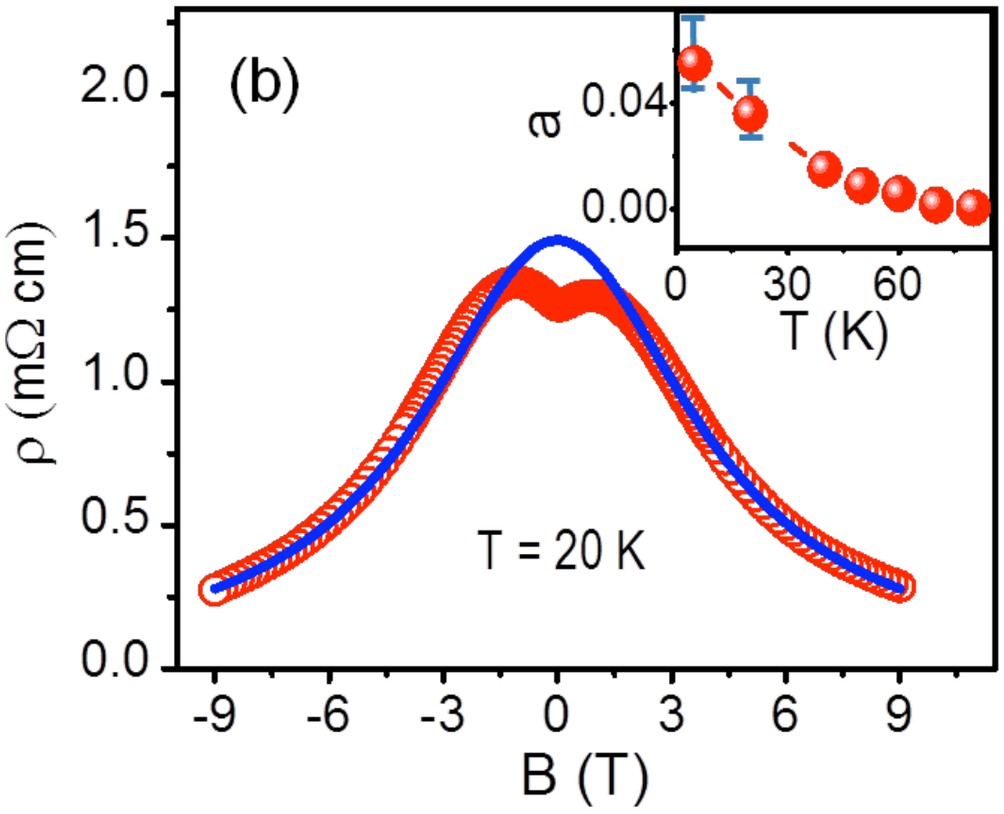


Chiral magnetic effect in $ZrTe_5$

Qiang Li[1*], Dmitri E. Kharzeev[2,3*], Cheng Zhang[1], Yuan Huang[4], I. Pletikosić[1,5], A. V. Fedorov[6], R. D. Zhong[1], J. A. Schneeloch[1], G. D. Gu[1] and T. Valla[1*]







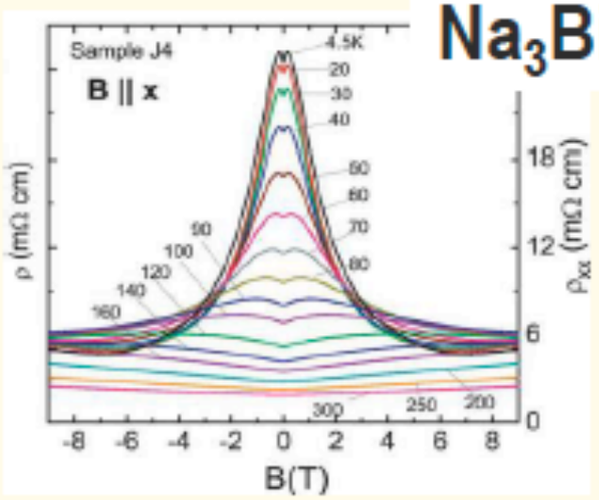
- When the electric field and magnetic field are parallel, the conductivity of CME can meet the expected B^2 dependence.

Quasiparticles in 3D Dirac semimetals

$$\sigma = \sigma_0 + \sigma_{CME} = \sigma_0 + a(T)B^2$$

CME in condensed matter physics

Dirac semimetals:

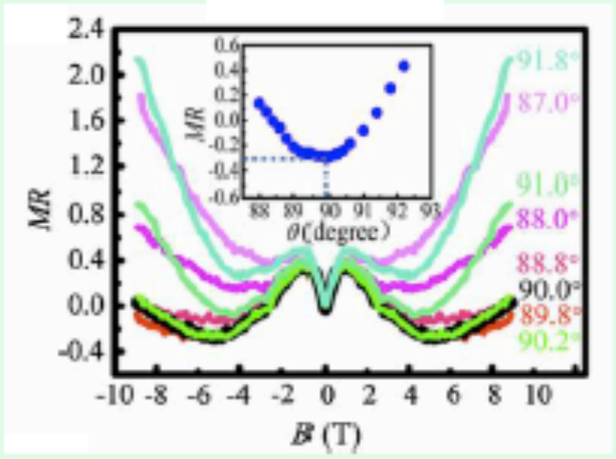


$ZrTe_5$ - Q. Li, D. Kharzeev, et al (BNL and Stony Brook Univ.)
arXiv:**1412.6543**; doi:10.1038/NPHYS3648

Na_3Bi - J. Xiong, N. P. Ong et al (Princeton Univ.)
arxiv:**1503.08179**; Science 350:413,2015

Cd_3As_2- C. Li et al (Peking Univ. China)
arxiv:**1504.07398**; Nature Commun. 6, 10137 (2015).

Weyl semimetals



TaAs - X. Huang et al (IOP, China)
arxiv:**1503.01304**; Phys. Rev. X 5, 031023

NbAs - X. Yang et al (Zhejiang Univ. China)
arxiv:**1506.02283**

NbP - Z. Wang et al (Zhejiang Univ. China)
arxiv:**1504.07398**

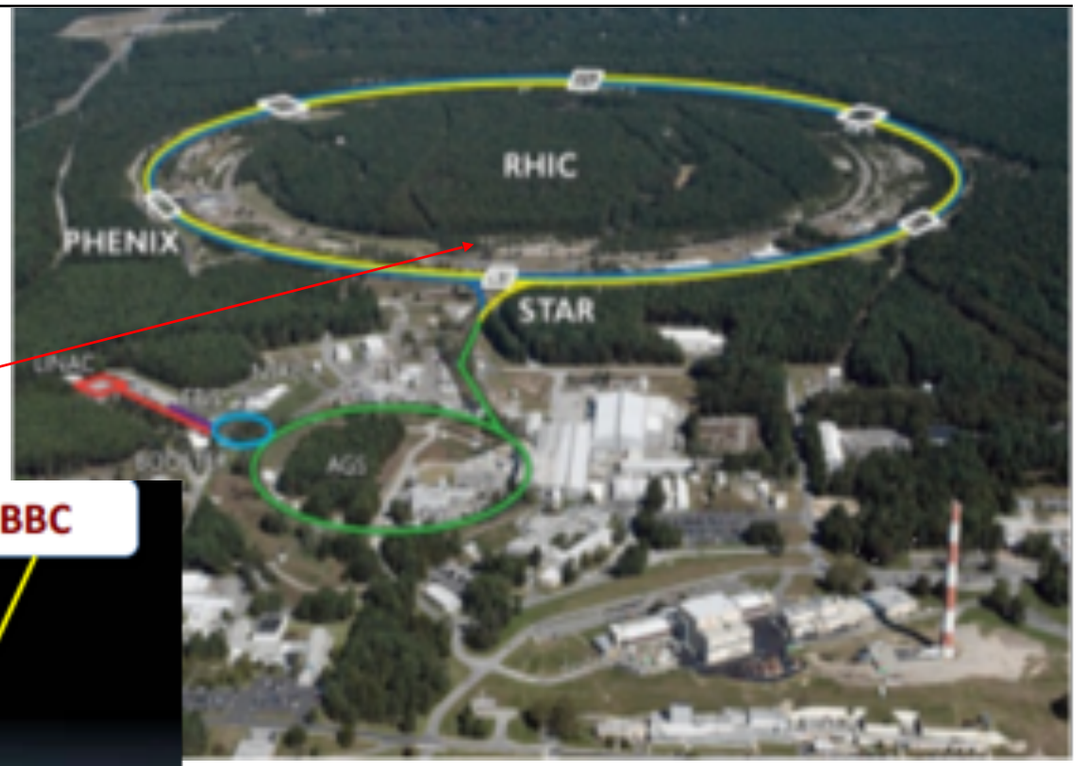
TaP - Shekhar, C. Felser, B. Yang et al (MPI-Dresden)
arxiv:**1506.06577**

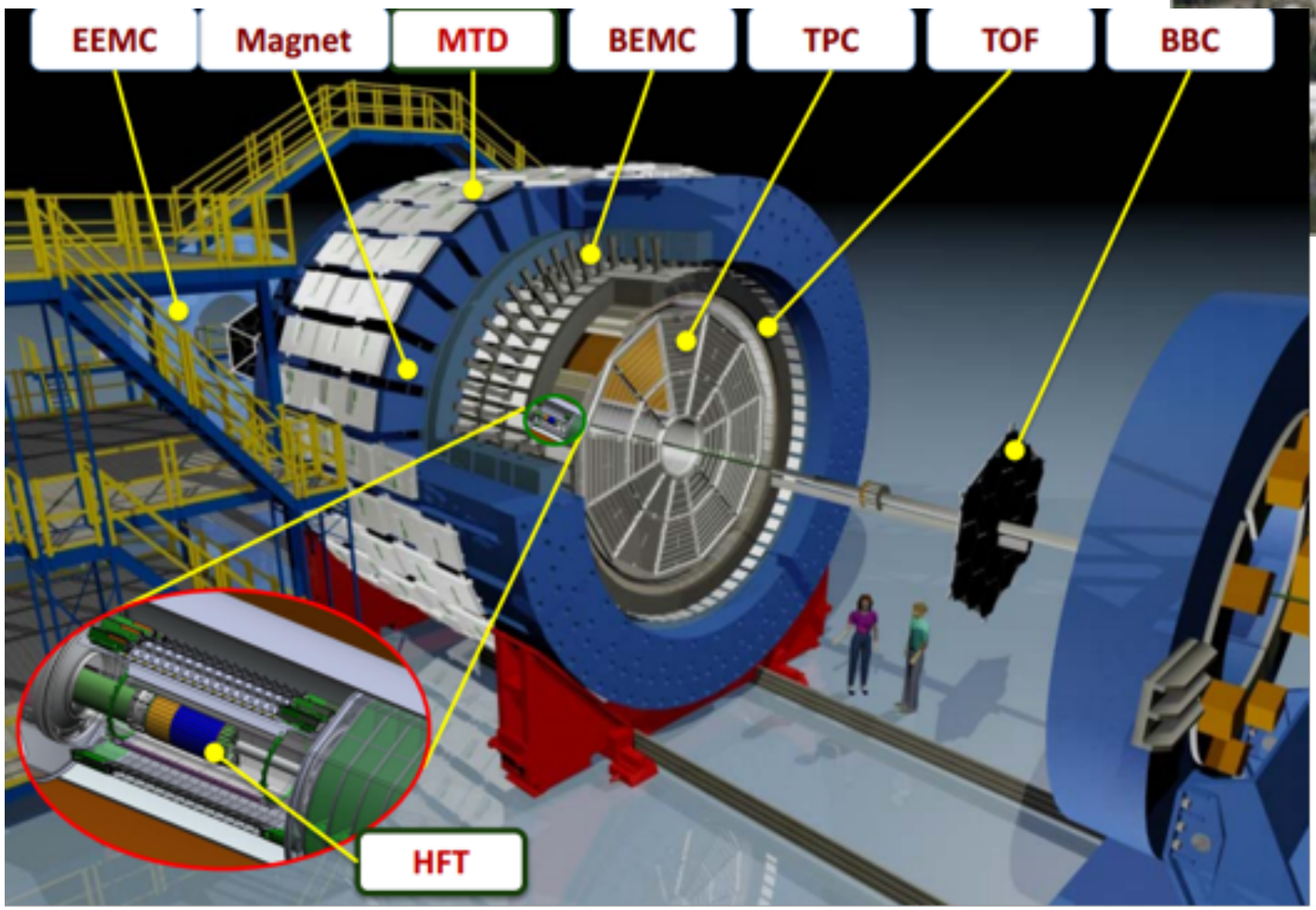
- CME found in condensed matter, a very important potential application prospect

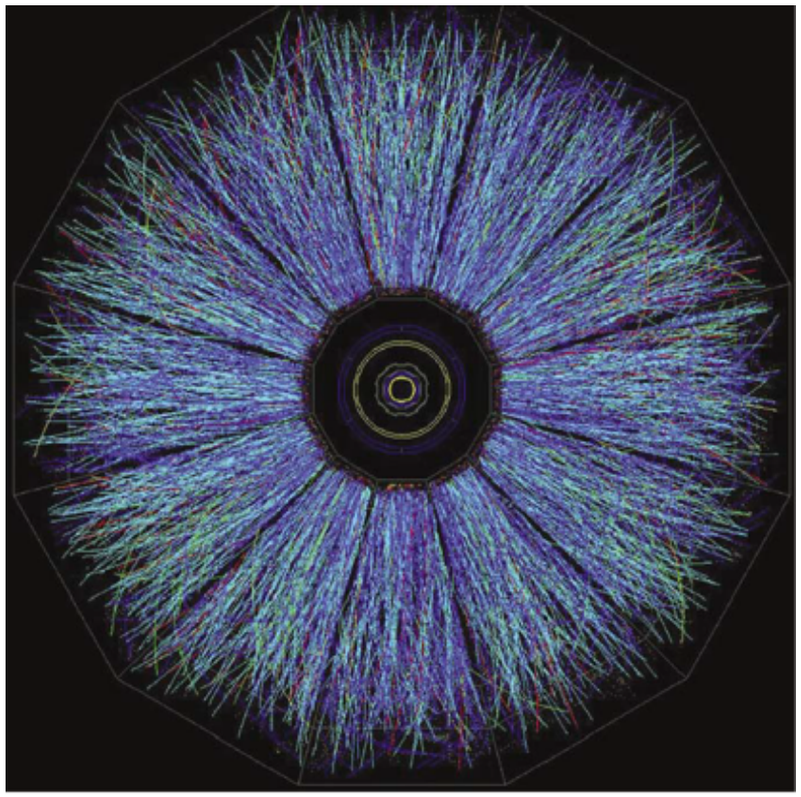
Heavy-ion collision experiment

Relativistic Heavy Ion Collider (RHIC)
&& Large Hadron Collider (LHC)

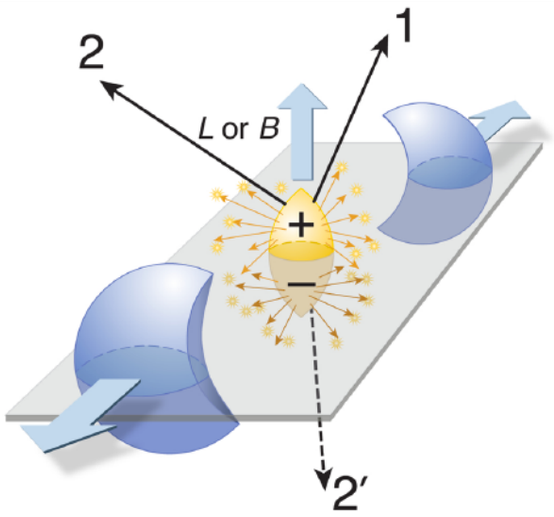
Solenoidal Tracker at RHIC (STAR)







CME probe: charge azimuthal correlation γ



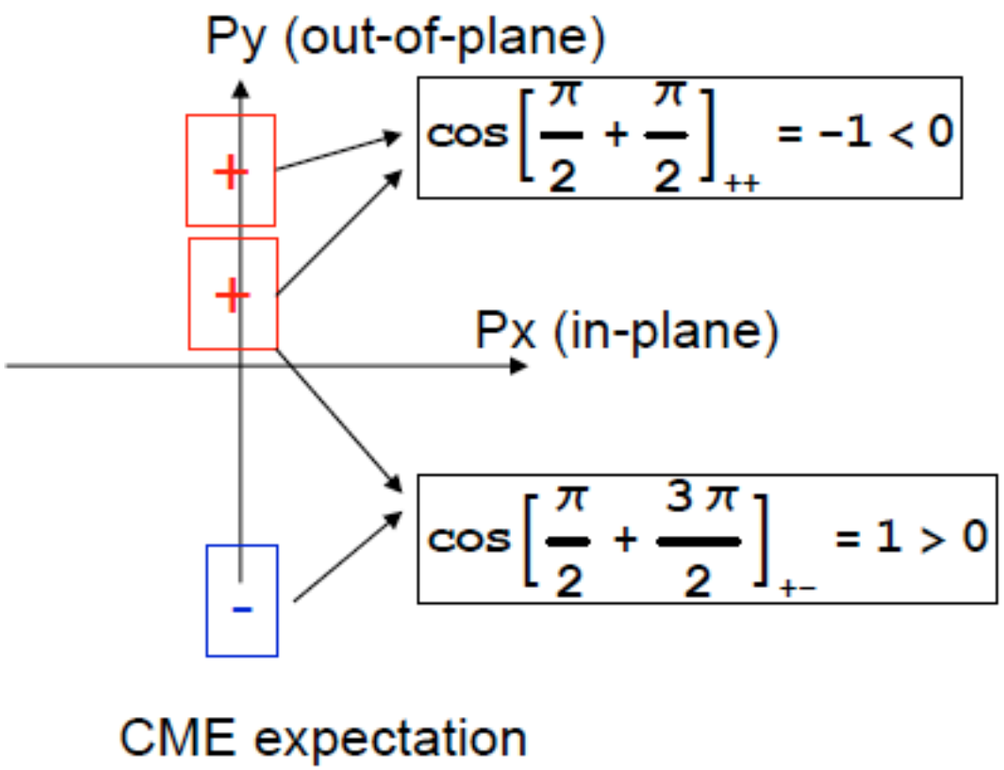
$$\gamma = \langle \cos(\phi_\alpha + \phi_\beta - 2\Psi_{RP}) \rangle = [\langle v_{1,\alpha} v_{1,\beta} \rangle + B_{in}] - [\langle a_\alpha a_\beta \rangle + B_{out}]$$

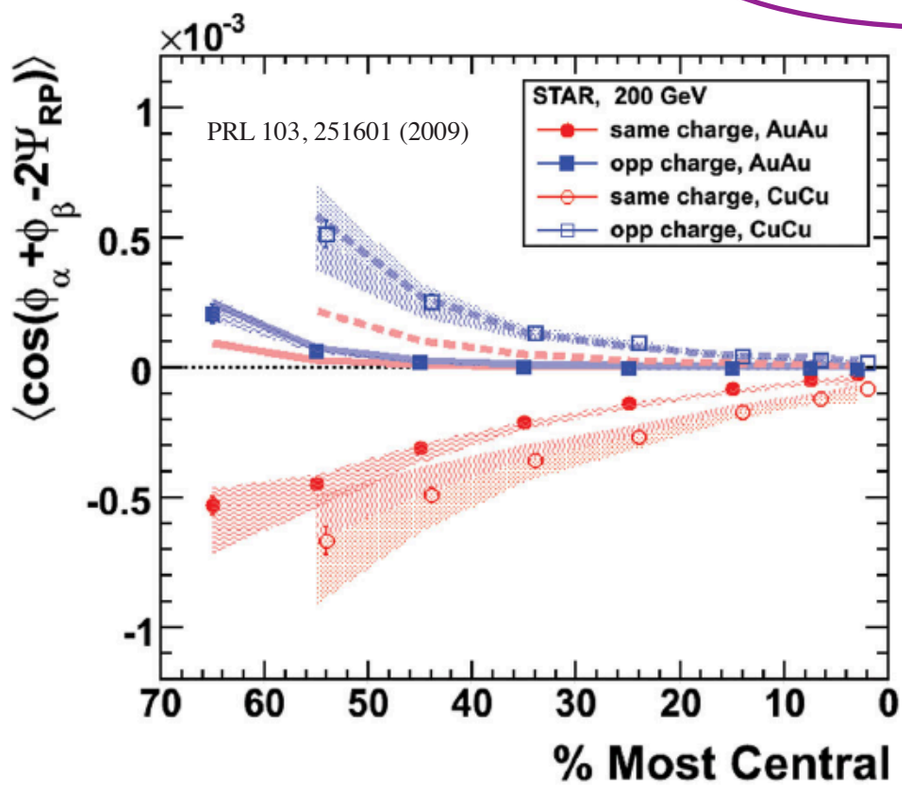
Directed flow: vanishes if measured in a symmetric rapidity range

Non-flow/non-parity effects: largely cancel out

P-even quantity: still sensitive to charge separation

$$\propto \langle B^2 \cos 2(\Psi_B - \Psi_2) \rangle.$$

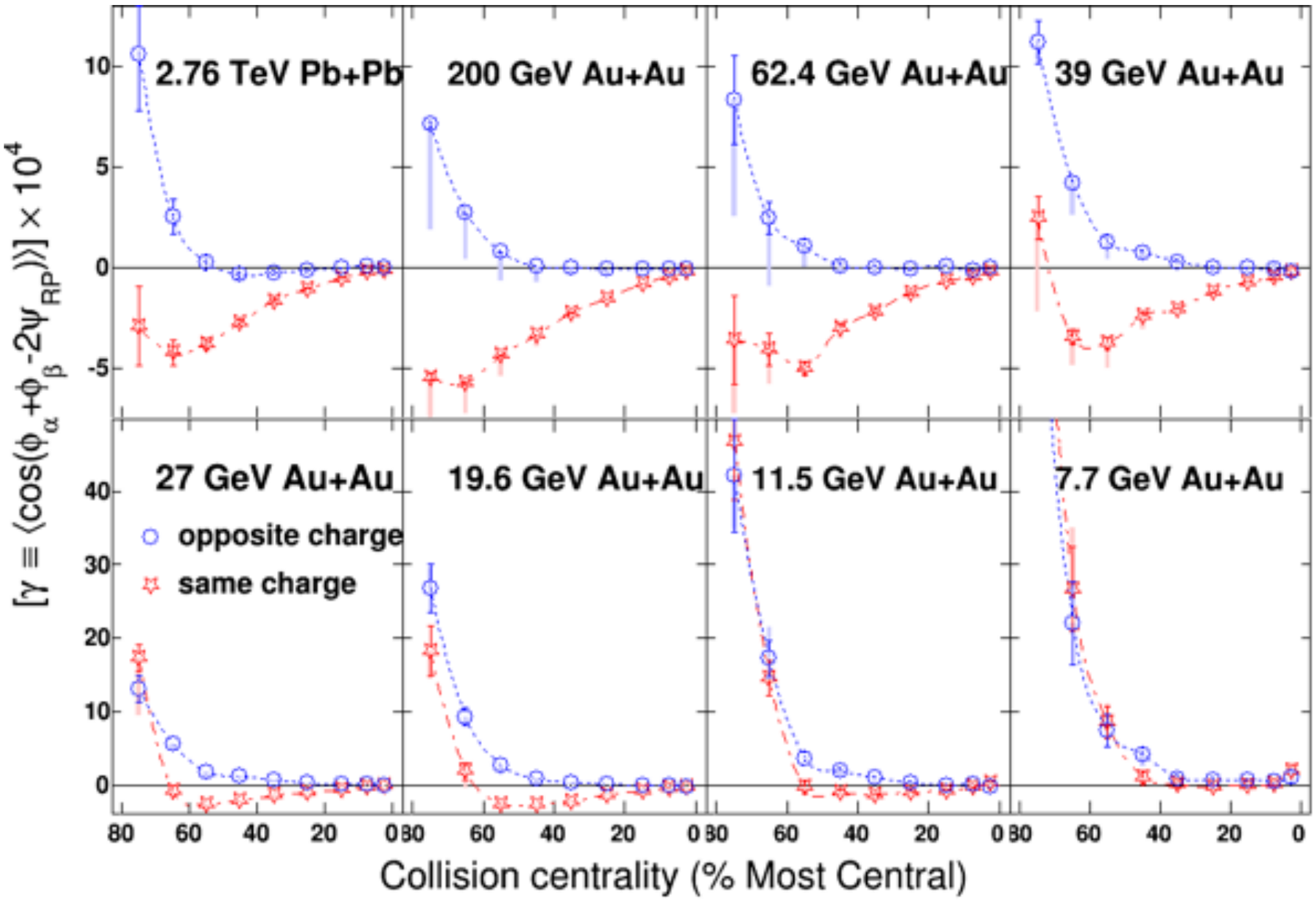




- RHIC data are consistent with the CME expectation that charges could be distributed asymmetrically w.r.t reaction plane, i.e. dipole charge separation.

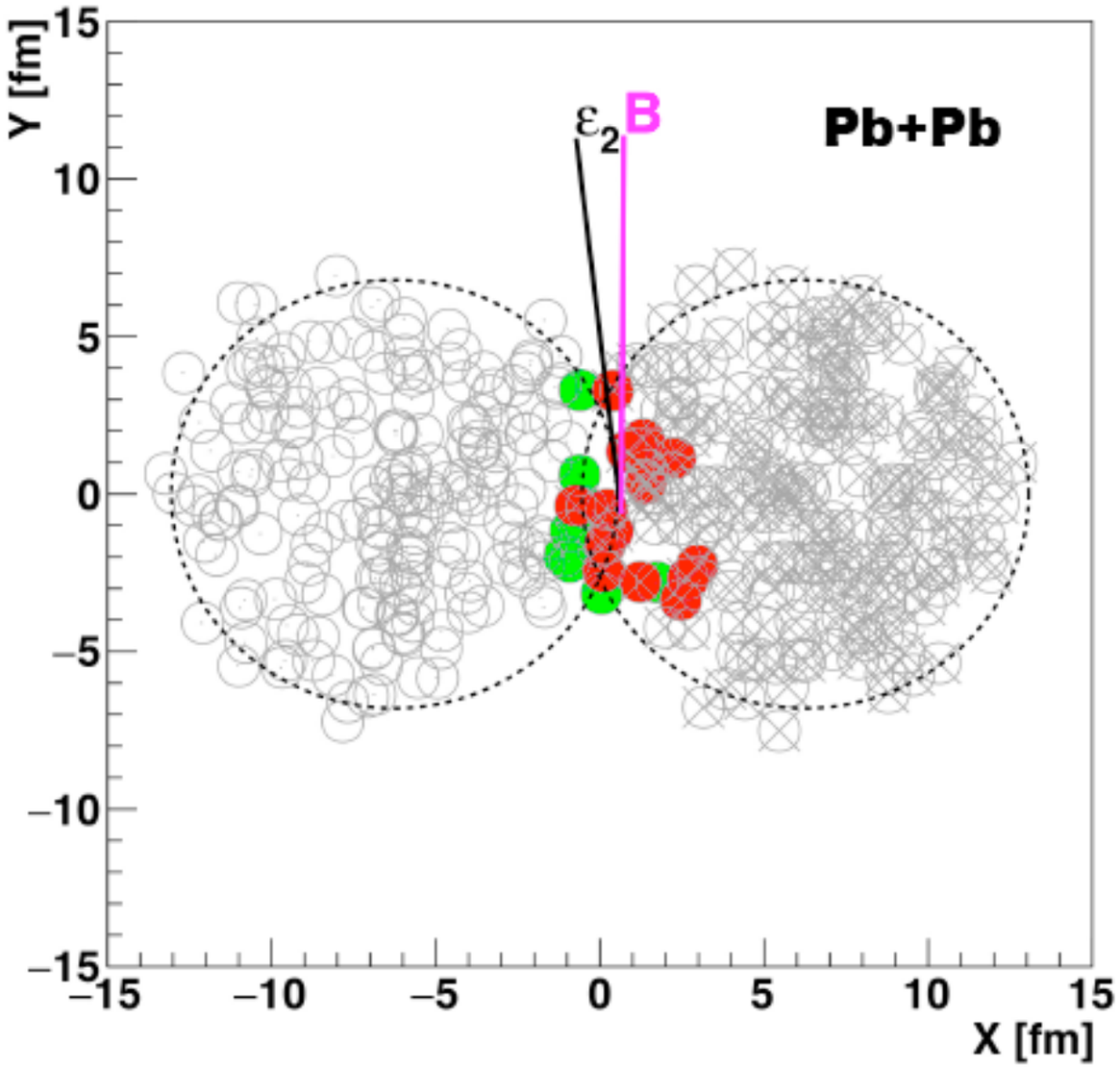
γ from Beam Energy Scan

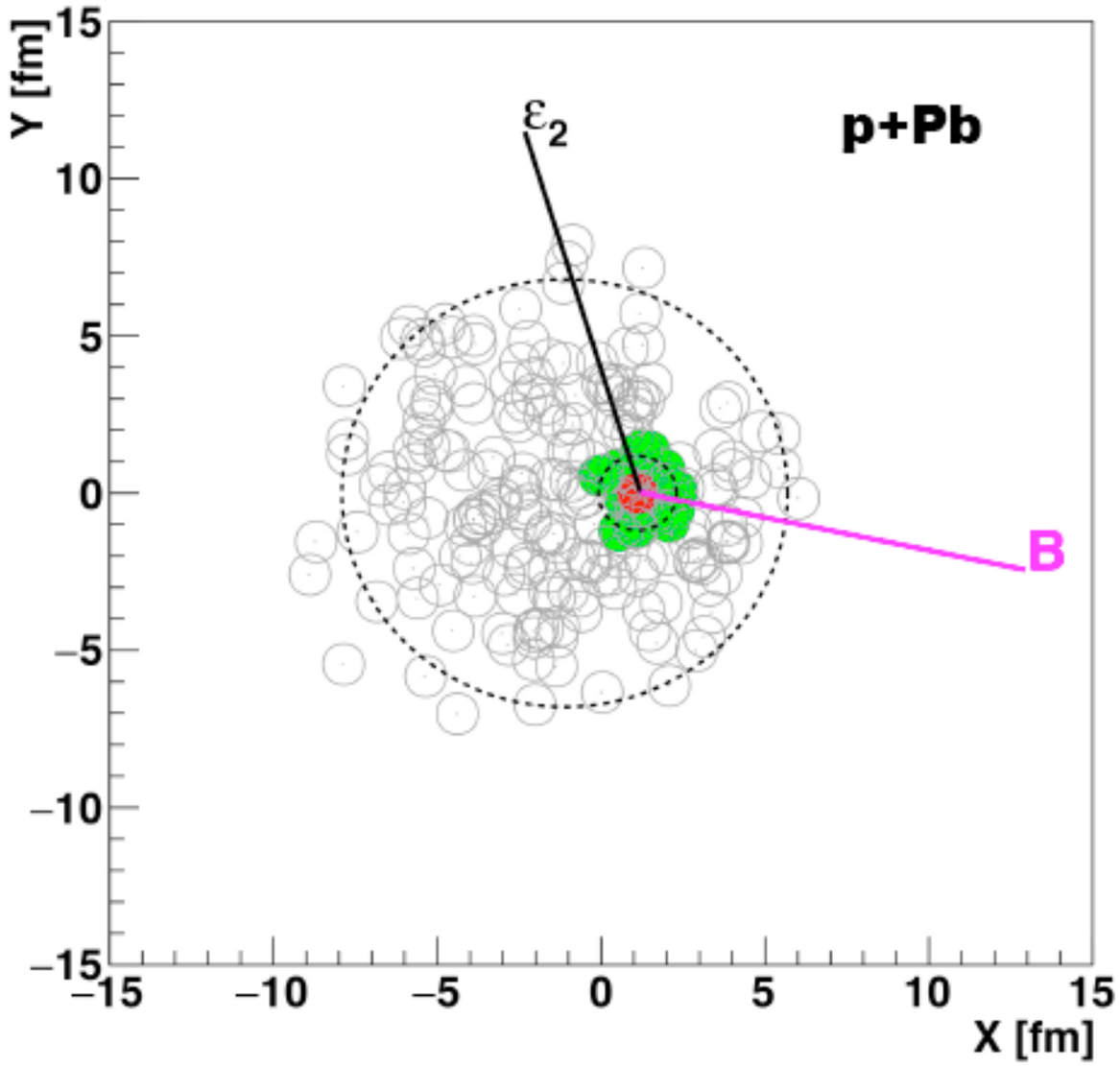
ALICE, Phys. Rev. Lett. 110, 012301 (2013); STAR, Phys. Rev. Lett 113 (2014) 052302



- The result from top RHIC energy is very similar to that from LHC.
- At lower energies, ‘charge separation’ starts to diminish.

CME in large vs small systems

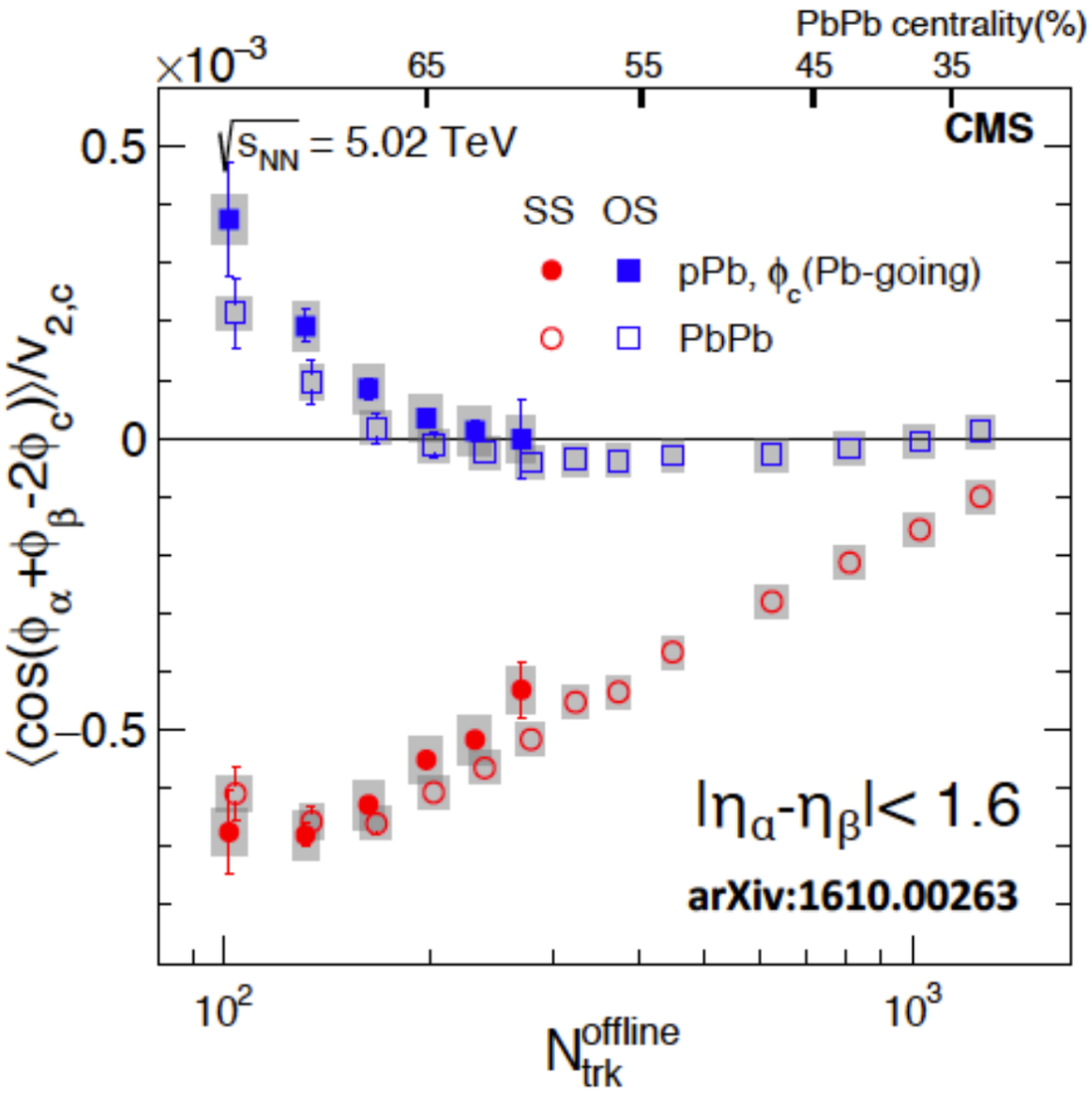


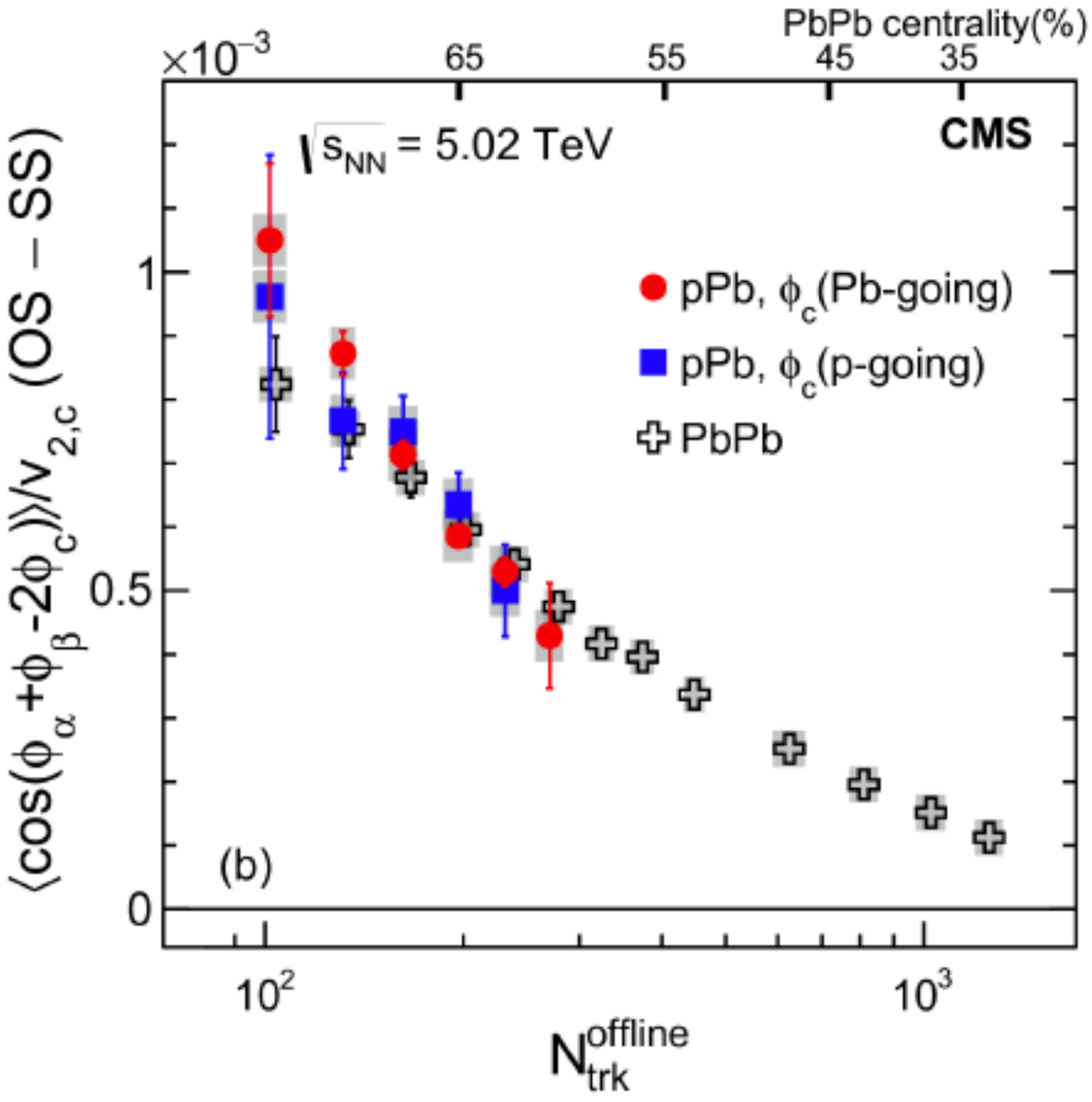


Charge separation signal: $\Delta\gamma \propto < B^2 \cos 2(\Psi_B - \Psi_{EP}) >$

In pA collisions, if $< \cos 2(\Psi_B - \Psi_{EP}) > \approx 0 \Longrightarrow \Delta\gamma^{CME} \approx 0$

Comparing $\Delta\gamma$ in pPb vs PbPb at LHC



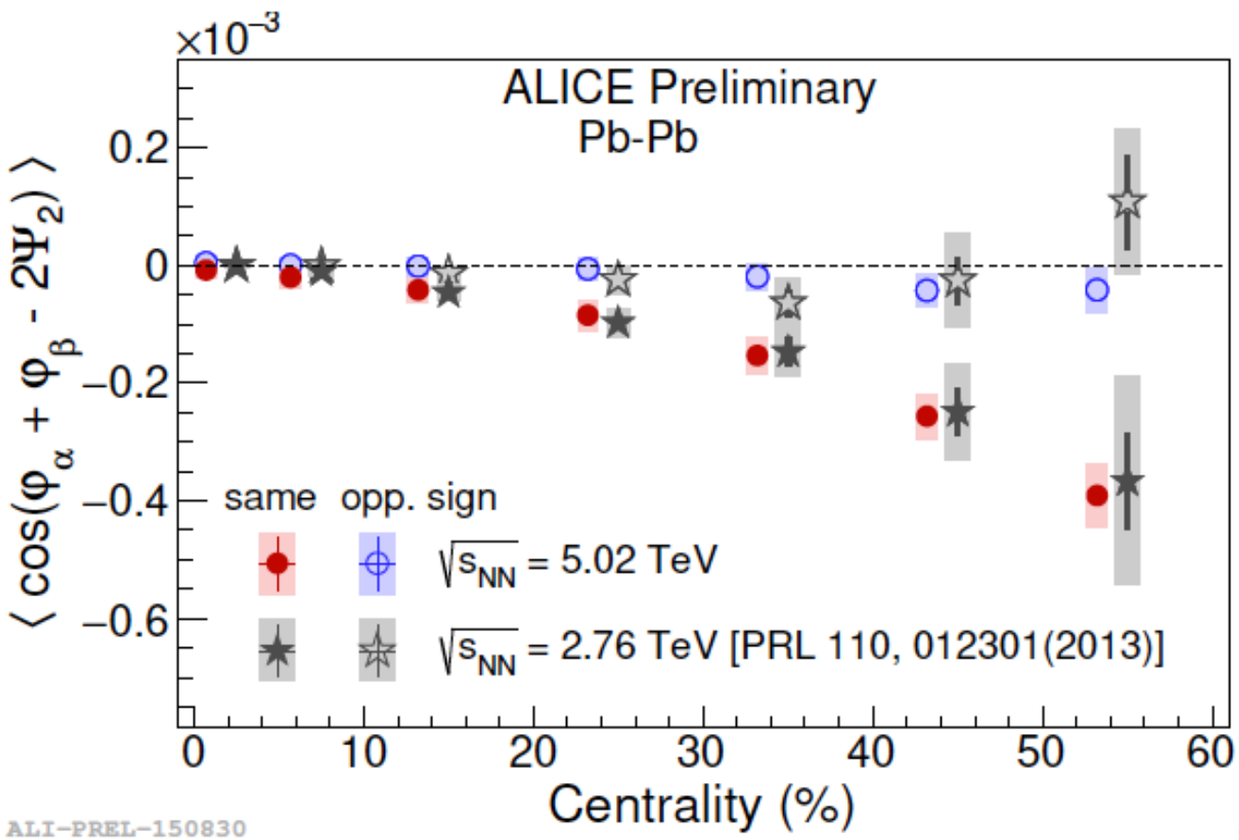


Almost all **BKG** in pPb and PbPb

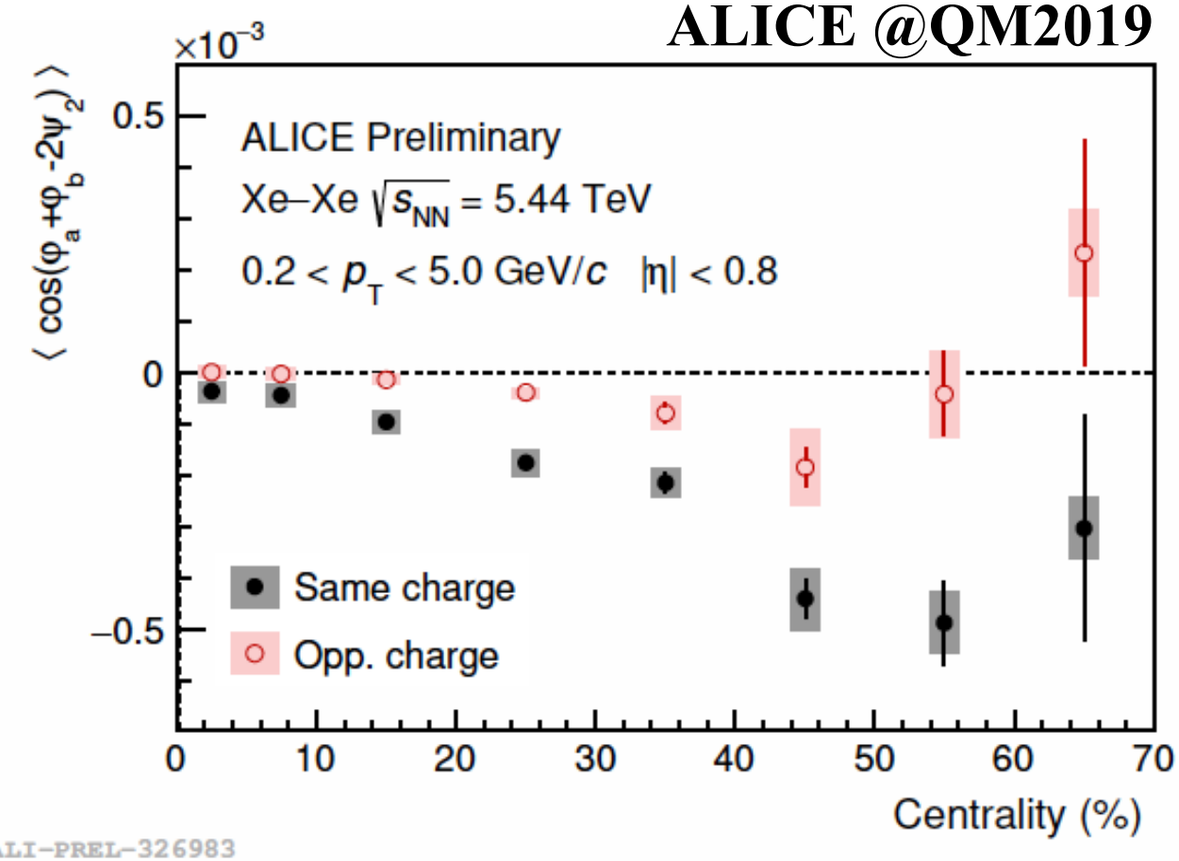
OR

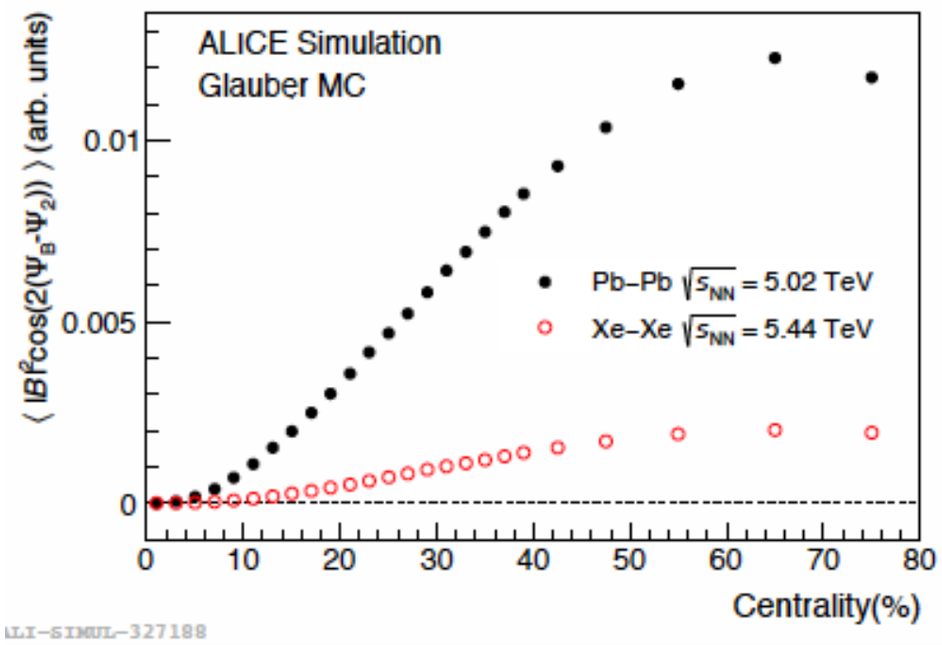
CME+**BKG** in PbPb ≈ **BKG** only in pPb

Comparing $\Delta\gamma$ in PbPb vs XeXe at LHC



ALICE @QM2019

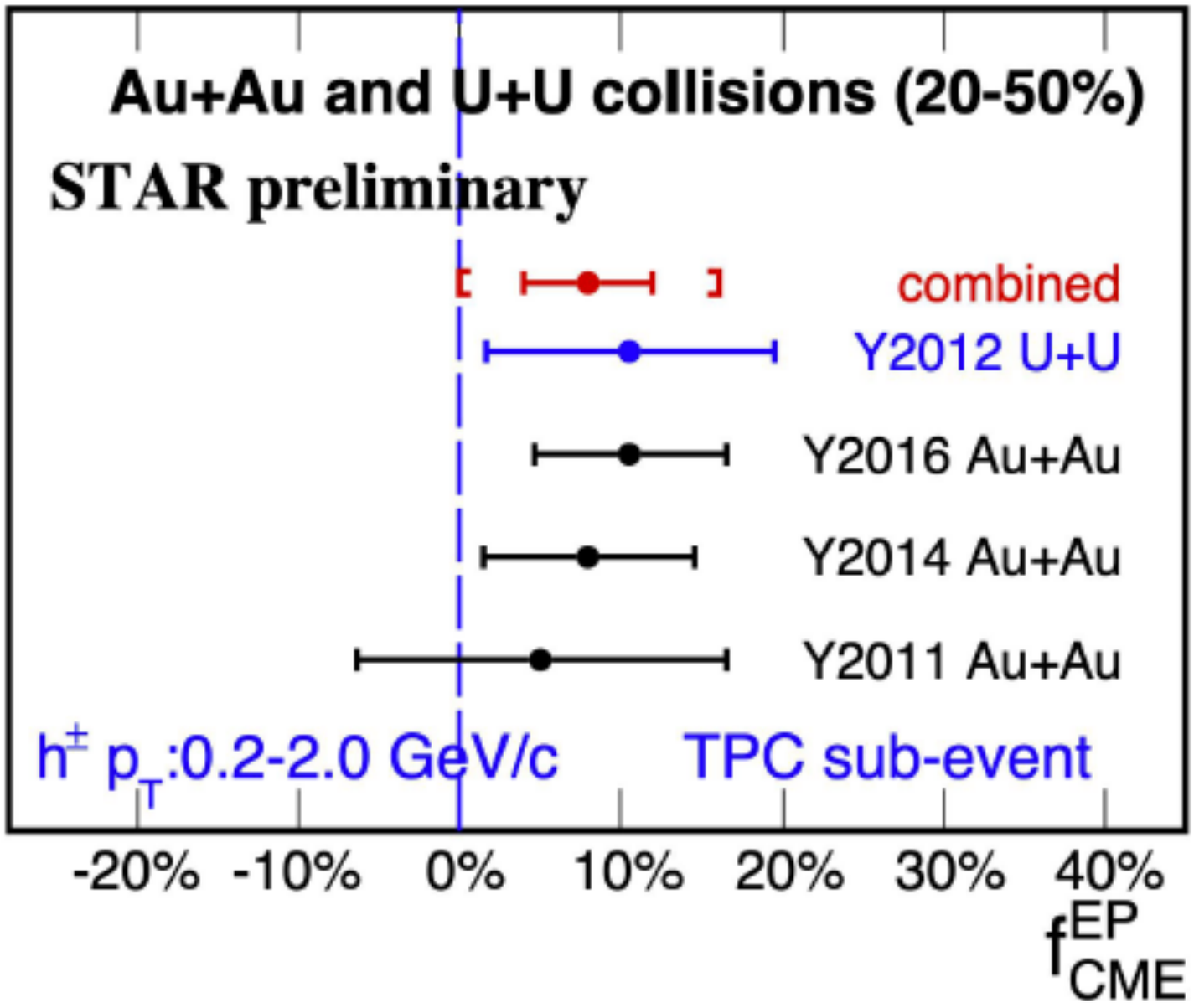




- **Non-CME contribution to $\Delta\gamma$ are significant**
- **Need to constrain background && CME to $\Delta\gamma$.**

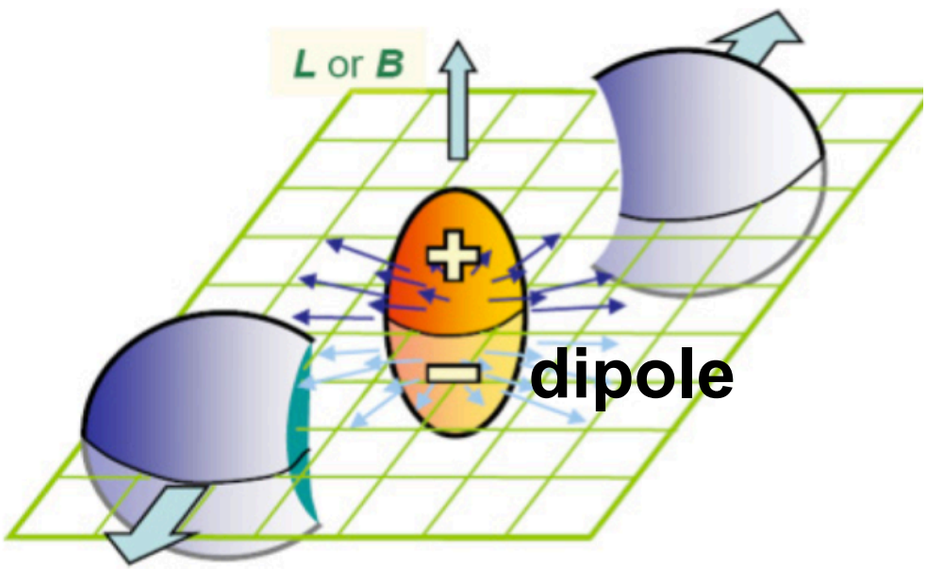
Constraint of CME from $\Delta\gamma$ at RHIC

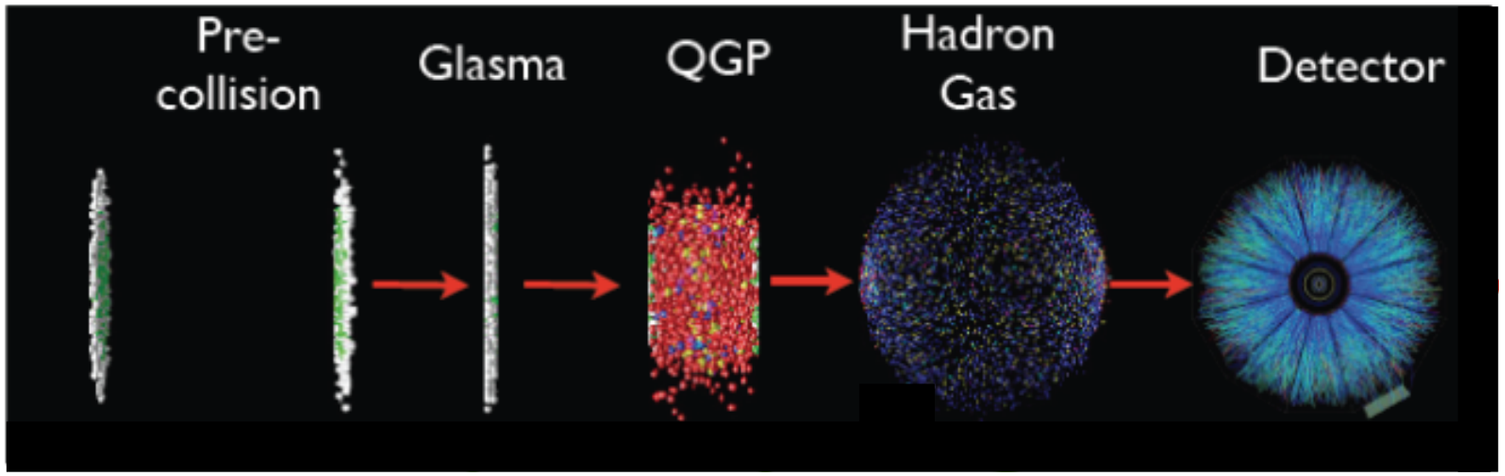
STAR @QM2019

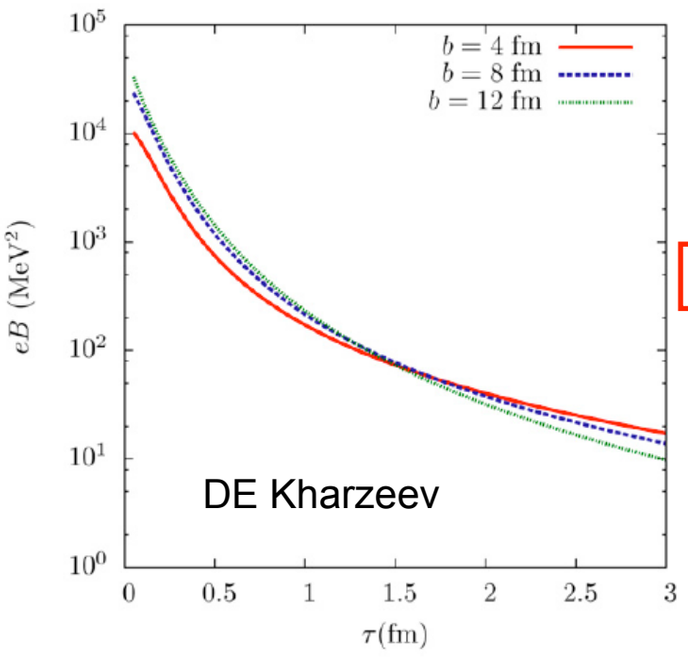


- **Results indicate possible CME signal fraction is small in Δγ**
- **possible CME signal is (8±4±8)% of the inclusive Δγ**

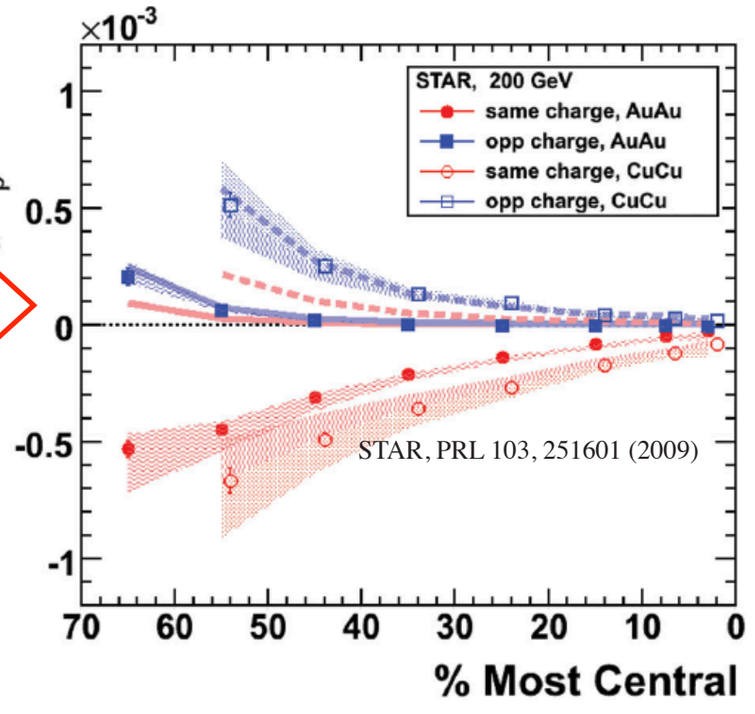
Can CME survive from final state interactions?







final state interaction effects



- To answer if CME can survive from final state interactions, it's important to investigate FSI effects on initial CME.

A multiphase transport (AMPT) model

Z. W. Lin, C. M. Ko et al. PRC 72, 064901 (2005)

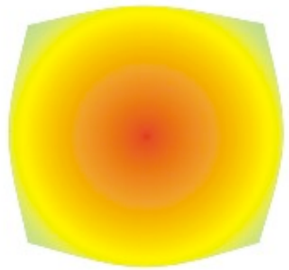
Melting AMPT Model

(1) initial condition

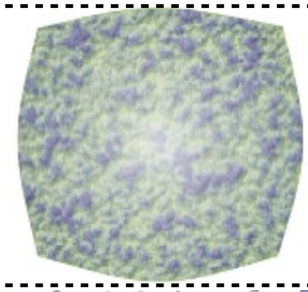


(2) parton cascade

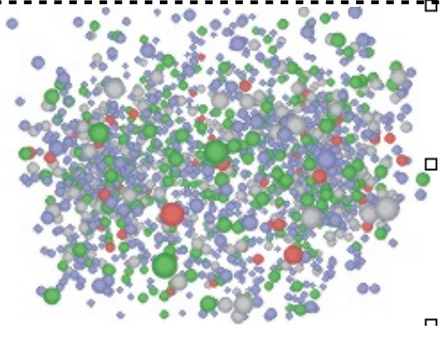
[2<->2 elastic collisions]

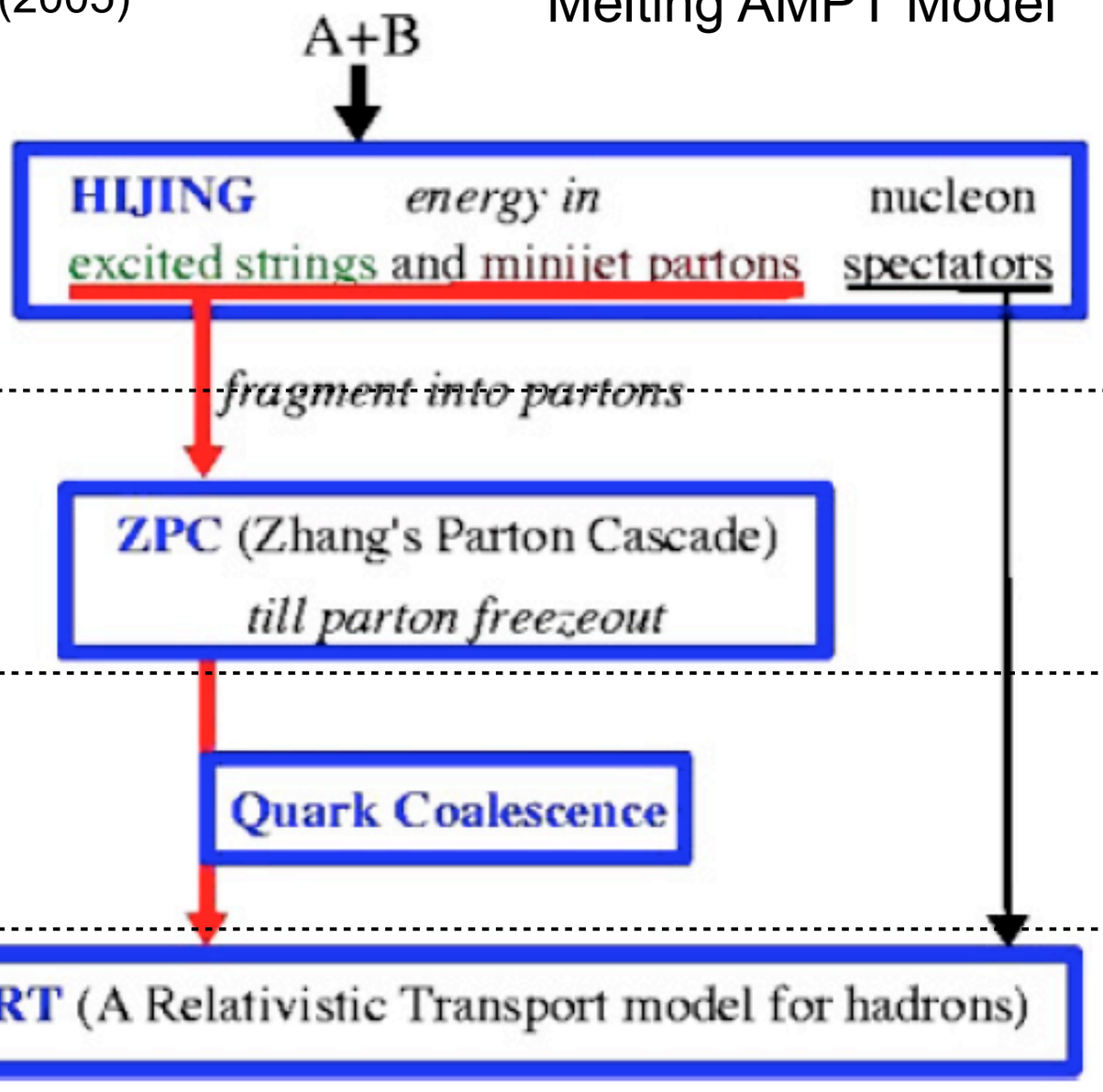


(3) hadronization

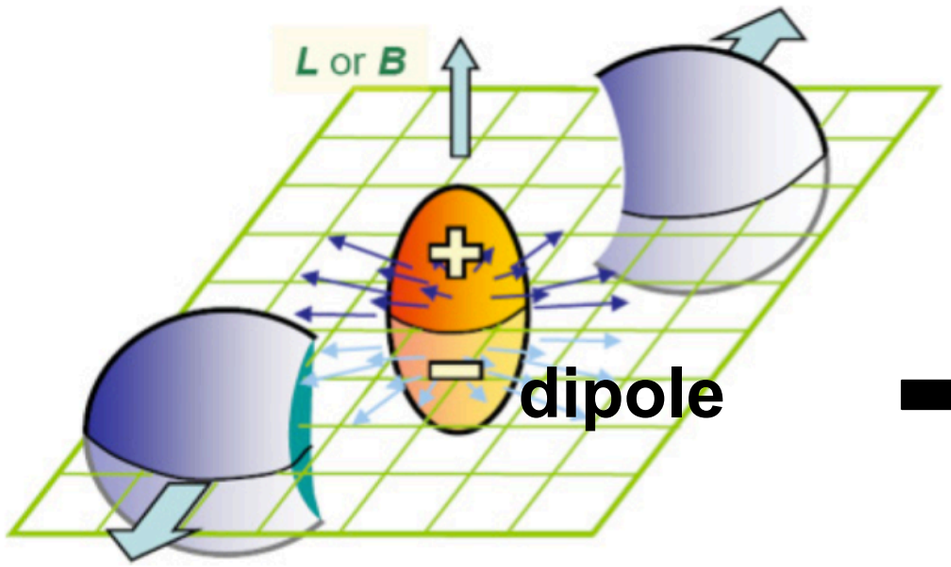


(4) hadronic rescatterings

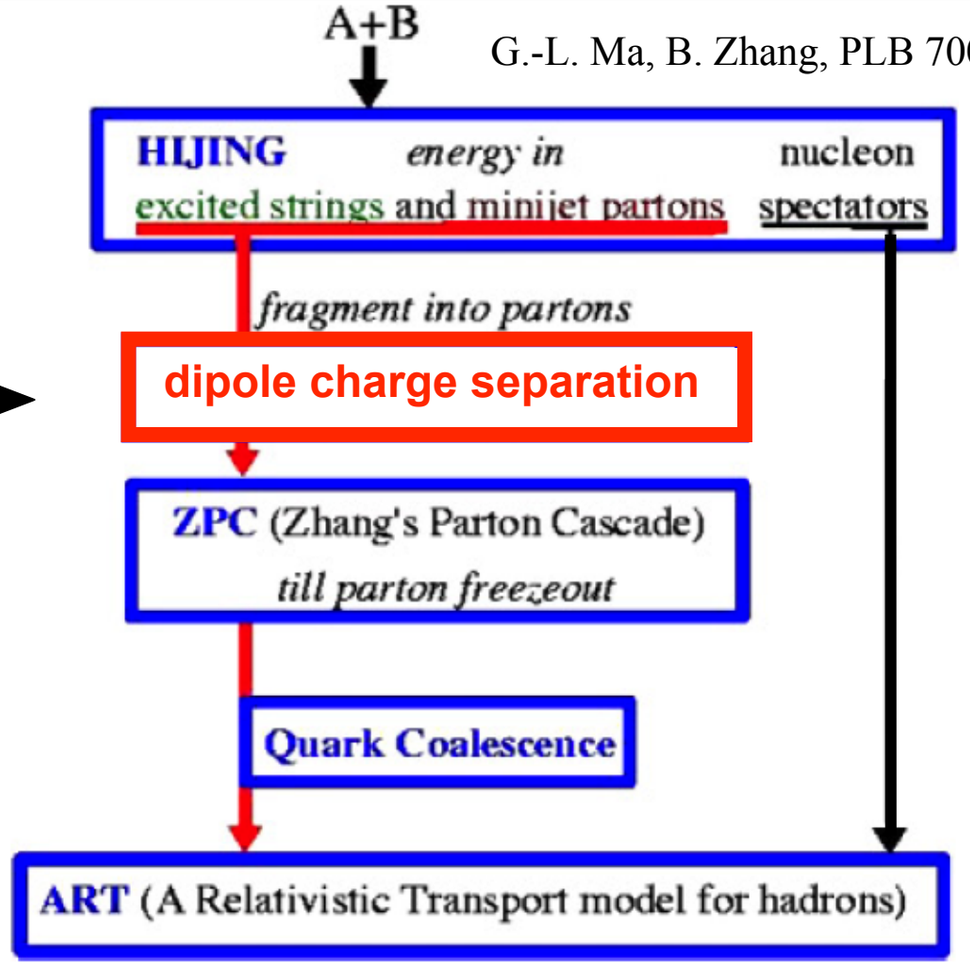




AMPT model with CME-type charge separation



$f\% = (N^{+}_{upward} - N^{+}_{downward})/(N^{+}_{upward} + N^{+}_{downward})$



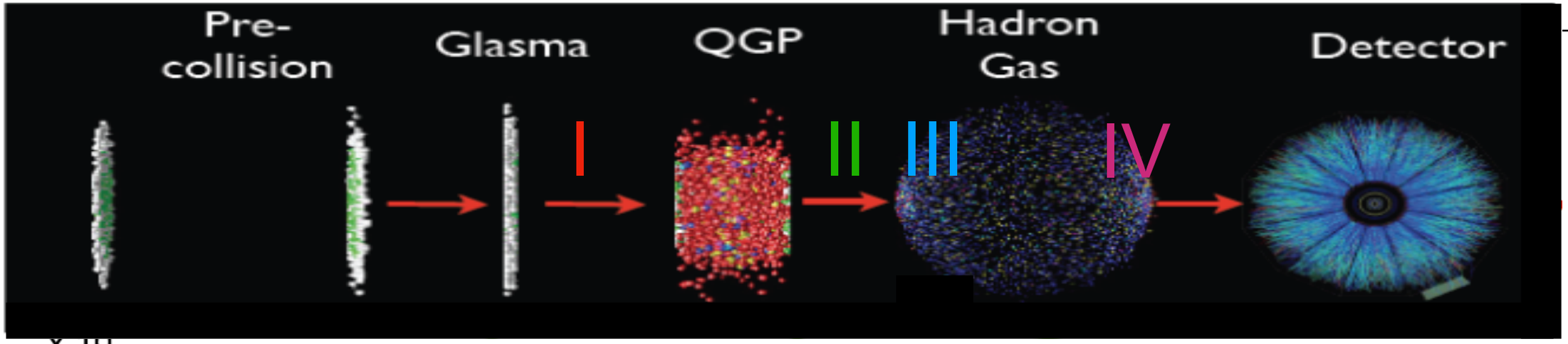
G.-L. Ma, B. Zhang, PLB 700 (2011) 39

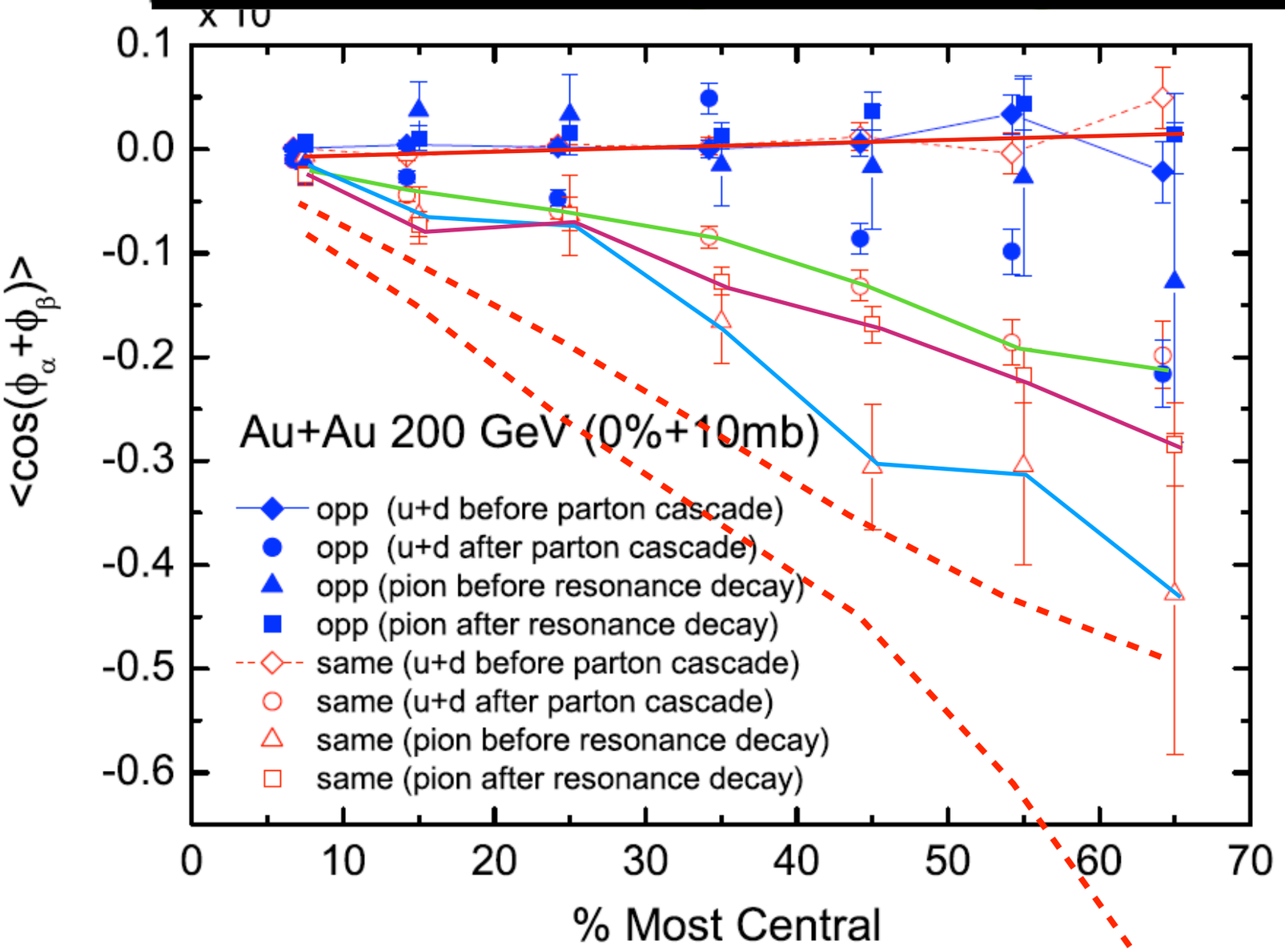
- **To include initial dipole charge separation (CME) into AMPT model,**

We switch p_y of f% of the downward moving u quarks with those of the upward moving u-bar quarks, and likewise for d-bar and d quarks.

- **We focus on FSI effects on the charge separation, including parton cascade, hadronization, resonance decays after $\vec{B}$ and $\vec{E}$ vanish quickly.**

Stage evolution of CME background in AMPT





I. Opp-charge and same-charge are consistent with zero initially.(◇)

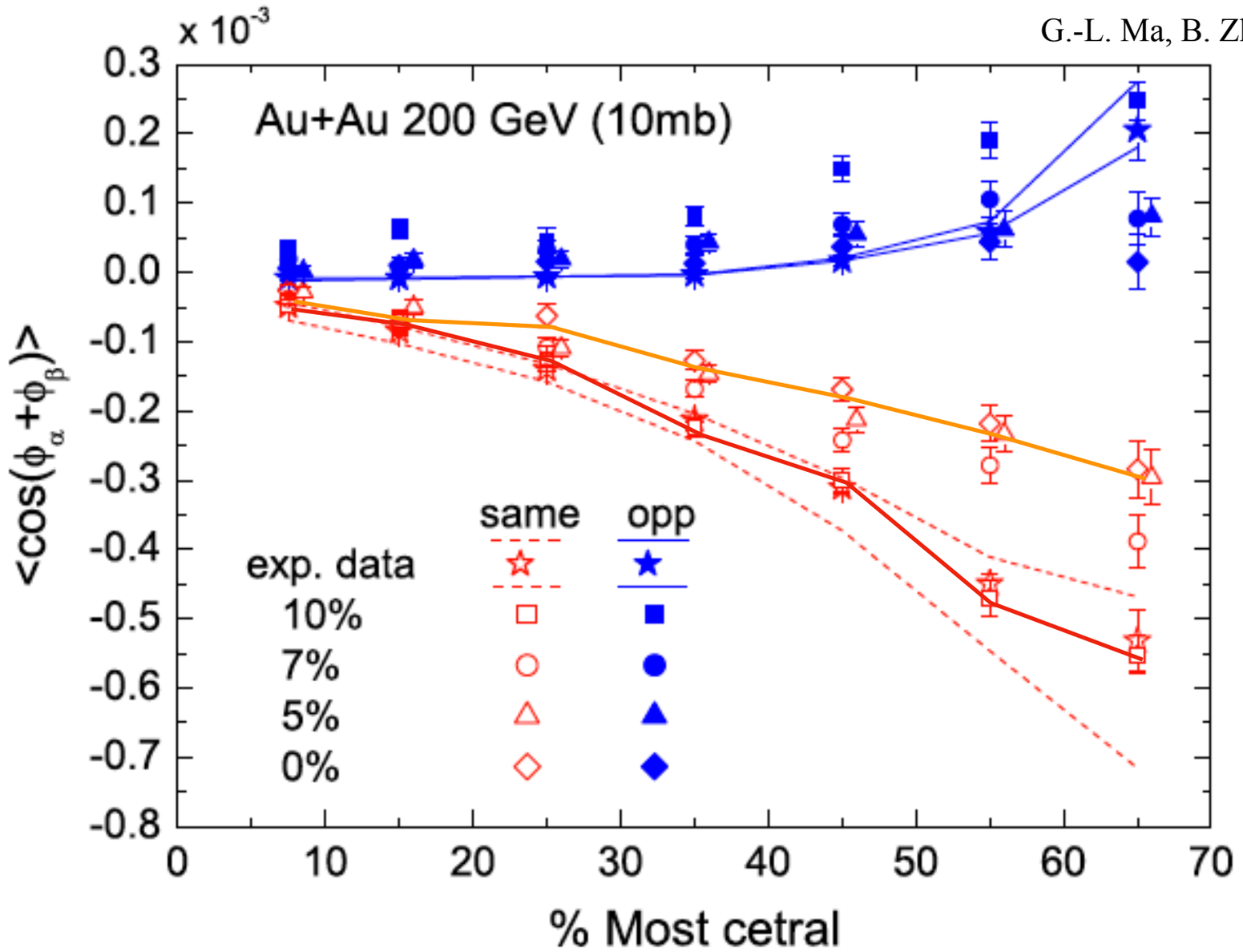
II. being negative through parton cascae due to Flow+TMC.(○)

III. Coalesce enhances same-charge and reduce opp-charge. (△)

IV. Resonance decays reduce signal. (□)

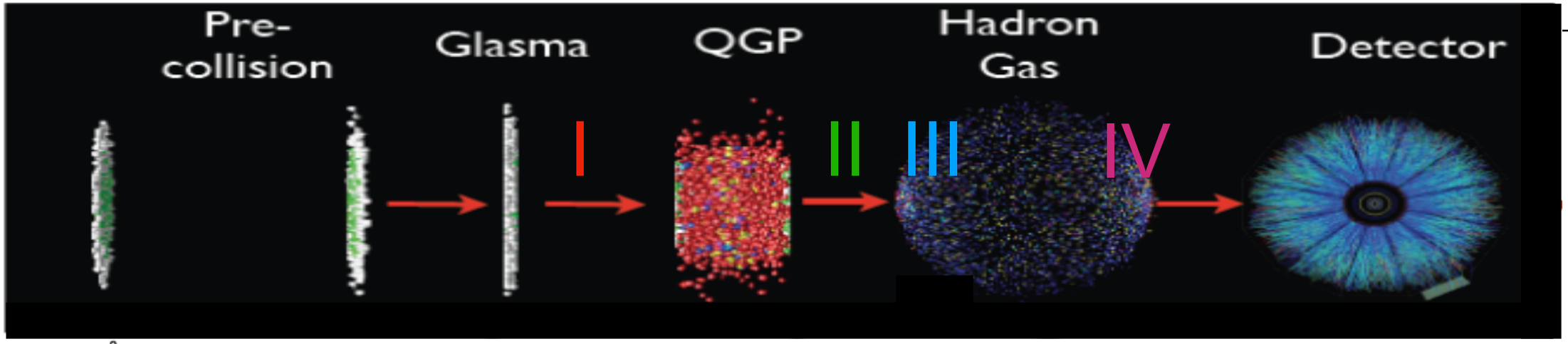
AMPT results on the CME obs. $\gamma=\langle\cos(\varphi_\alpha+\varphi_\beta)\rangle$

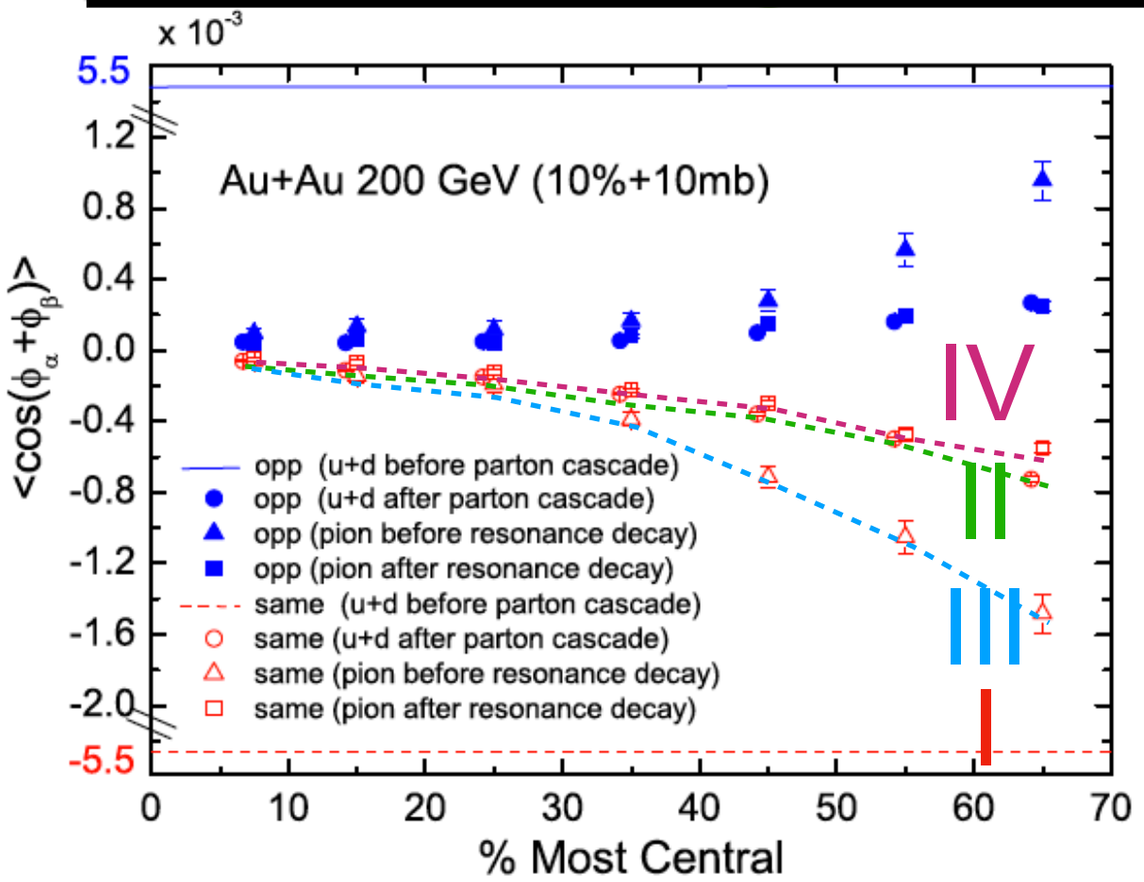
G.-L. Ma, B. Zhang, PLB 700 (2011) 39

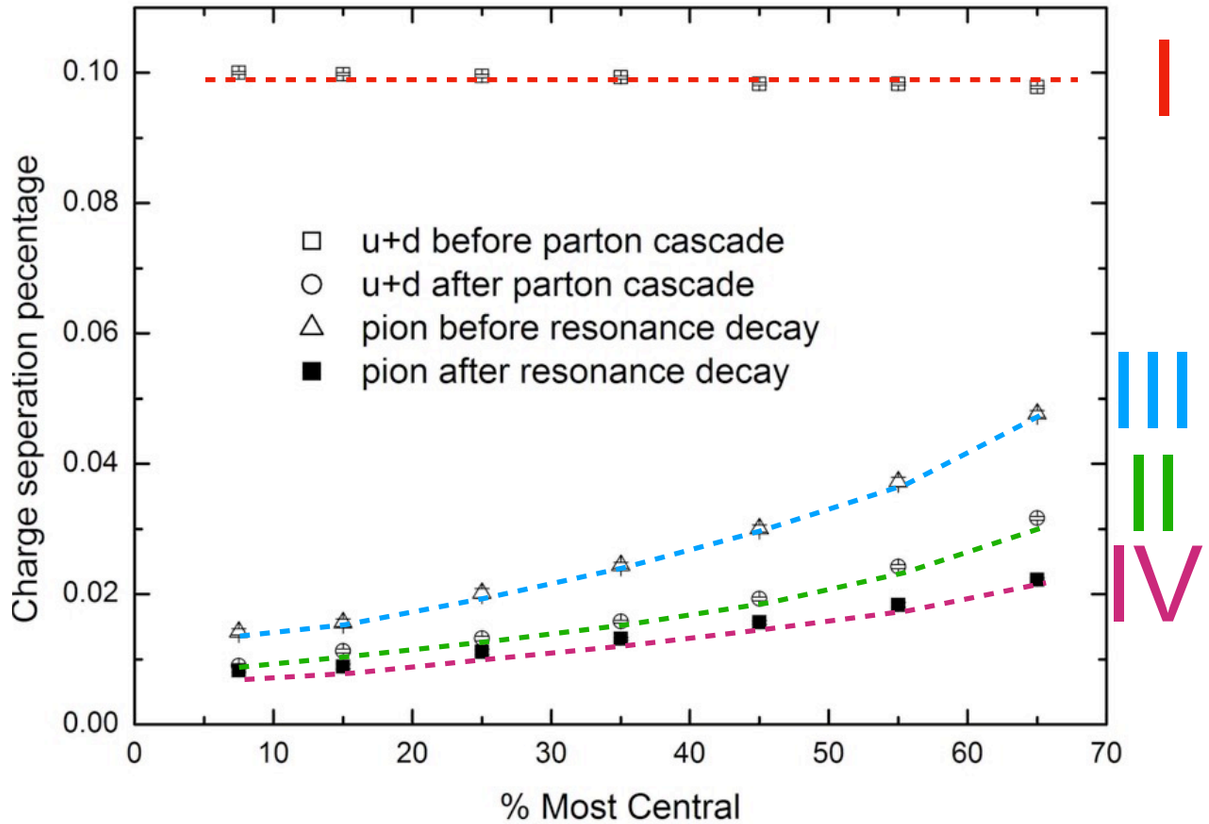


- Original AMPT (f=0%,◇) underestimates exp. data. ~2/3.
- AMPT+CME (f=10%,□) can describe same-charge data.

Stage evolution of CME signal in AMPT





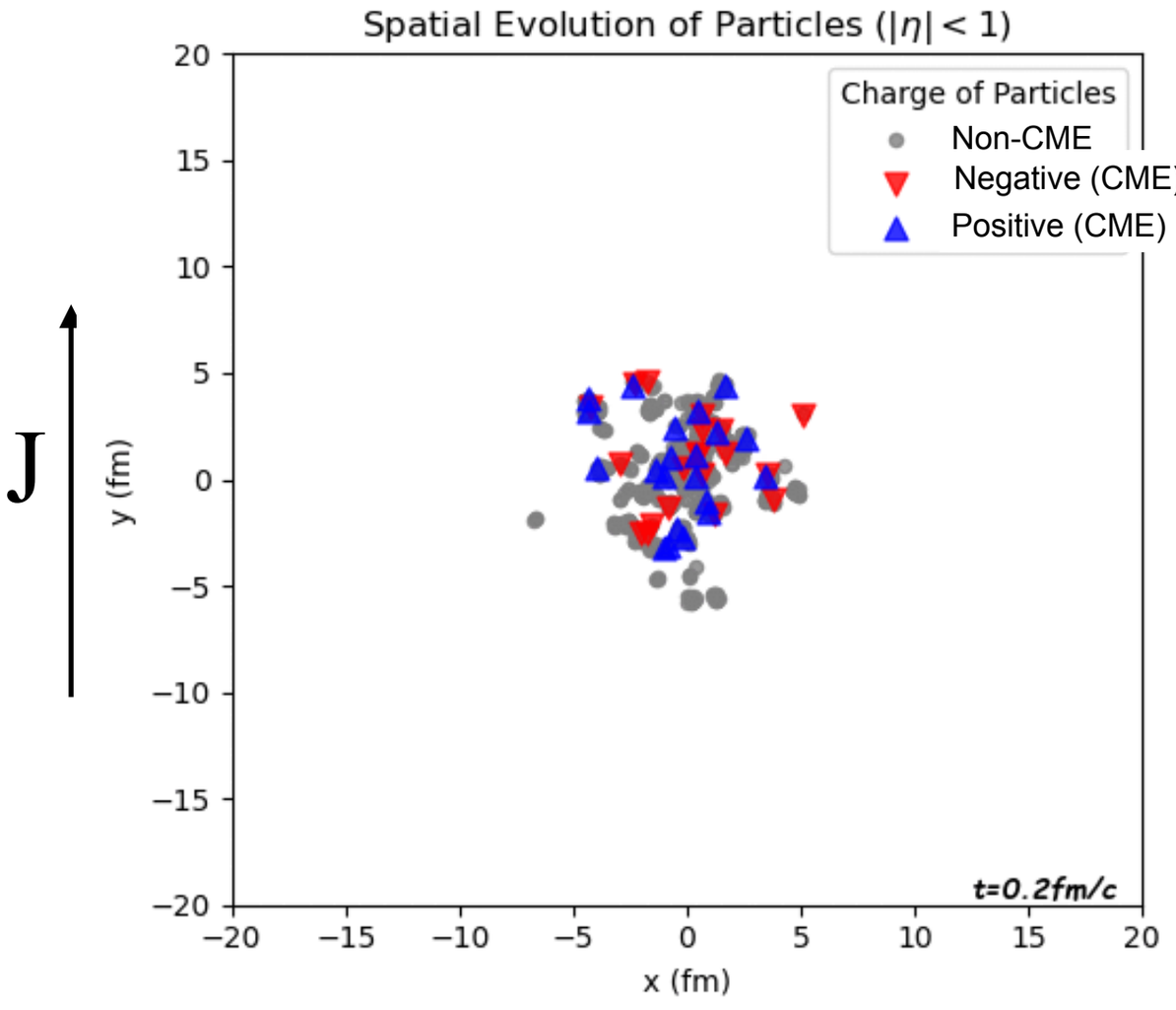


- Parton cascade reduces charge separation significantly; Coalescence enhances some charge separation; Resonance decays reduce charge separation.
- **FSI effect: 10% in the beginning →1-2% percentage at the end.**

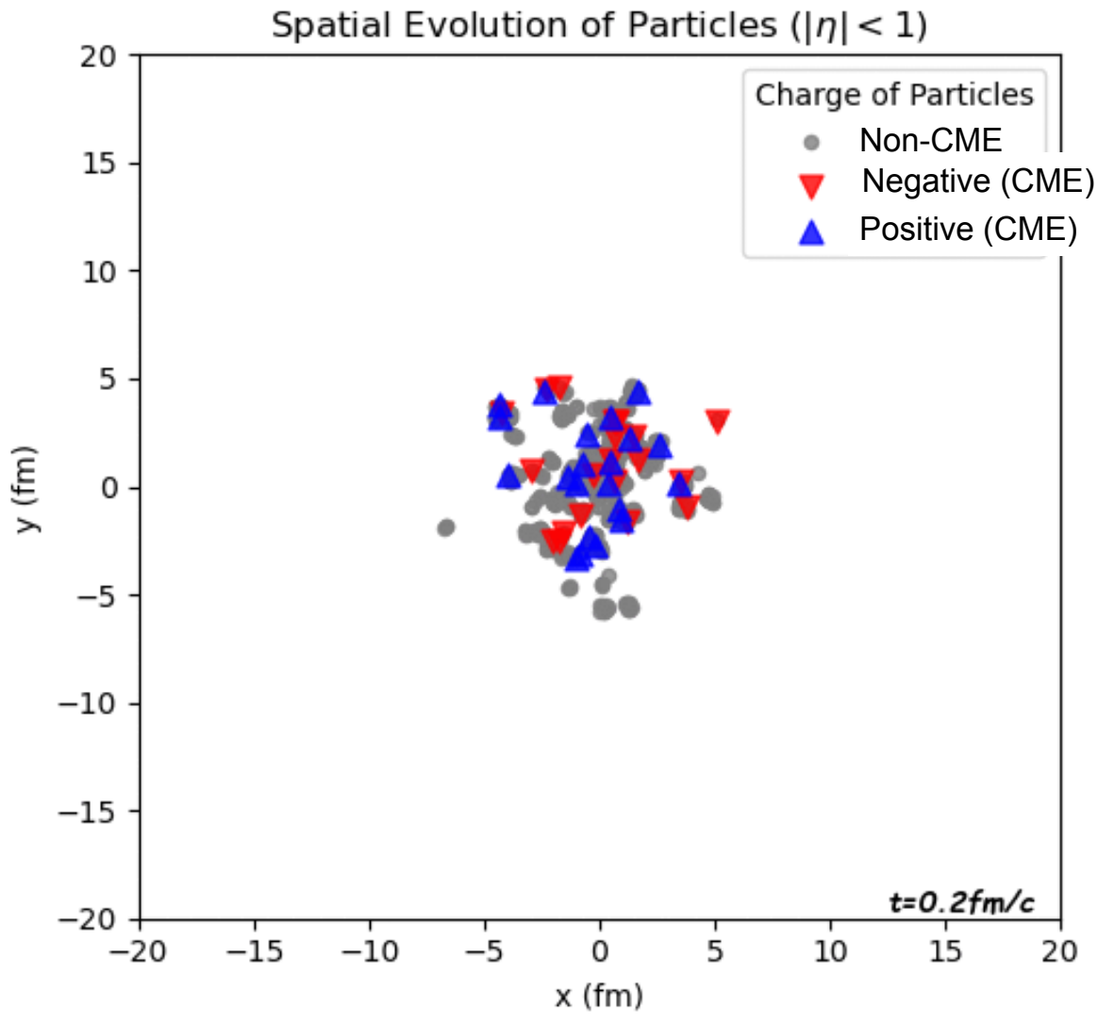
Parton cascade effect on the CME signal

Au+Au 200 GeV (b=8fm), AMPT+CME(10%)

0 mb

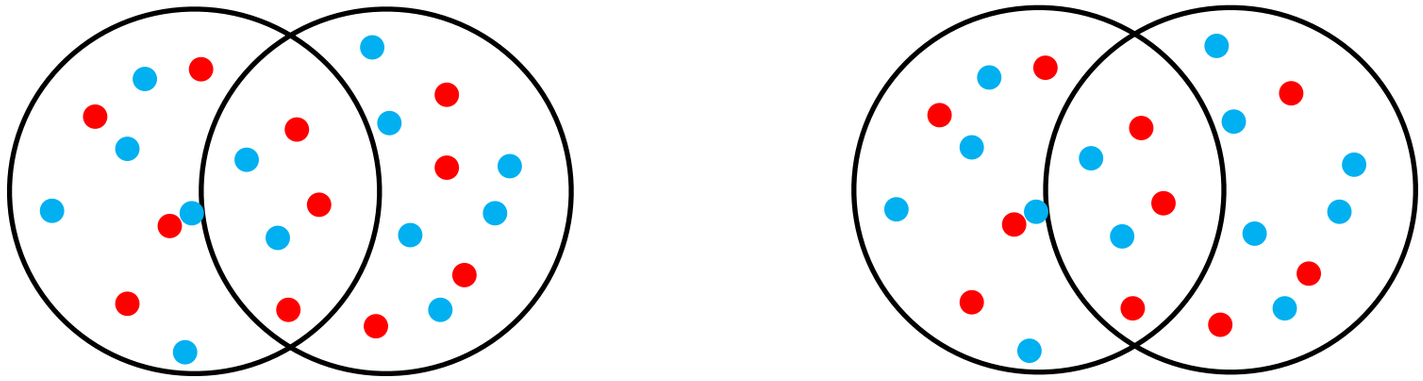


3 mb



Isobar collisions : a promising way to see CME

$$\mathbf{J} = \frac{Qe}{2\pi^2}\mu_5\mathbf{B}$$



$^{96}_{44}\mathrm{Ru} + {}^{96}_{44}\mathrm{Ru}$ $^{96}_{40}\mathrm{Zr} + {}^{96}_{40}\mathrm{Zr}$

钌+钌 锆+锆

Identical nucleon number → Identical background

Different proton number → Different magnetic field

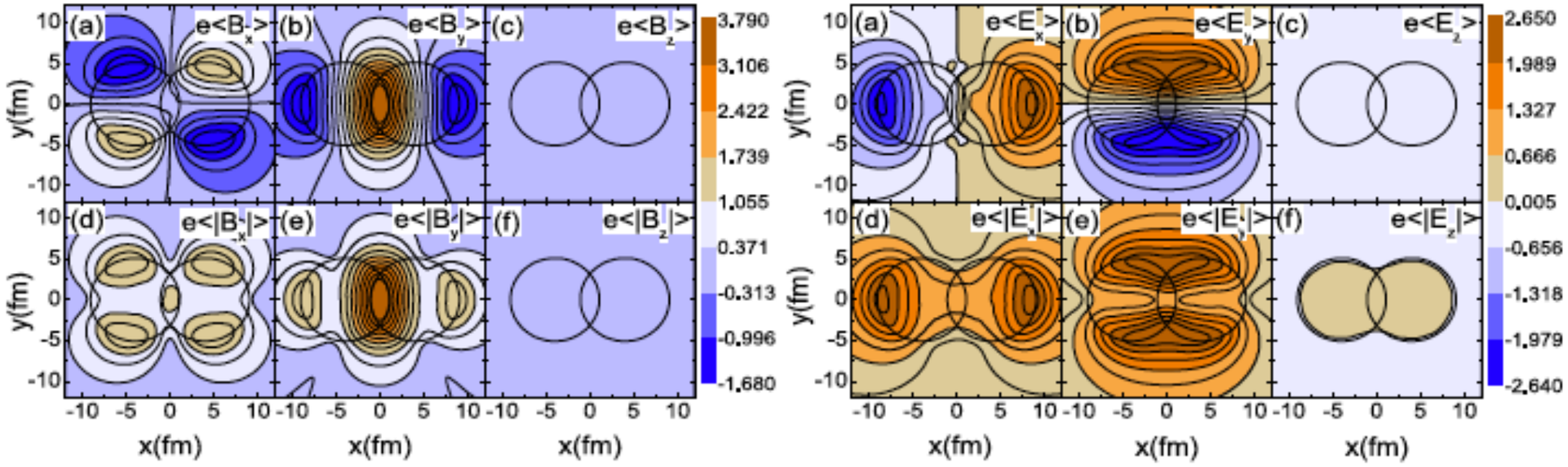
Electromagnetic field in isobaric collisions

From Lienard-Wiechert potential:

$$e\mathbf{E}(t,\mathbf{r}) = \frac{e^2}{4\pi}\sum_n Z_n \frac{\mathbf{R}_n - R_n\mathbf{v}_n}{(R_n - \mathbf{R}_n\cdot\mathbf{v}_n)^3}(1-v_n^2),$$

$$e\mathbf{B}(t,\mathbf{r}) = \frac{e^2}{4\pi}\sum_n Z_n \frac{\mathbf{v}_n \times \mathbf{R}_n}{(R_n - \mathbf{R}_n\cdot\mathbf{v}_n)^3}(1-v_n^2),$$

b = 8 fm

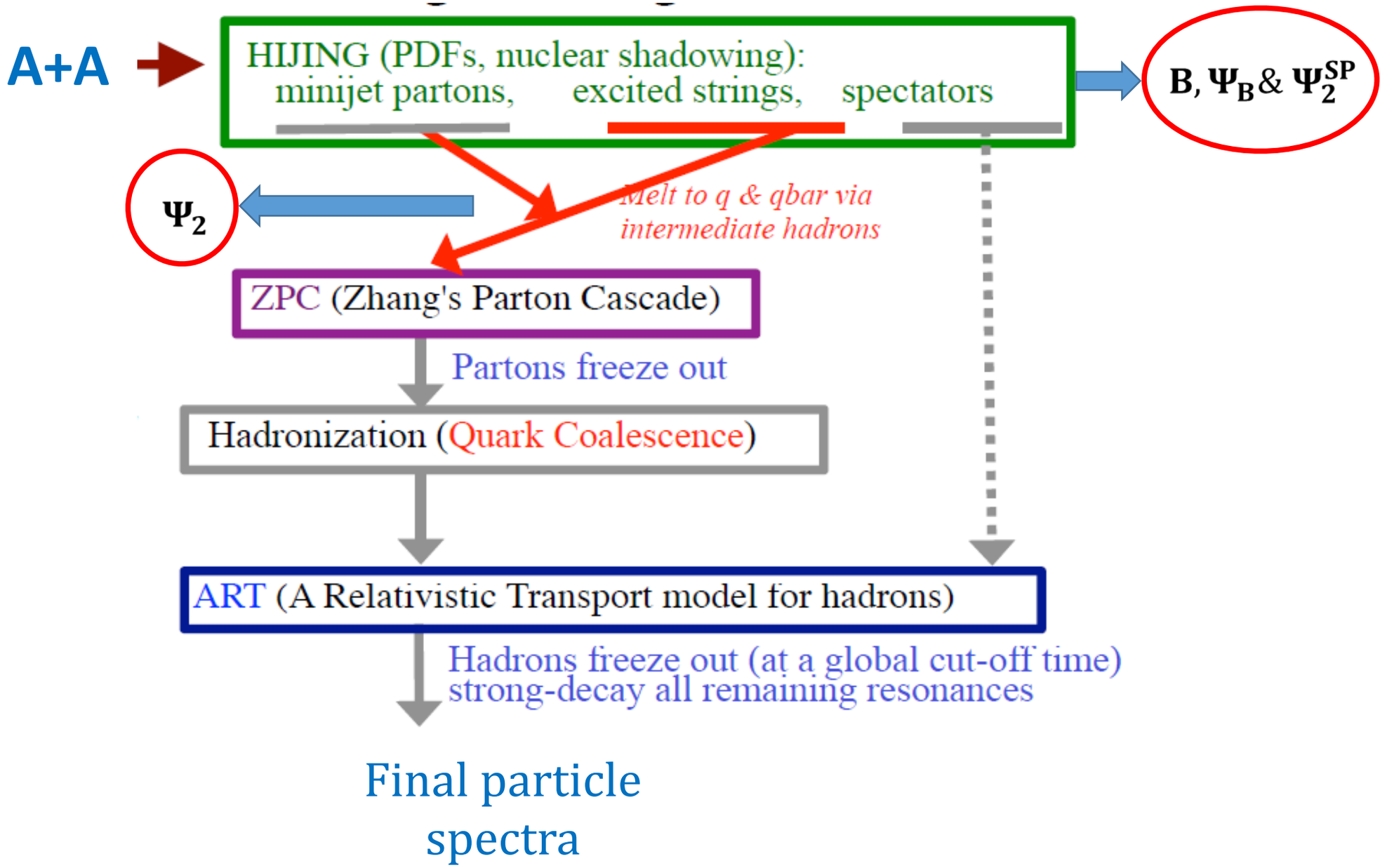


The distributions of RuRu collisions for case 1.

$\mathbf{r} = (0,0,0)\ \&\ t = 0$

CME-induced signal: $\Delta\gamma \propto \langle B^2 \cos 2(\Psi_B - \Psi_{EP})\rangle$

Key ingredients for CME signal



Geometry Configuration of Isobaric Collisions

Woods-Saxon form of spatial distribution of nucleons:

$$\rho(r,\theta) = \rho_0/(1+exp((r-R_0-\beta_2 R_0 Y_2^0(\theta))/a))$$

Case 1	R_0	a	β_2	β_4
Ru96	5.13	0.46	0.13	0.00
Zr96	5.06	0.46	0.06	0.00
Case 2	R_0	a	β_2	β_4
Ru96	5.13	0.46	0.03	0.00
Zr96	5.06	0.46	0.18	0.00

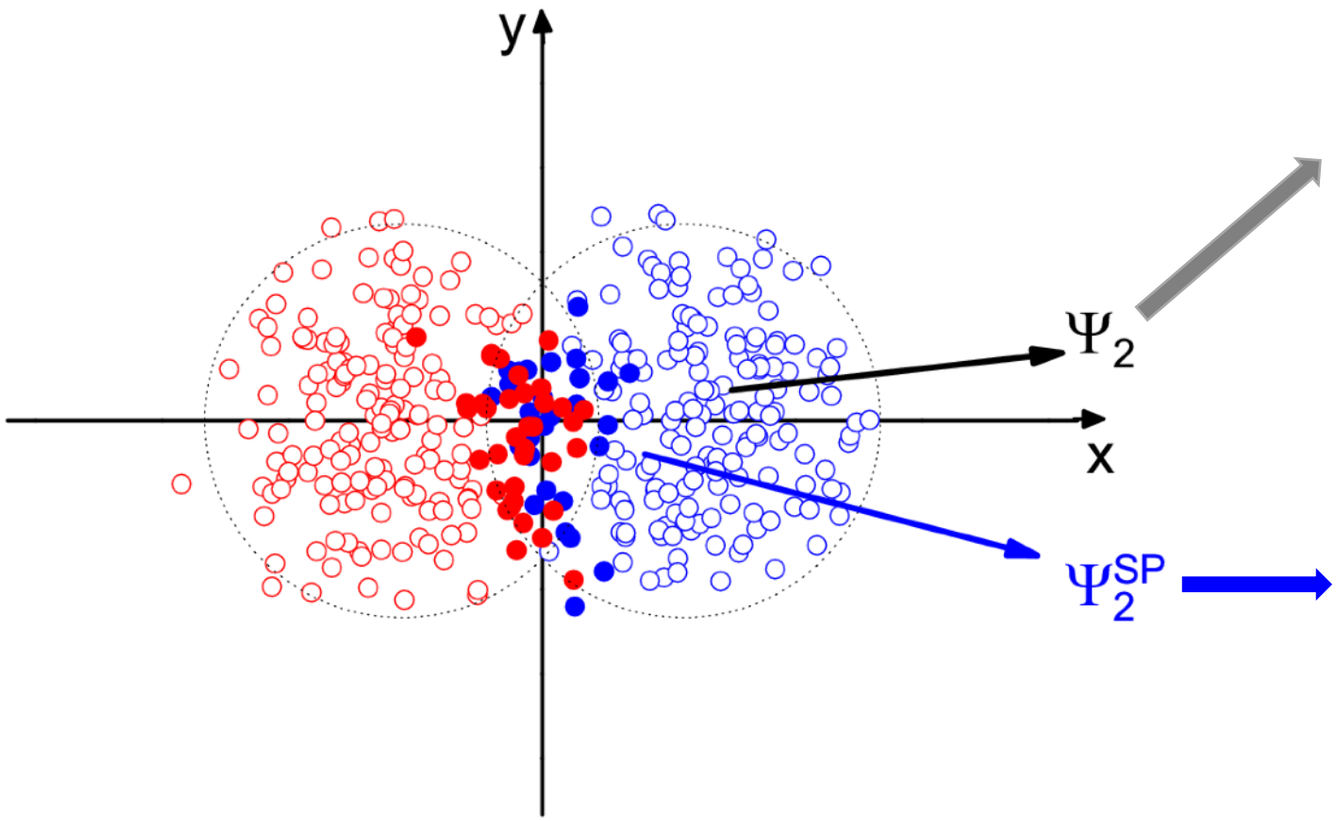
Relative ratio (RR): $R_Q = \frac{2(Q^{Ru}-Q^{Zr})}{Q^{Ru}+Q^{Zr}}$

e.g. for case 1, $R_{\beta_2} = \frac{2(0.13-0.06)}{0.13+0.06} = 0.33$; for case 2, $R_{\beta_2} = \frac{2(0.03-0.18)}{0.03+0.18} = -1.43$

Q can represent $|B|$, $\cos2(\Psi_B-\Psi_2)$, $B^2\cos2(\Psi_B-\Psi_2)$, $\cos2(\Psi_B-\Psi_2^{SP})$ and $B^2\cos2(\Psi_B-\Psi_2^{SP})$.

X. L. Zhao, G. L. Ma, Y. G. Ma, PRC 99, 034903 (2019)

Calculation Method of Ψ_2 & Ψ_2^{SP}



In model,

$$\Psi_2 = \frac{1}{2}[arctan\frac{\langle r_p^2 sin(2\phi_p)\rangle}{\langle r_p^2 cos(2\phi_p)\rangle} + \pi]$$

X. L. Zhao, Y. G. Ma, G. L. Ma, PRC 97, 024910 (2018)

Ψ_2 is participant plane which is constructed by initial geometry of partons.

$$\Psi_2^{SP} = \frac{1}{2} arctan\frac{\langle r_s^2 sin(2\phi_s)\rangle}{\langle r_s^2 cos(2\phi_s)\rangle}$$

Sandeep Chatterjee *et al*, PRC 92, 011902(R) (2015)

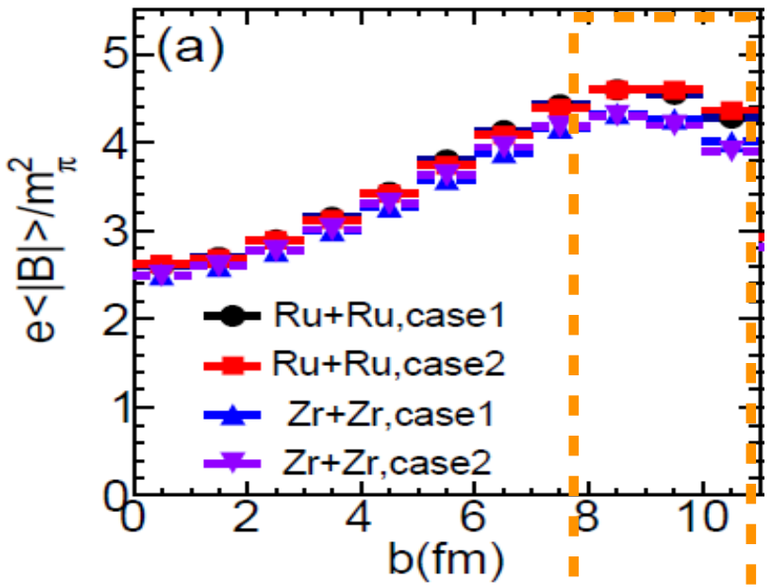
Ψ_2^{SP} is spectator plane which is constructed by spectator neutrons from one projectile.

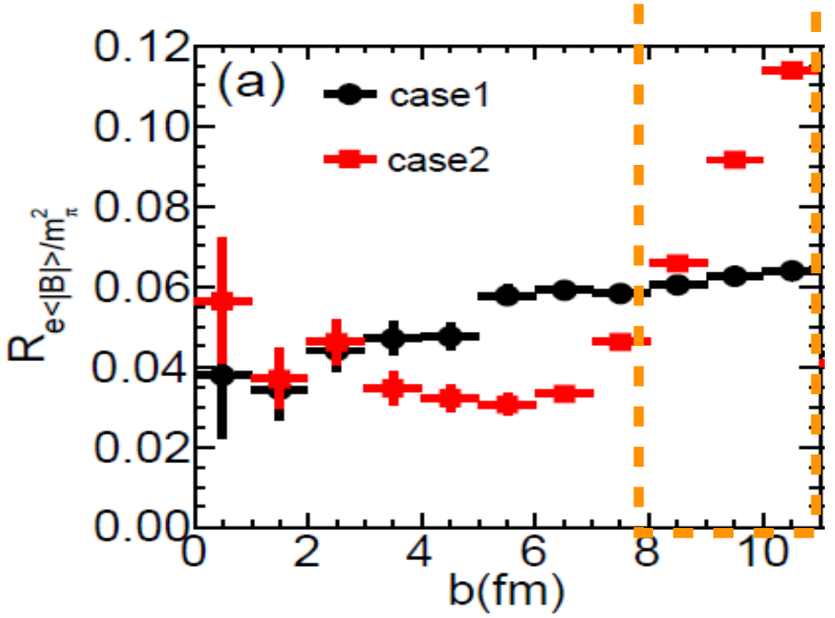
In experiment, Ψ_2 is the 2nd-harmonic event plane measured by the TPC, and Ψ_2^{SP} is assessed by spectator neutrons measured by ZDC.

Jie Zhao *et al*, arXiv:1807.05083; Hao-Jie Xu *et al*, arXiv:1710.07265; Sergei A. Voloshin, arXiv:1805.05300

|B|

40-70%

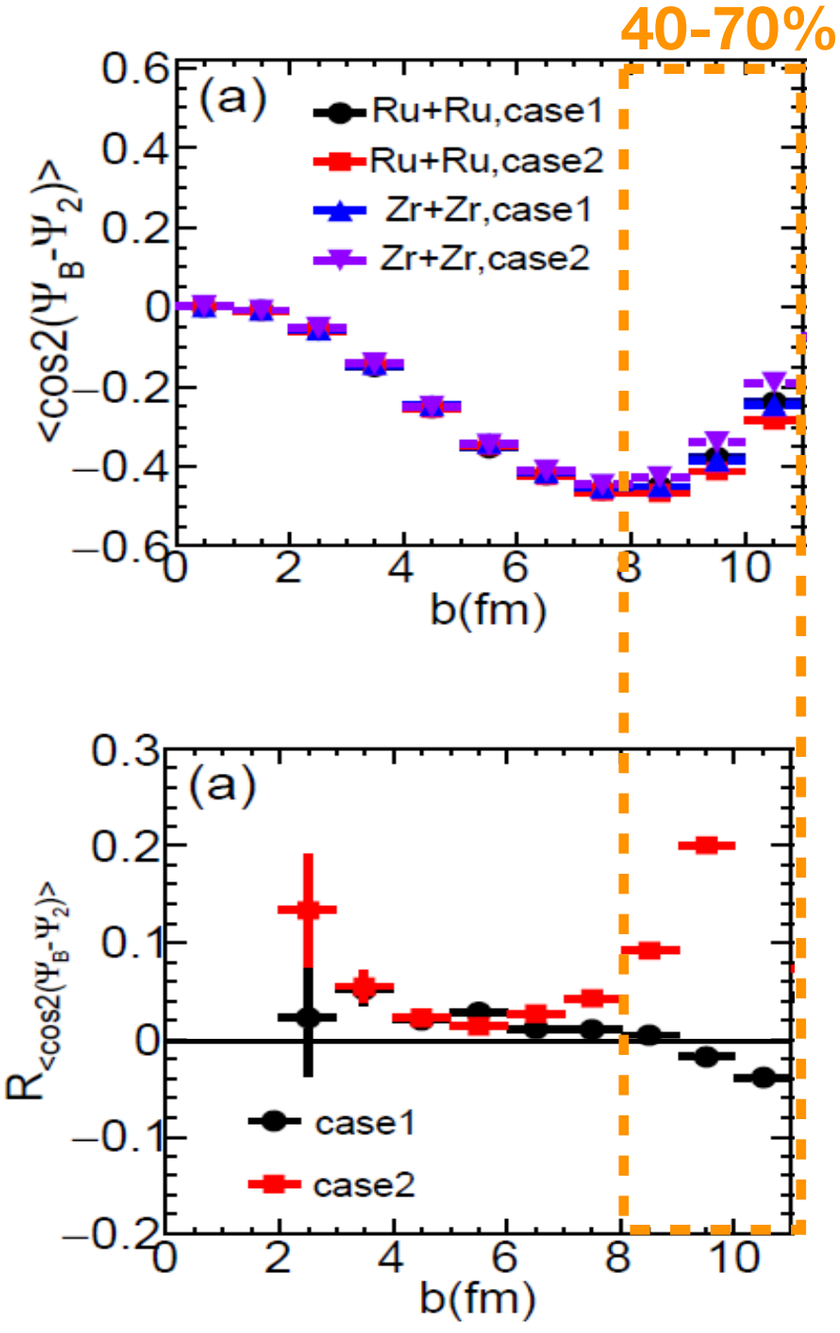




- |B|_{Ru} > |B|_{Zr}
- For case 1, RR is about 4% - 6%.
- For case 2, RR is about 4% - 12%.
- Deformation info. causes difference in |B|

$$R_Q = \frac{2(Q^{Ru} - Q^{Zr})}{Q^{Ru} + Q^{Zr}}$$

$\cos2(\Psi_B - \Psi_2)$



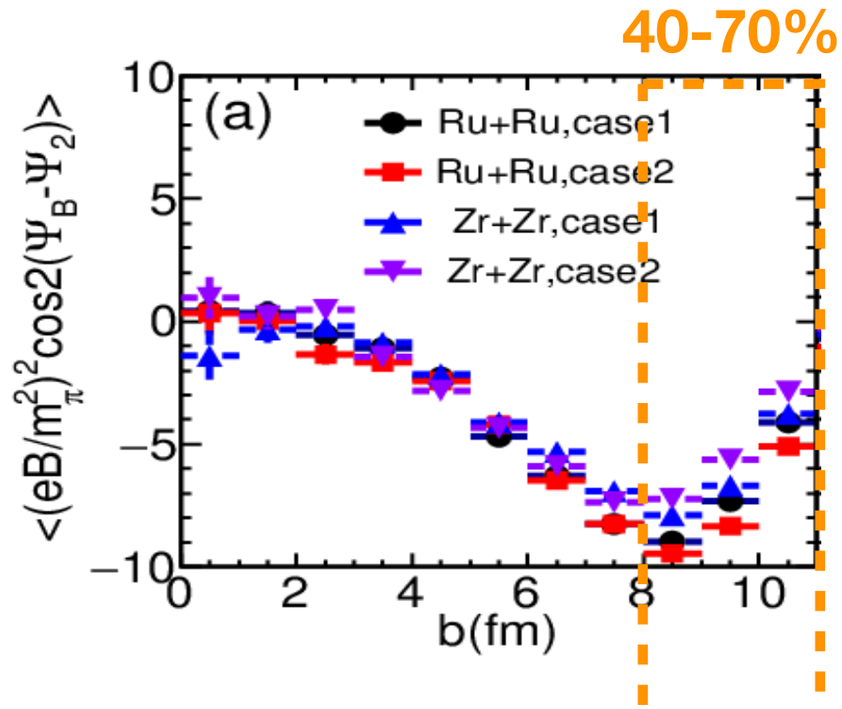
- The maximum of $\cos2(\Psi_B - \Psi_2)$ is about -0.5.
- In central and mid-central collisions, $\cos2(\Psi_B - \Psi_2)$ are similar in the four cases but different in peripheral collisions.

- **In mid-central collisions, RR are similar for case 1 and 2.**
- **In peripheral collisions, RR are different.**

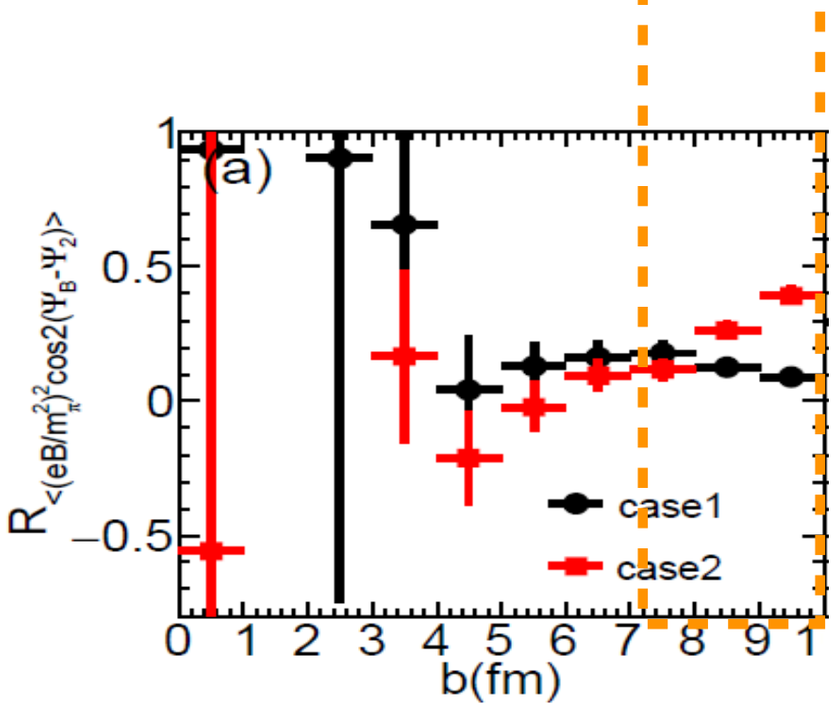
$$R_Q = \frac{2(Q^{Ru} - Q^{Zr})}{Q^{Ru} + Q^{Zr}}$$

A bad news for looking for CME!

$B^2 cos2(\Psi_B - \Psi_2)$



- The maximum of $B^2 cos2(\Psi_B - \Psi_2)$ is about -10.
- In central and mid-central collisions, $B^2 cos2(\Psi_B - \Psi_2)$ are similar in the four cases but different in peripheral collisions.

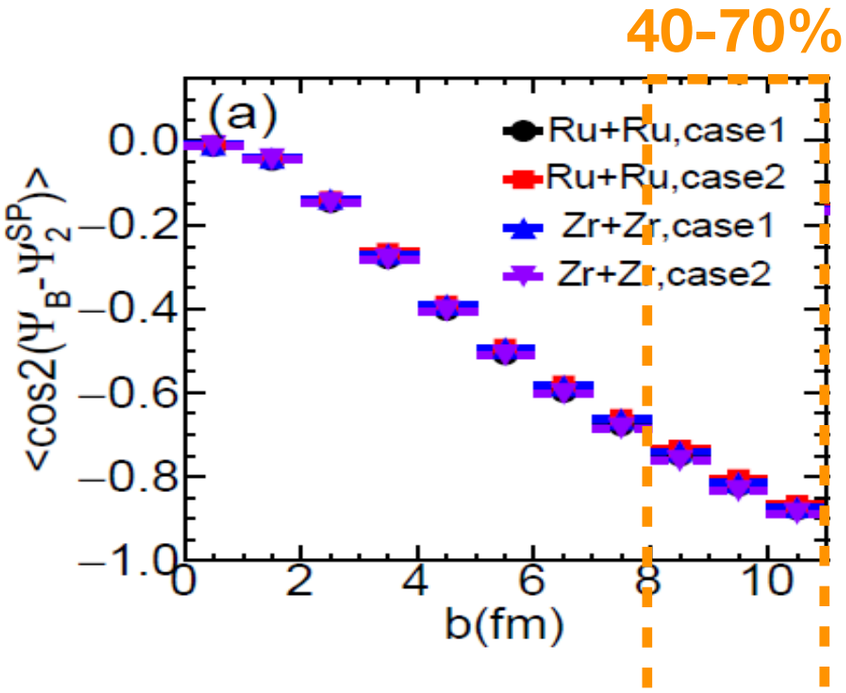


- RR of $B^2 cos2(\Psi_B - \Psi_2)$ are similar to RR of $cos2(\Psi_B - \Psi_2)$.

contaminated by deformation

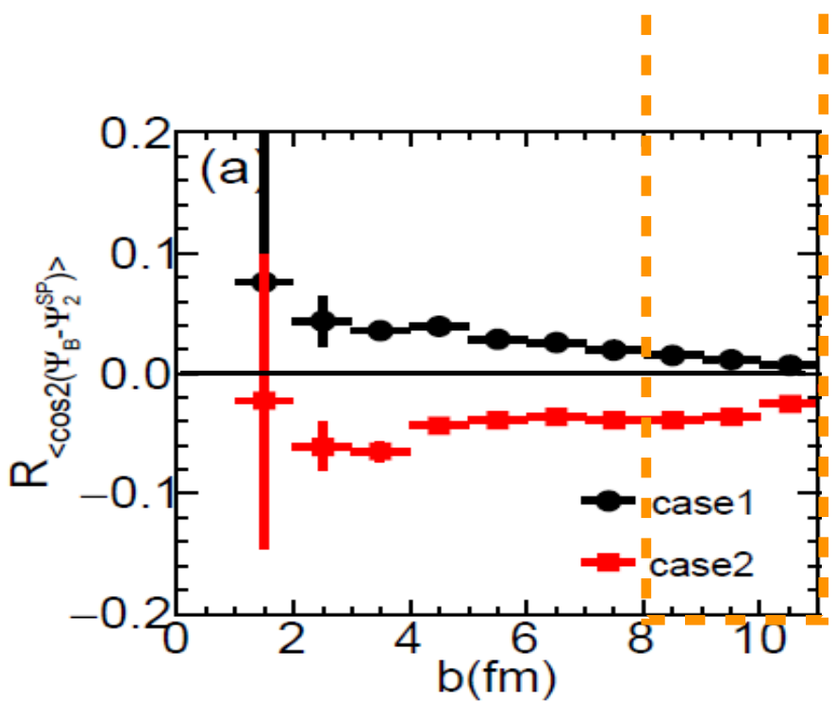
$$R_Q = \frac{2(Q^{Ru} - Q^{Zr})}{Q^{Ru} + Q^{Zr}}$$

$\cos2(\Psi_B - \Psi_2^{SP})$



- $\cos2(\Psi_B - \Psi_2^{SP})$ are around two times larger than $\cos2(\Psi_B - \Psi_2)$.
- In peripheral collisions, this correlation $\cos2(\Psi_B - \Psi_2^{SP}) = -0.9$.

Ψ_2^{SP} has stronger correlation with Ψ_B than Ψ_2.

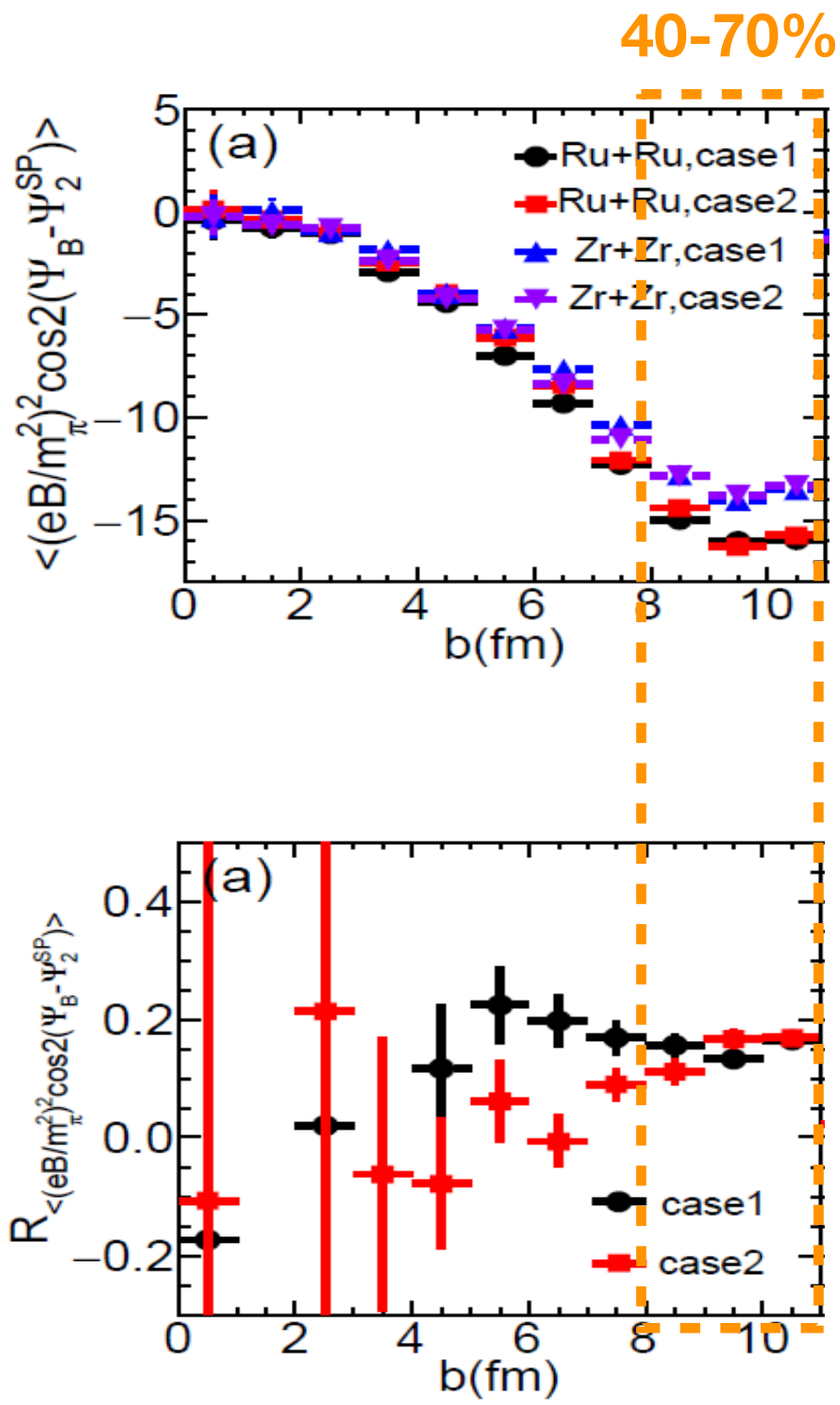


- RR of $\cos2(\Psi_B - \Psi_2^{SP})$ for the two cases are close to zero in peripheral collisions.

A good news for looking for CME!

$$R_Q = \frac{2(Q^{Ru} - Q^{Zr})}{Q^{Ru} + Q^{Zr}}$$

$B^2 \cos 2(\Psi_B - \Psi_2^{SP})$



CME-induced Δγ:

- $B^2 \cos 2(\Psi_B - \Psi_2^{SP}) > B^2 \cos 2(\Psi_B - \Psi_2)$.

~15 **~10**

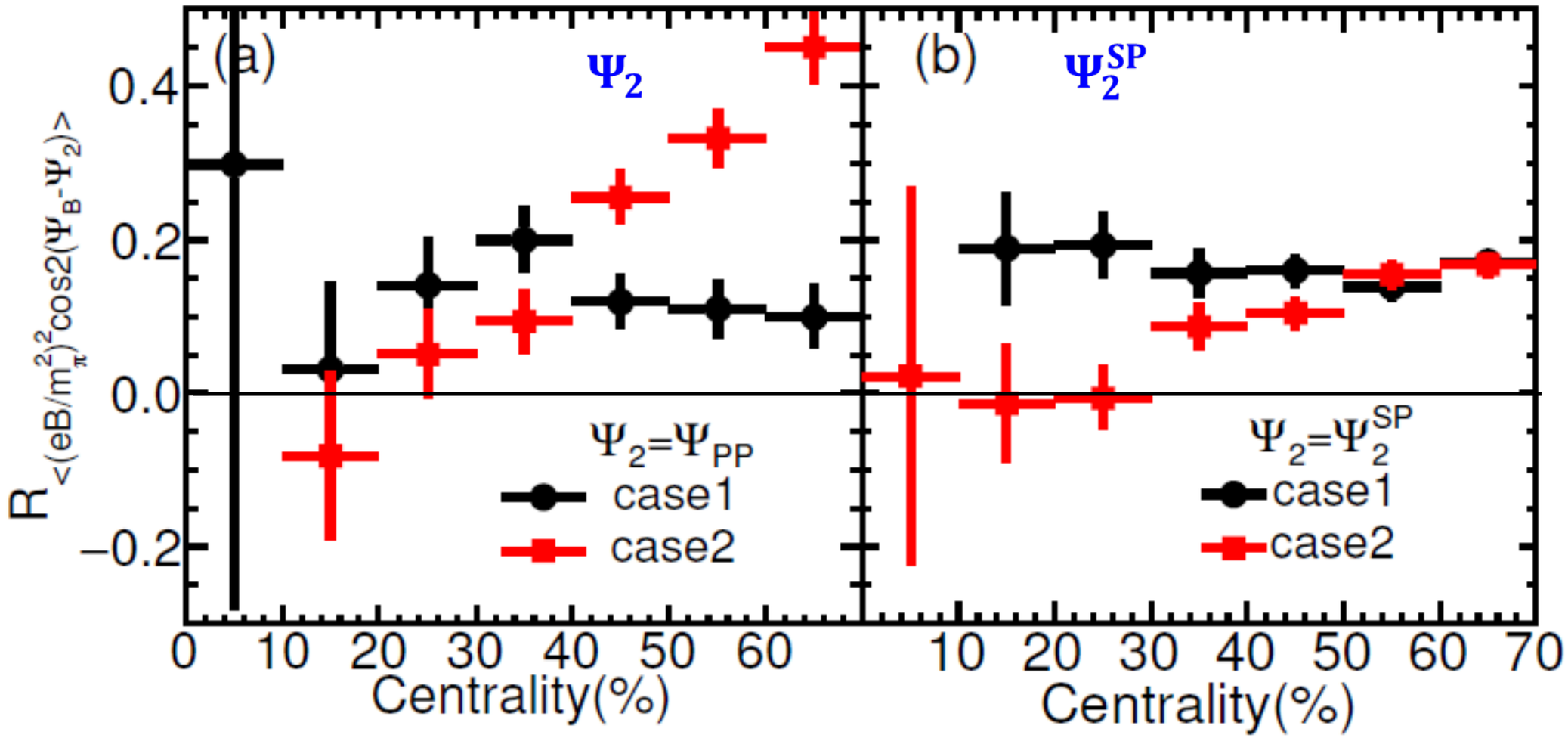
- **For case 1, RR is near 15%.**
- **For case 2, RR increases from 0 to 15% from central to peripheral events.**

Less contaminated by deformation in peripheral events

$$R_Q = \frac{2(Q^{Ru} - Q^{Zr})}{Q^{Ru} + Q^{Zr}}$$

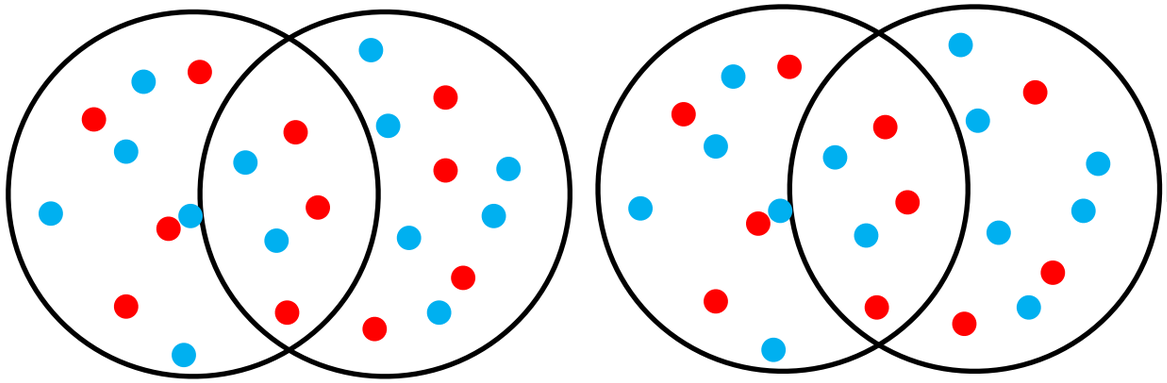
CME signal difference from Ψ_2 VS Ψ_2^{SP}

X. L. Zhao, G. L. Ma, Y. G. Ma, PRC 99, 034903 (2019)



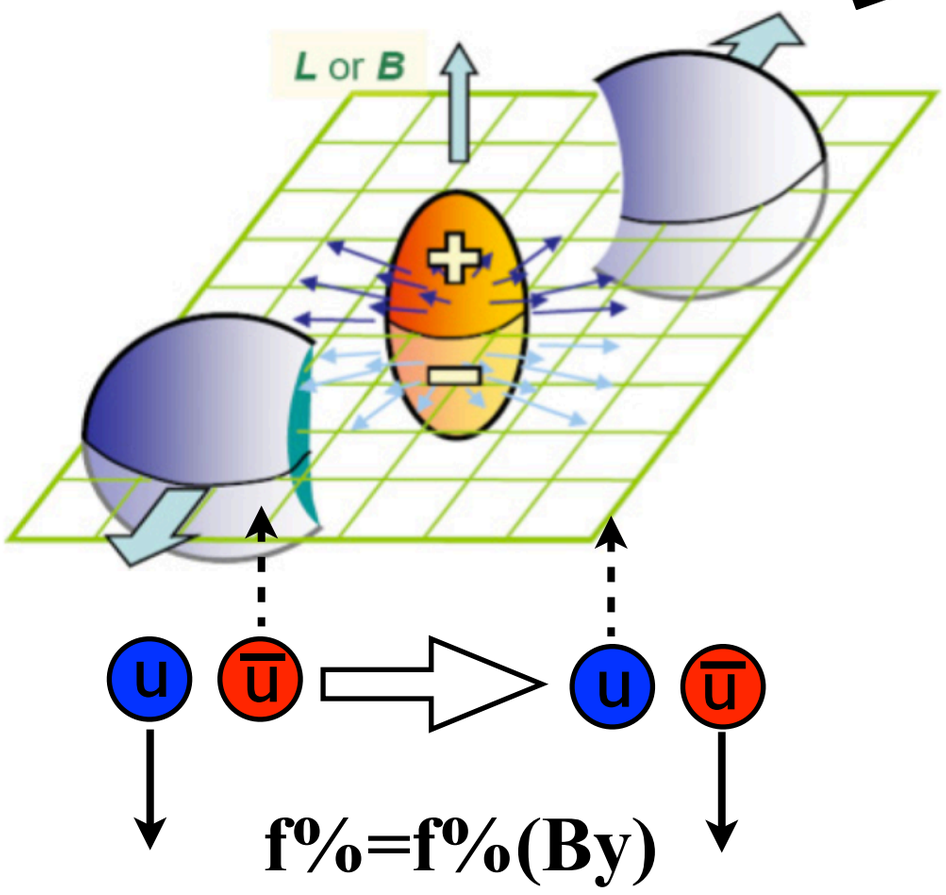
- For case 1, RR of $B^2 cos2(\Psi_B - \Psi_2)$ and $B^2 cos2(\Psi_B - \Psi_2^{SP})$ are similar.
- For case 2, RR of Ψ_2 is larger than RR of Ψ_2^{SP}.
- Ψ_2^{SP} is expected to reflect much cleaner information about the CME signal.

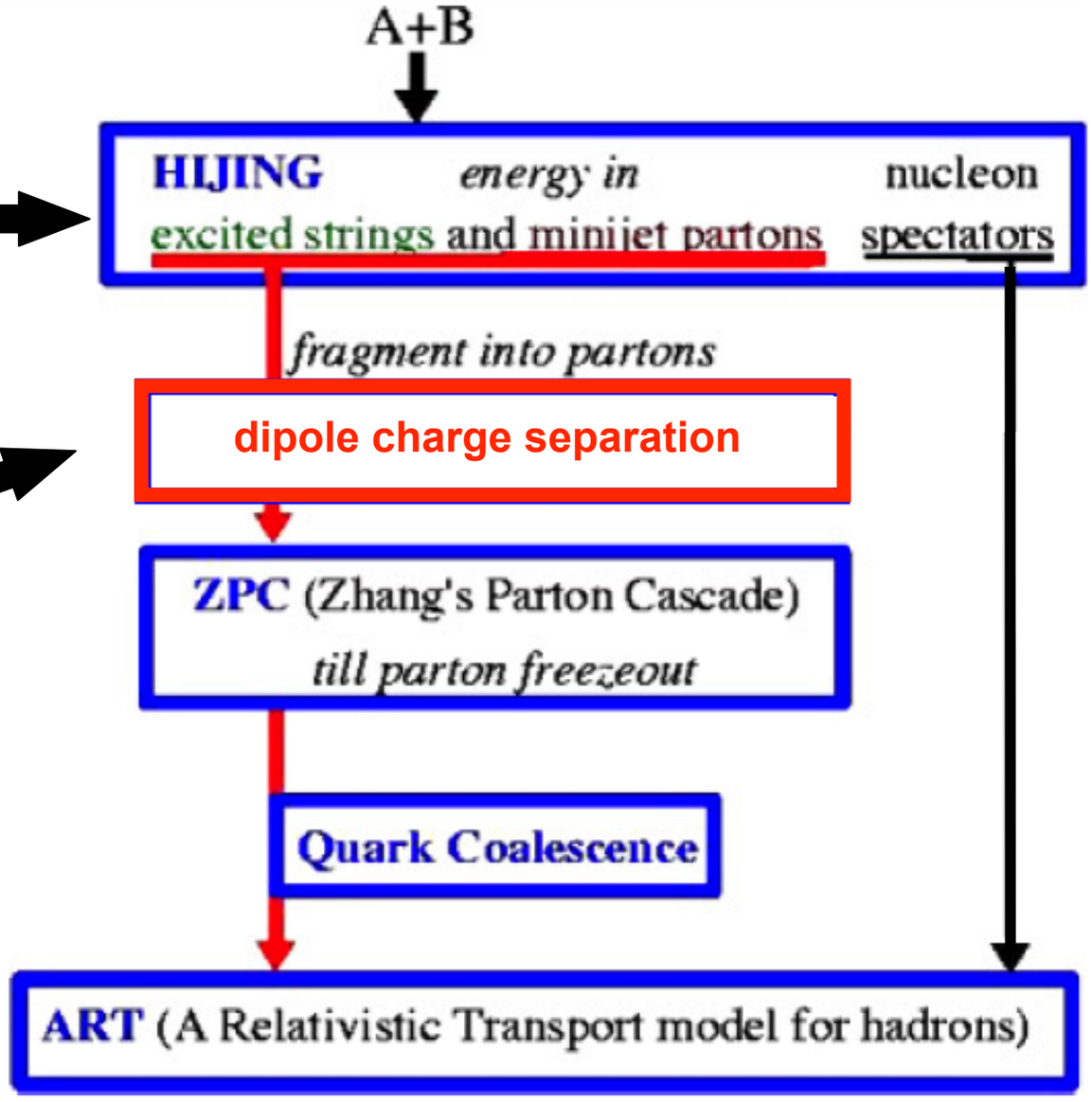
Simulating isobaric collisions with AMPT+CME



$^{96}_{44}Ru + ^{96}_{44}Ru$

$^{96}_{40}Zr + ^{96}_{40}Zr$



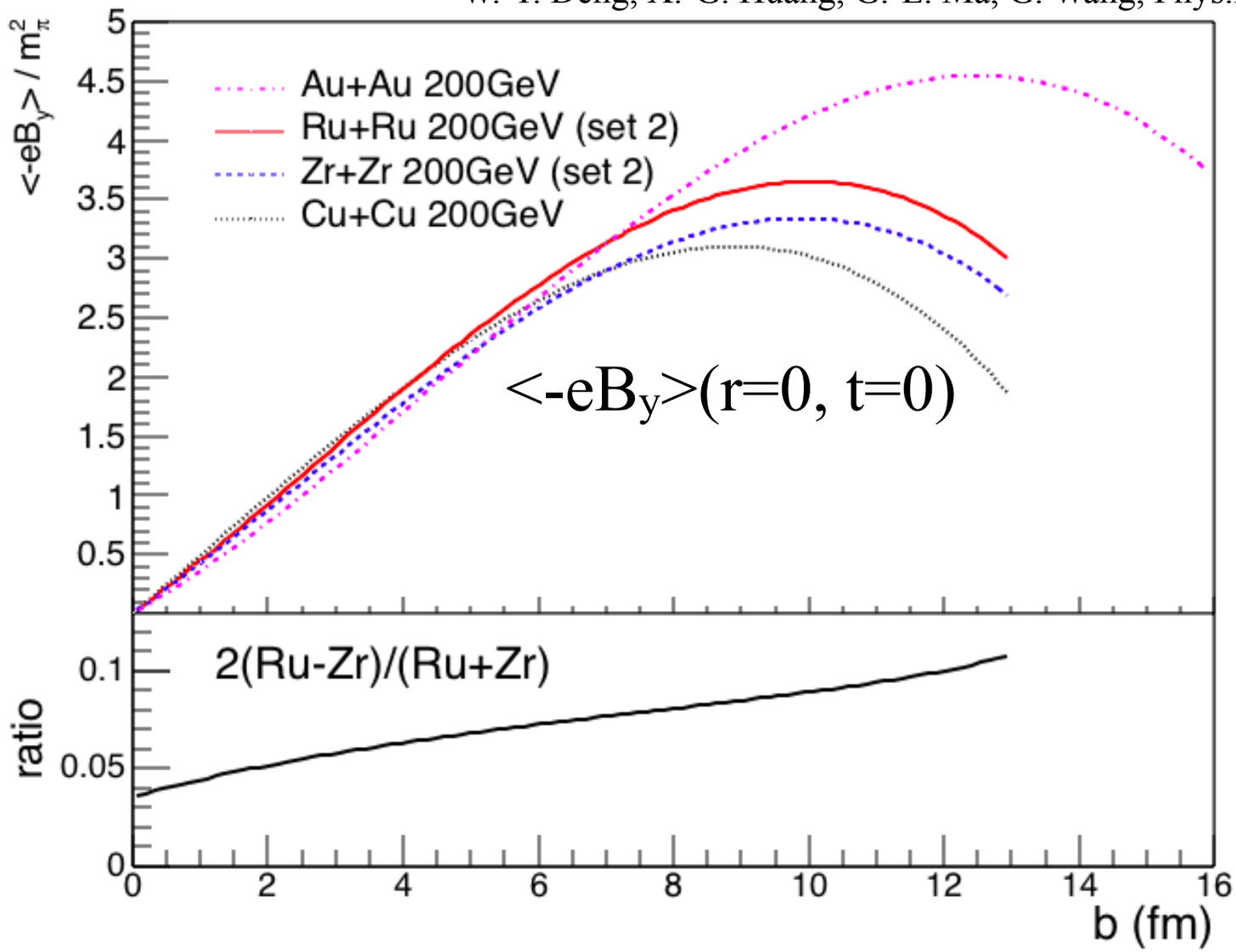


Two key facts:

- Initialization of isobars
- By-dependent CME percentage

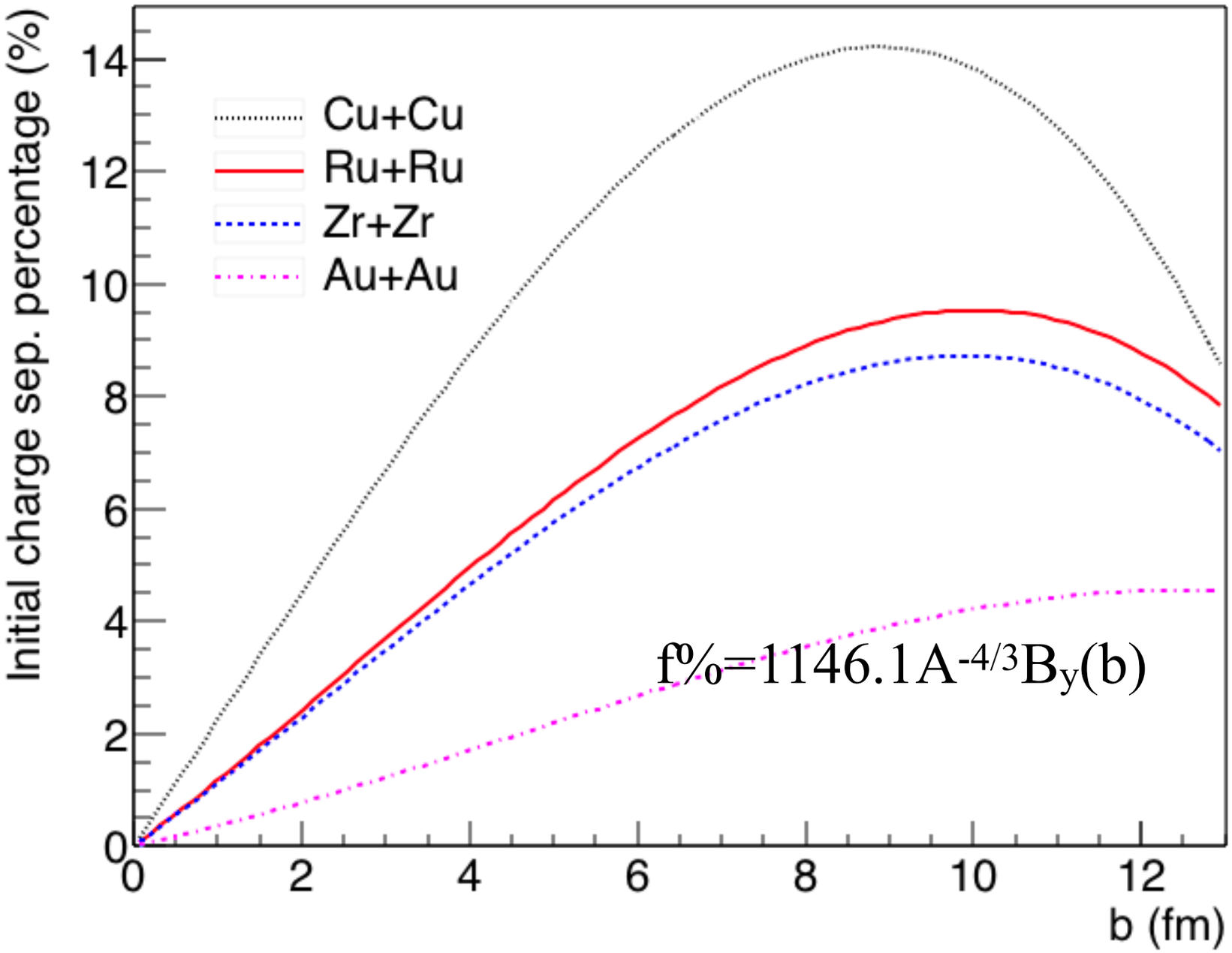
b-dependent B field

W.-T. Deng, X.-G. Huang, G.-L. Ma, G. Wang, Phys.Rev. C97 (2018), 044901



- We use Lienard-Wiechert potential to calculate b-dependent <By> .
- $\langle B_y \rangle$(Ru+Ru) is larger than $\langle B_y \rangle$(Zr+Zr) by 10% at large b.

b-dependent initial charge sep. percent

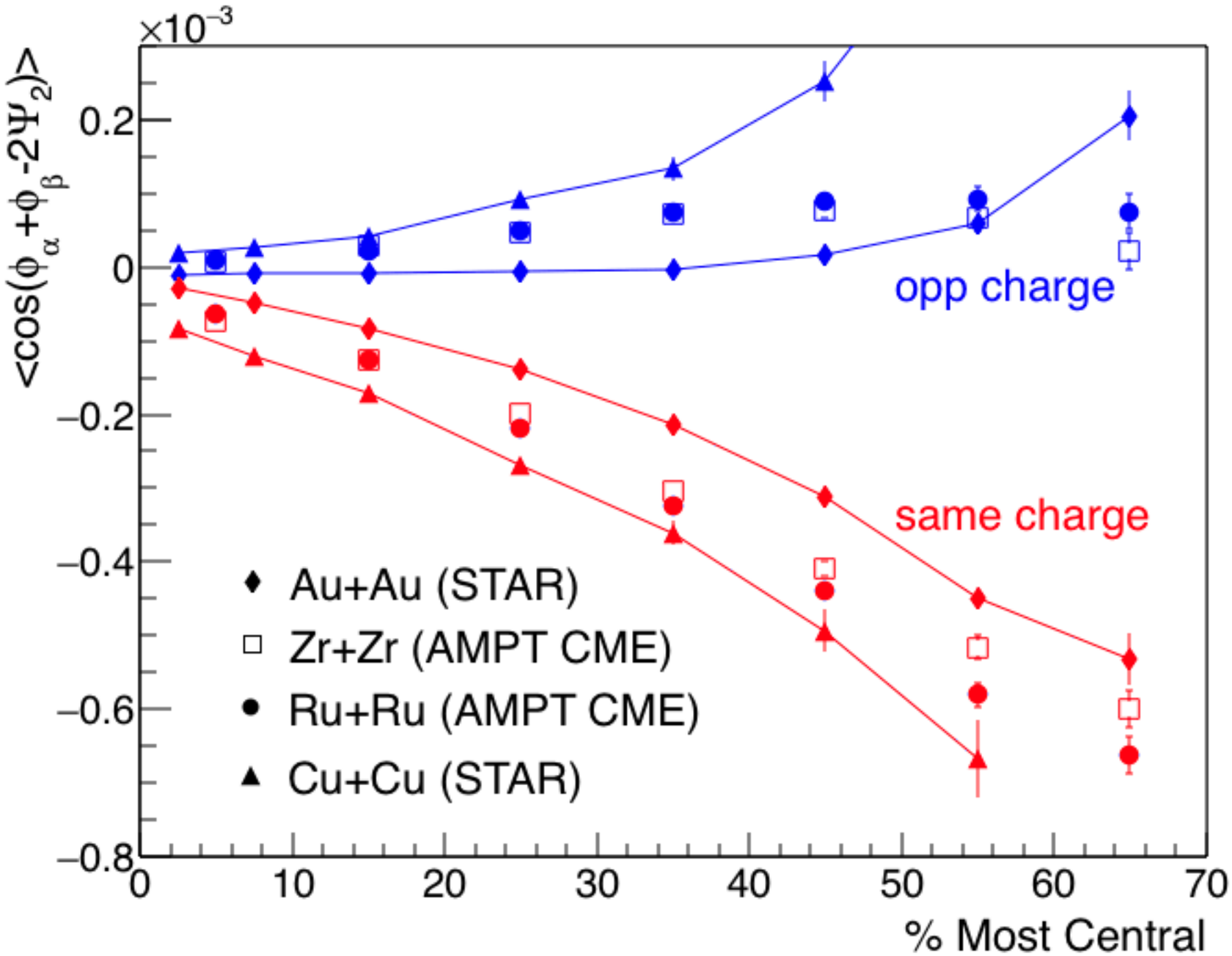


Centrality cuts for Ru+Ru and Zr+Zr

Centrality	b_{min} (fm)	b_{max} (fm)
0-10%	0	3.9
10-20%	3.9	5.5
20-30%	5.5	6.8
30-40%	6.8	7.8
40-50%	7.8	8.8
50-60%	8.8	9.6
60-70%	9.6	10.3

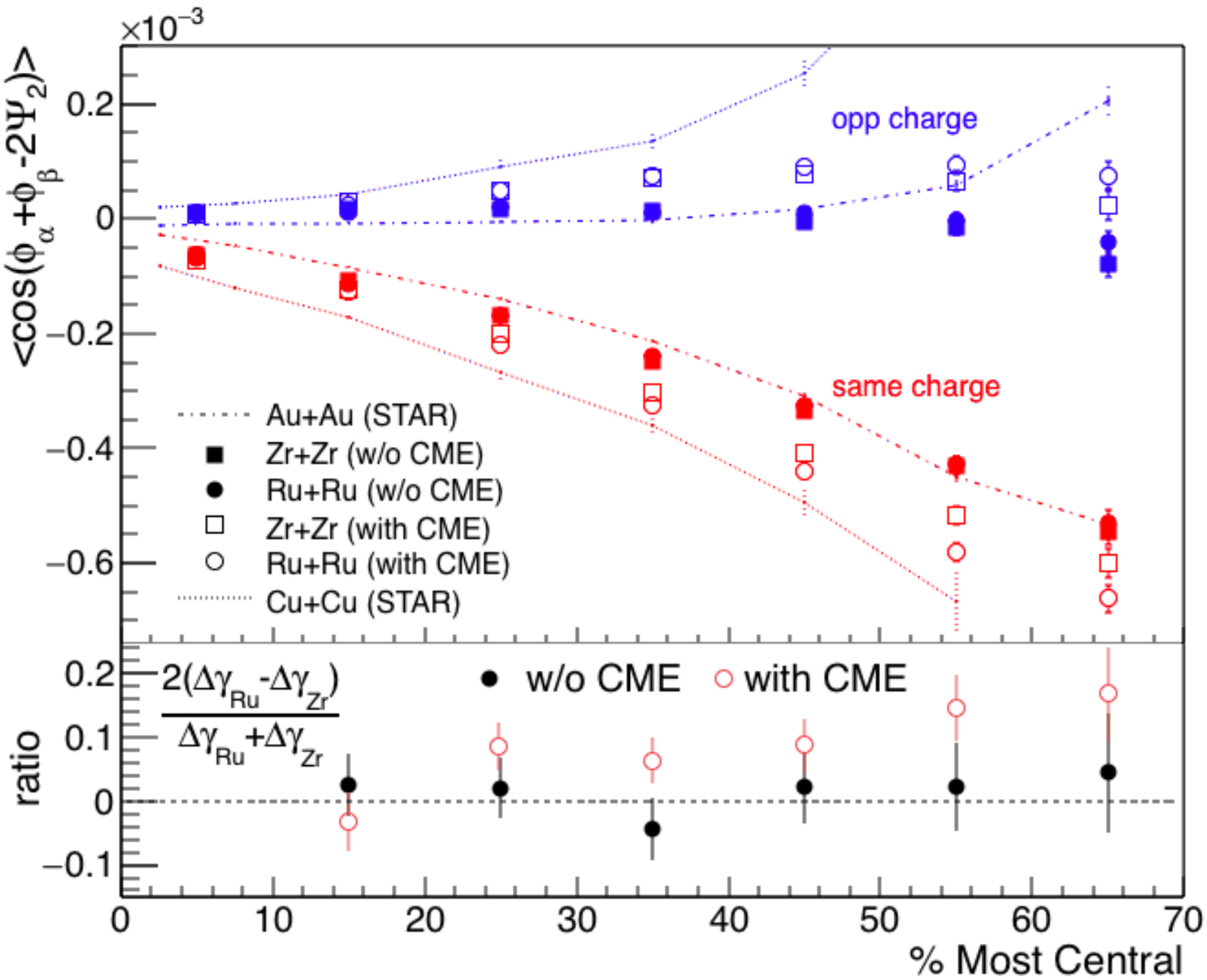
- We apply $f\%=1146.1A^{-4/3}B_y(b)$ to introduce the initial charge separation into Ru+Ru and Zr+Zr.

AMPT (CME) results on γ=<cos(ϕa+ϕβ-2ψ2)>



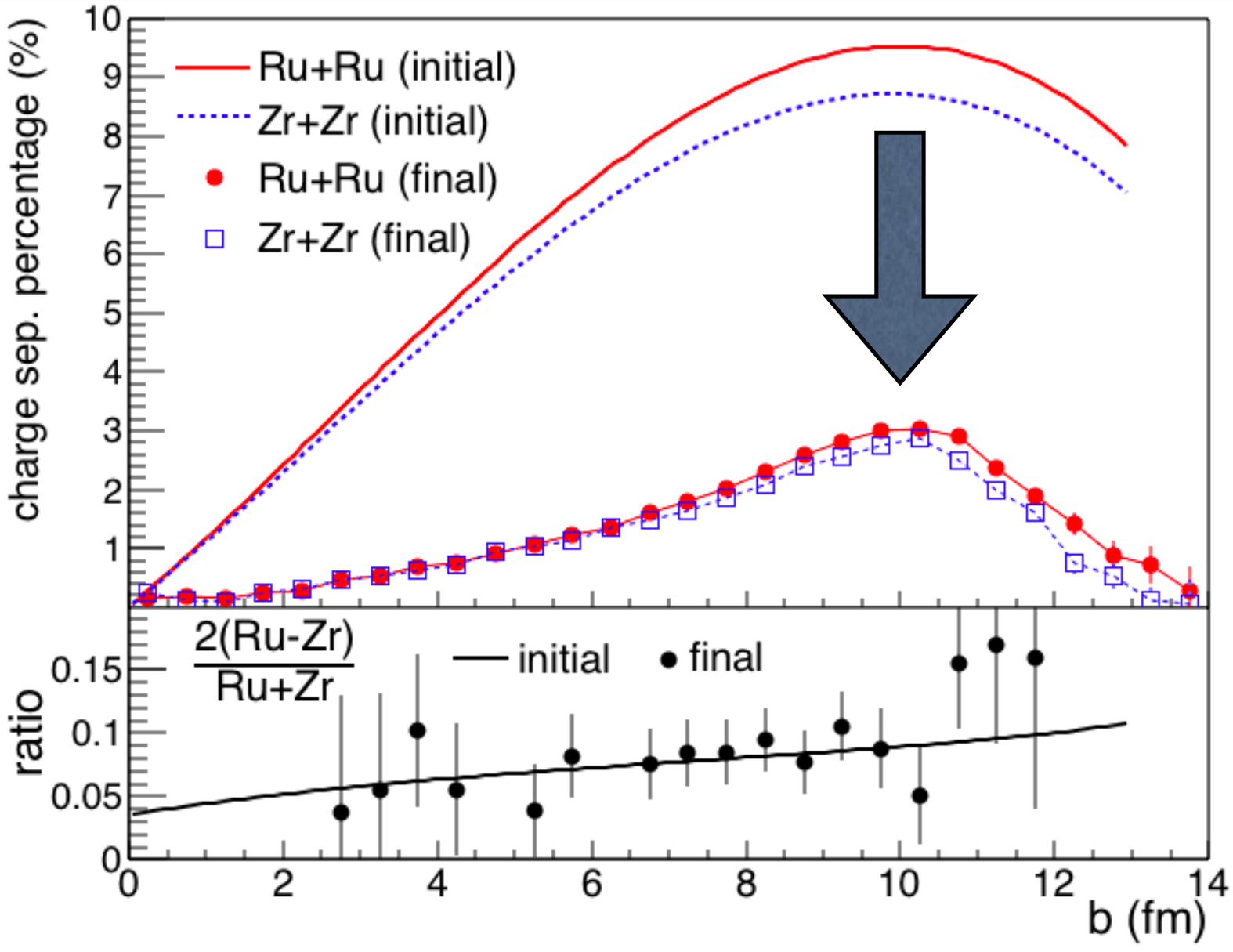
- We see a magnitude relation of | <cos(ϕa+ϕβ-2ψ2)> |, i.e., Au+Au < Zr+Zr < Ru+Ru < Cu+Cu.

CME effect in isobar collisions



- **If w/o CME(solid symbol),** the signals are almost same between Ru+Ru and Zr+Zr from the original AMPT model.
- **If with CME (open symbol),** the magnitudes of signals increase, the ratio between Ru+Ru and Zr+Zr appears ~10%.

FSI effect on CME signal difference



initial state

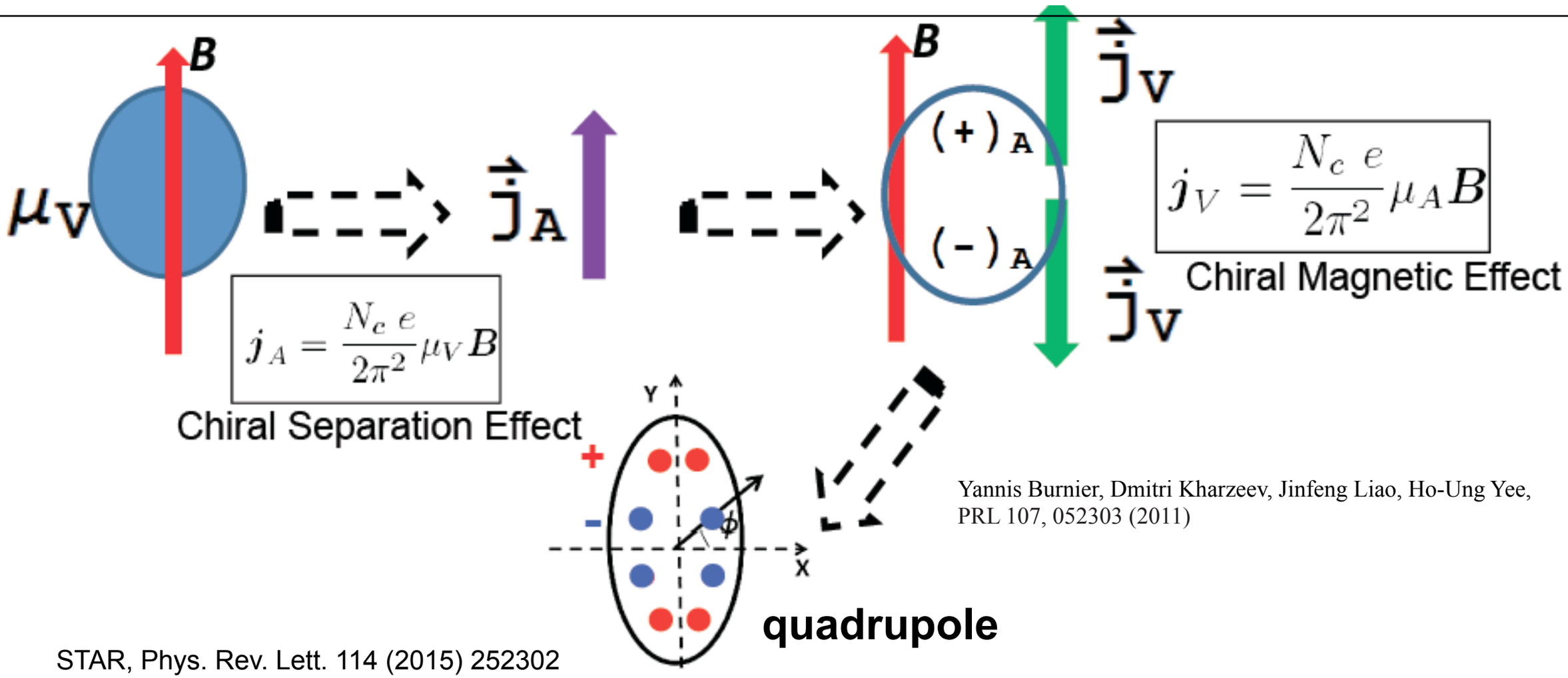
(parton cascade, hadronization, resonance decays)

final state

- Initial charge sep. percent. is reduced by final state interactions.
- Relative ratio of charge sep. percent. is kept, same as $\langle B_y \rangle$ ratio.

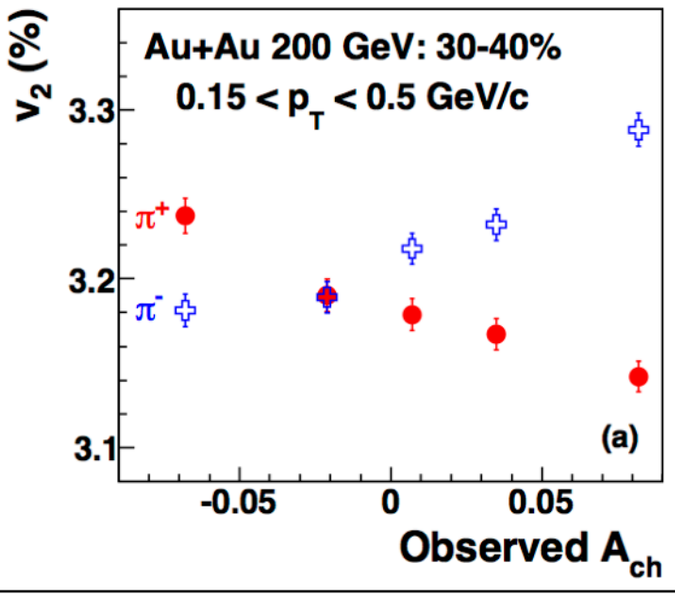
W.-T. Deng, X.-G. Huang, G.-L. Ma, G. Wang, Phys.Rev. C97 (2018), 044901

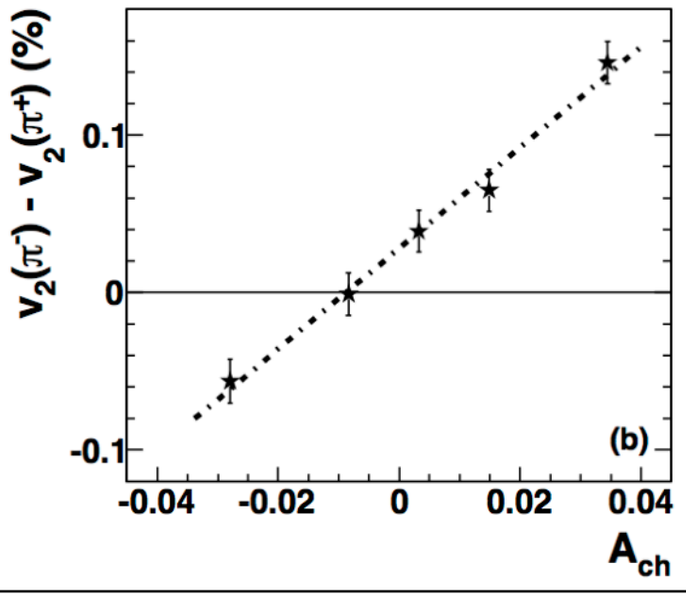
Chiral Magnetic Wave (CMW)



Yannis Burnier, Dmitri Kharzeev, Jinfeng Liao, Ho-Ung Yee, PRL 107, 052303 (2011)

STAR, Phys. Rev. Lett. 114 (2015) 252302



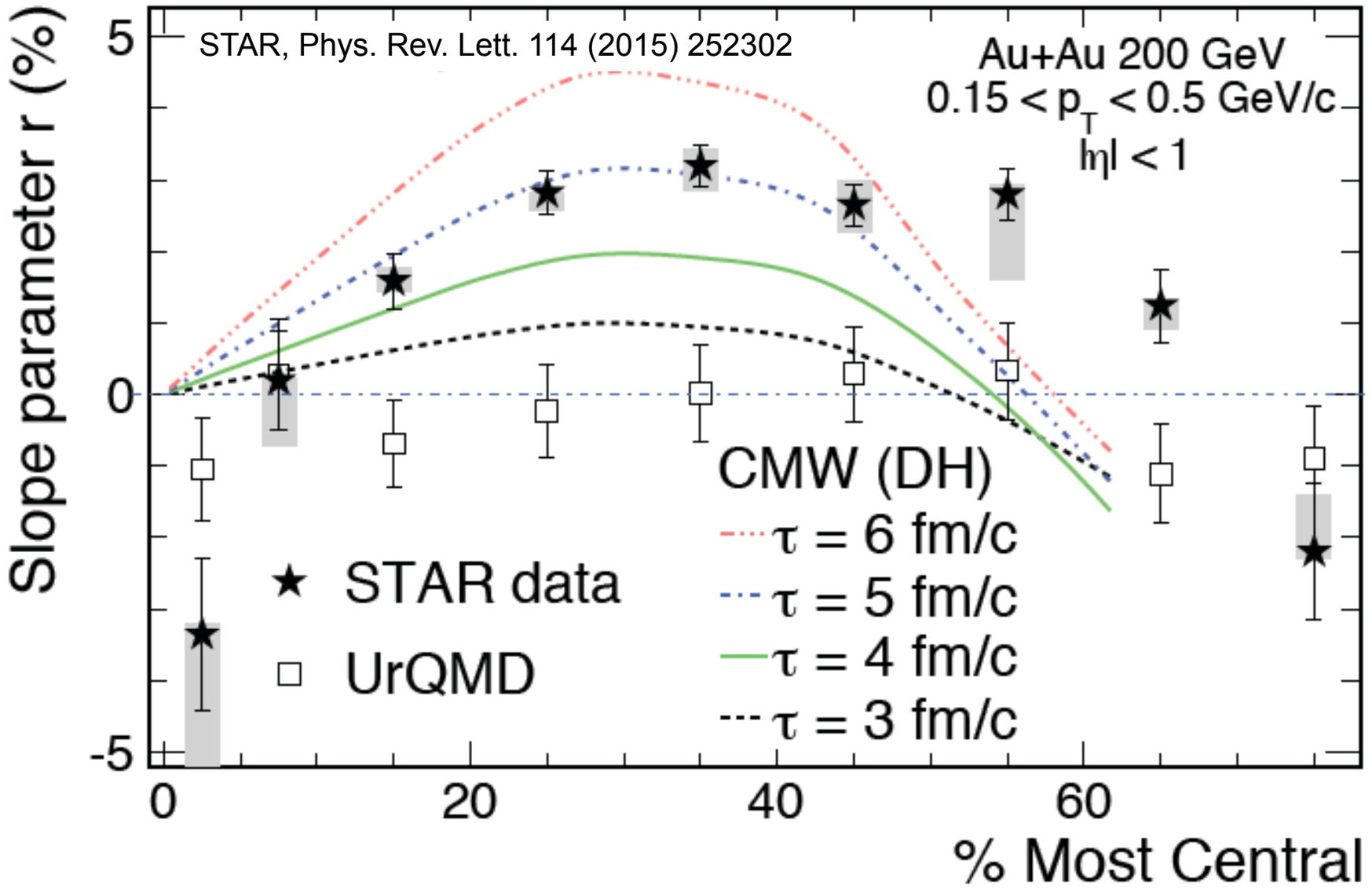


$$v_2^{\pm} = v_2 \mp \frac{r}{2} A_{ch}$$

$$v_2^{-} - v_2^{+} = r A_{ch}$$

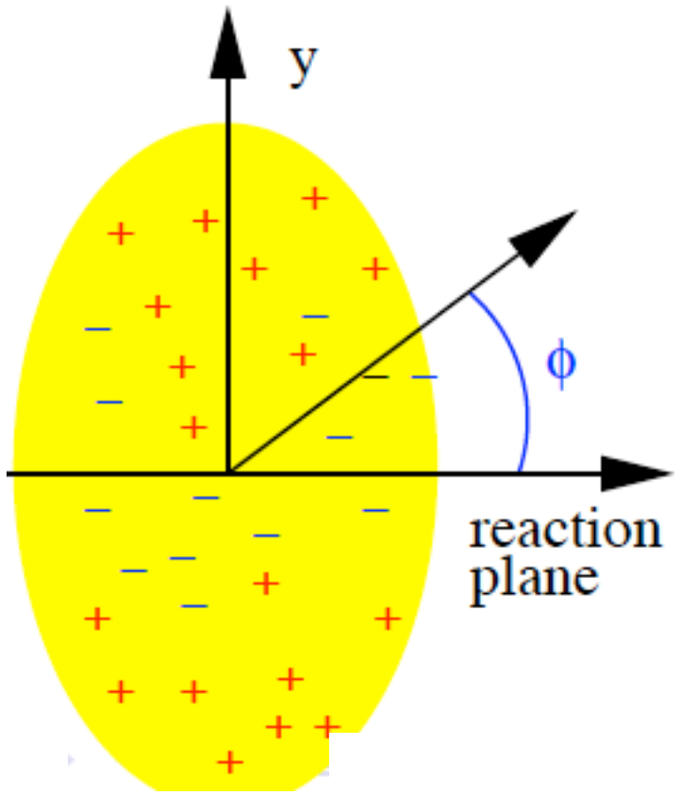
- CMW (CME+CSE) signal: v2 splitting of positive and negative charged particles (slope para. *r*)

CMW probe: slope r of pions' v2 charge asymmetry

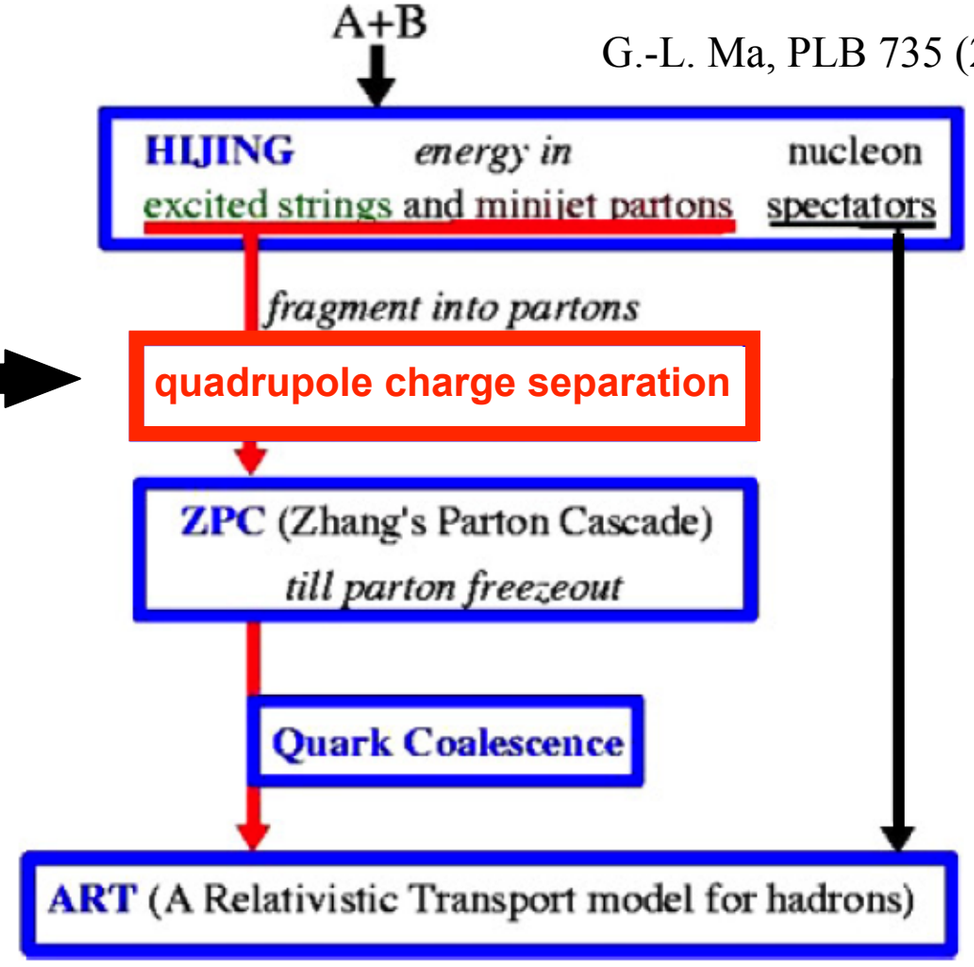


- RHIC-STAR data can be described by the CMW expectation with different CMW duration times.
- UrQMD can not reproduce the slopes r.

AMPT model with CMW-type charge separation



Type II



G.-L. Ma, PLB 735 (2014) 383

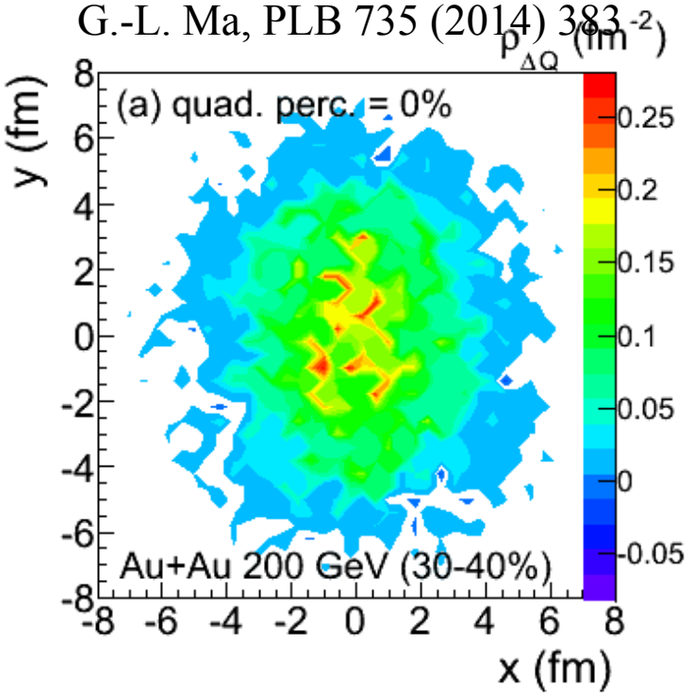
- **To include initial quadrupole charge separation (CMW) into the AMPT model:**

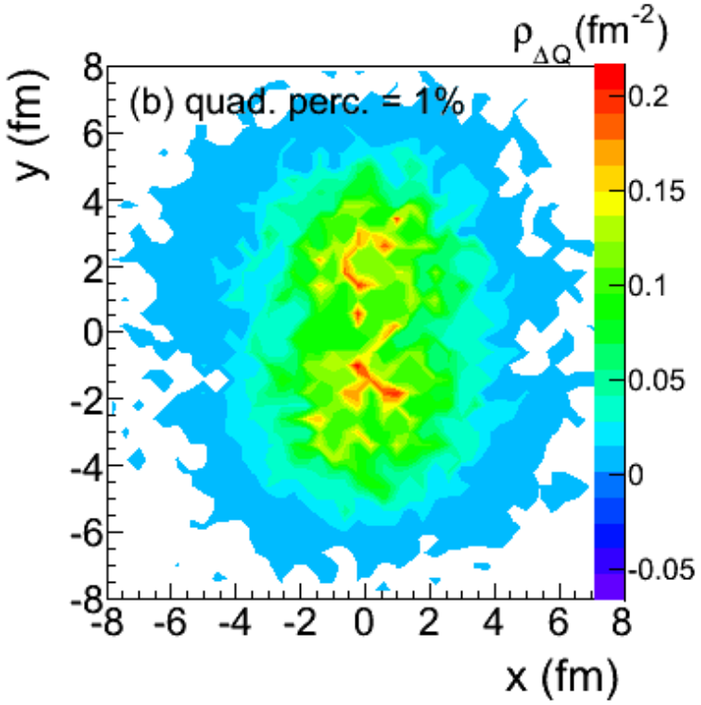
We switch the positions (x,y,z) of a percentage of the small-|y| u quarks with those of large-|y| u-bar quarks, and likewise for d-bar and d quarks for Ach>-0.01 events(Type II); A contrary manner for A_{ch}<-0.01 events(Type I)

- **The goal is to learn about transport properties of CMW** through how final charge asymmetry of pion v_2 depends on the quadrupole fraction after $\vec{B}$ and $\vec{E}$ vanish.

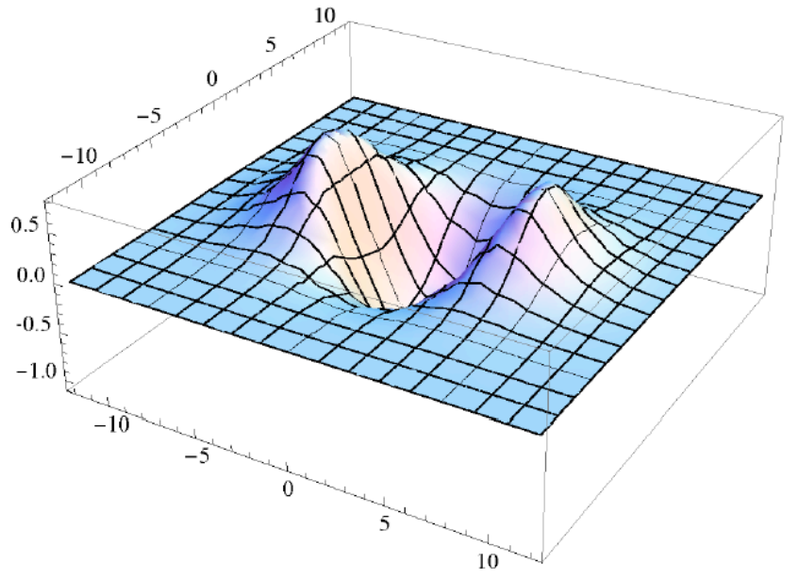
Initial charge quadrupole distribution

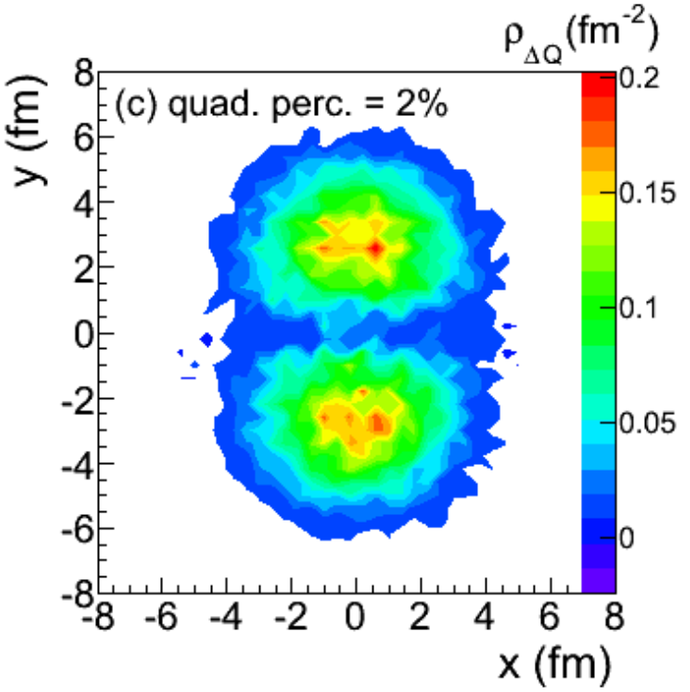
G.-L. Ma, PLB 735 (2014) 383

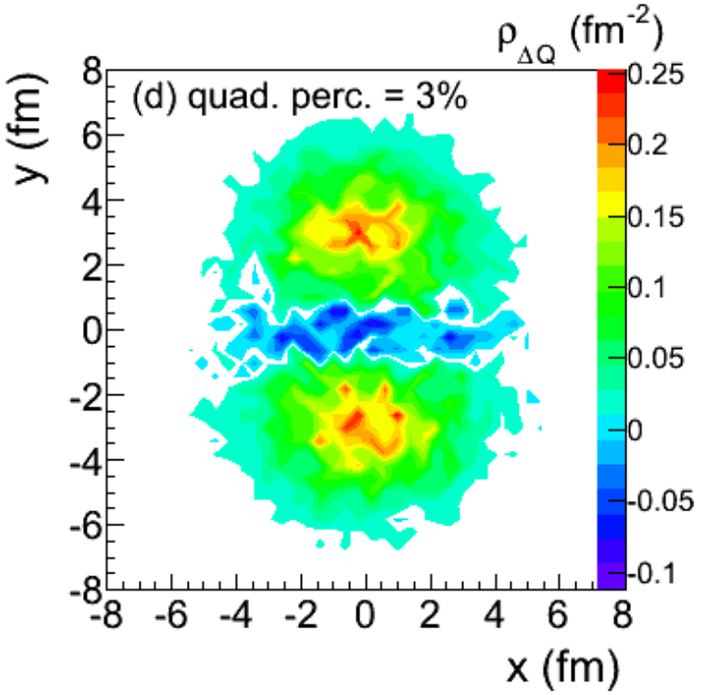


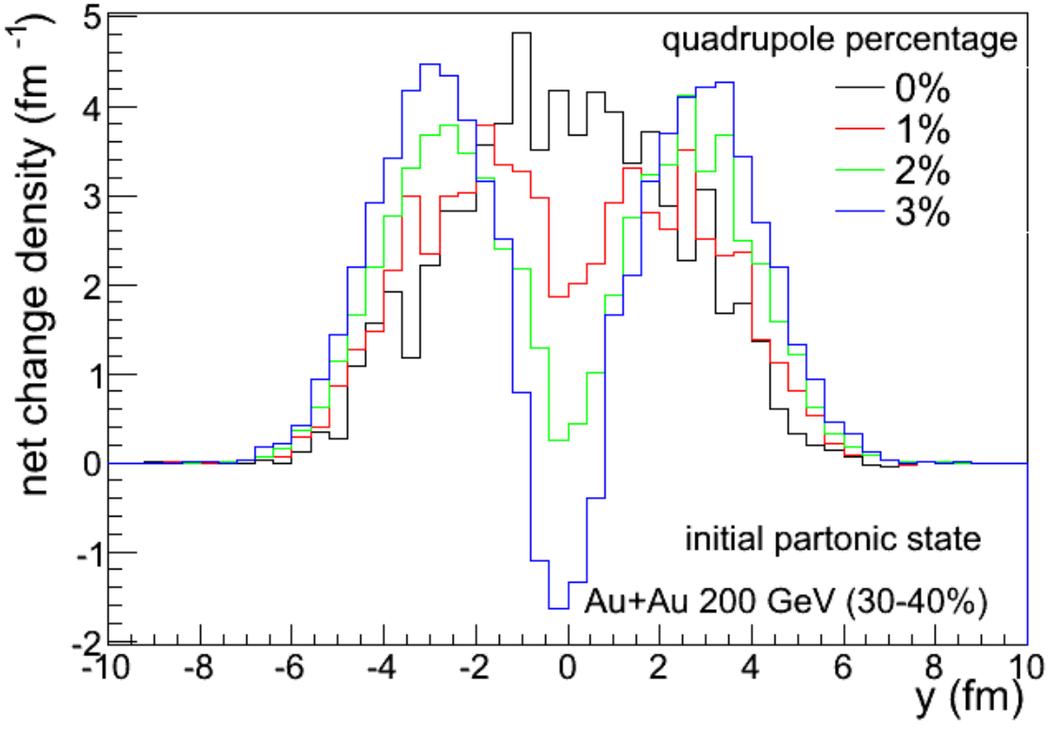


Yannis Burnier, Dmitri Kharzeev, Jinfeng Liao, Ho-Ung Yee,PRL 107, 052303 (2011)





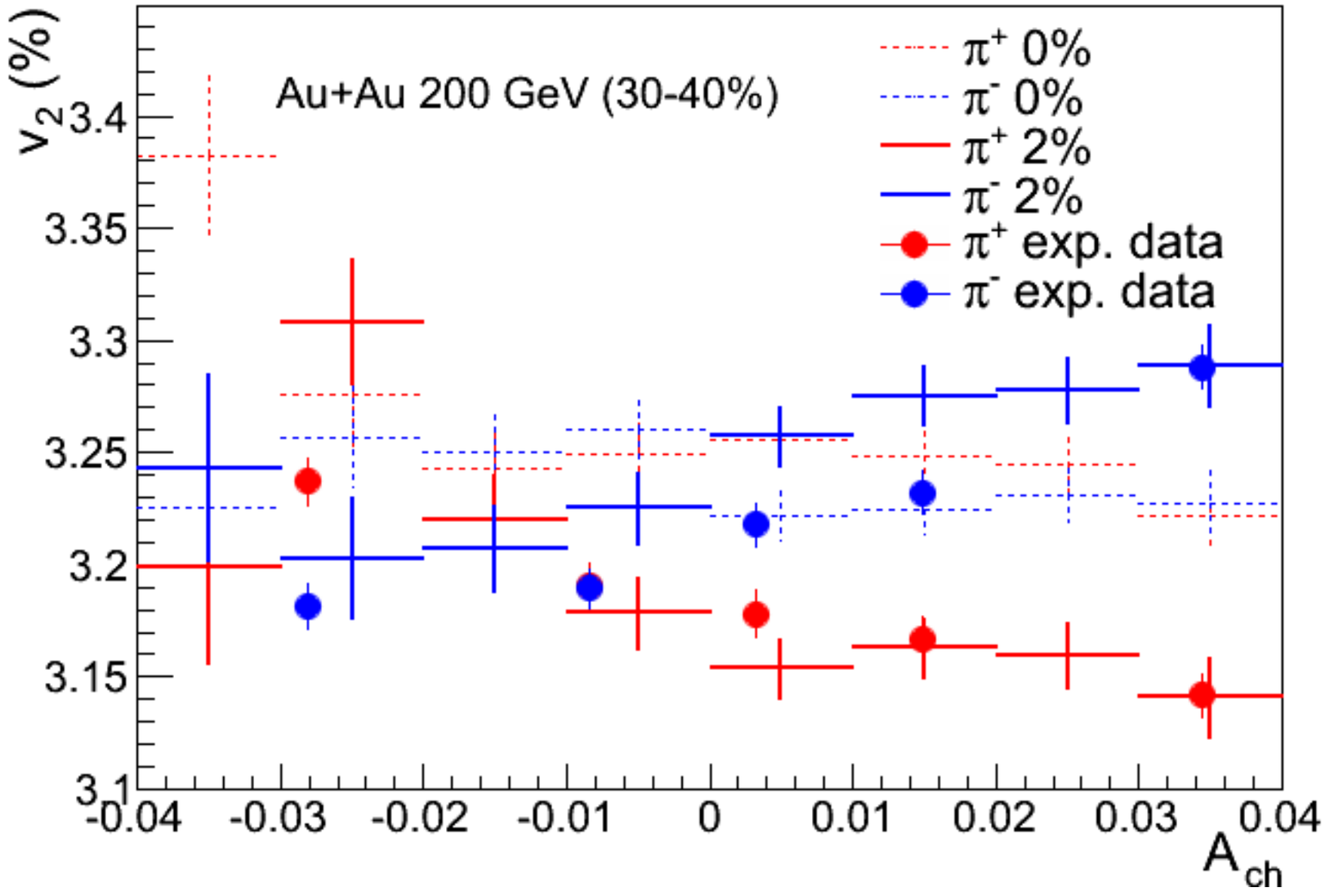




- Initial partonic net charge distribution (~2 fm/c) changes with quadrupole percentage.

Charge asymmetry of pion v2

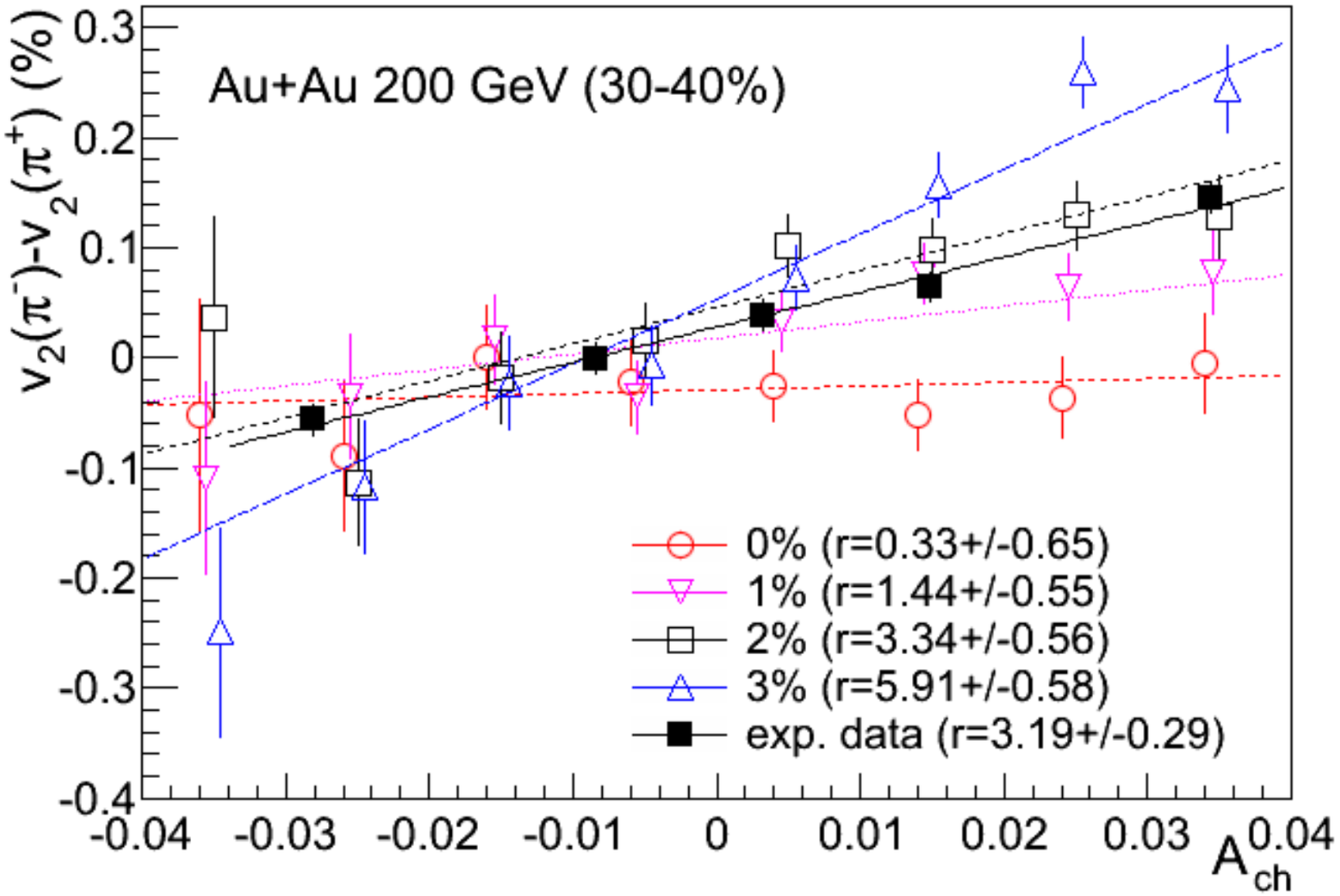
G.-L. Ma, PLB 735 (2014) 383



- **The Ach dependences of pions' v_2 appear with a non-zero initial charge quadrupole.**

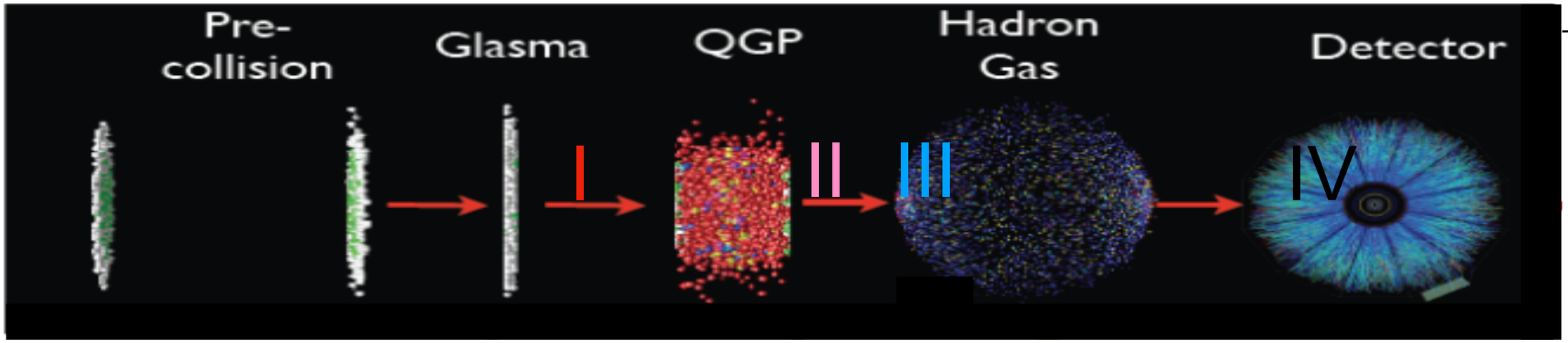
Δv_2 vs A_{ch}

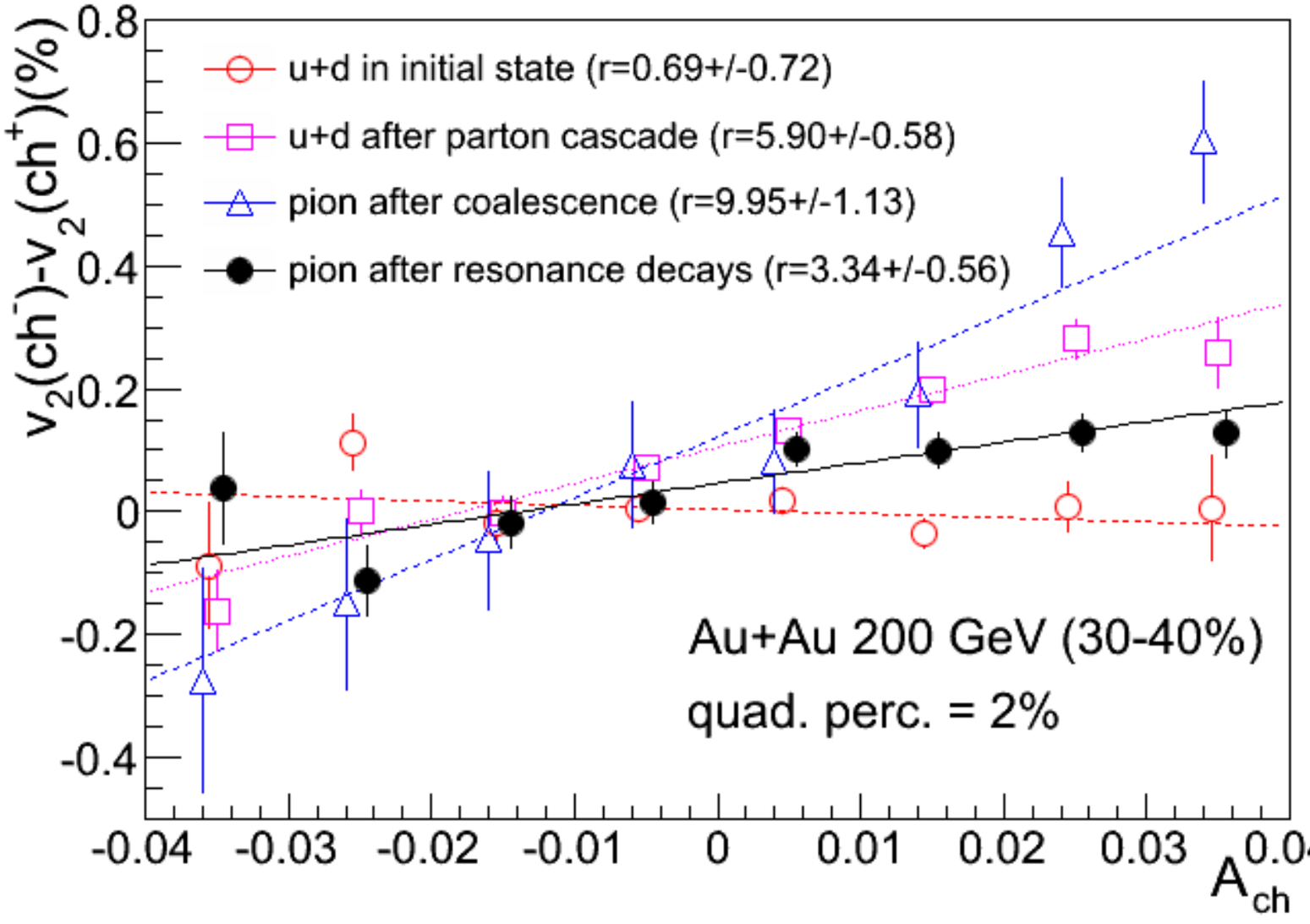
G.-L. Ma, PLB 735 (2014) 383



- The slope of Δv_2 is larger with larger initial quadrupole percentage.

Stage evolution for the slope r



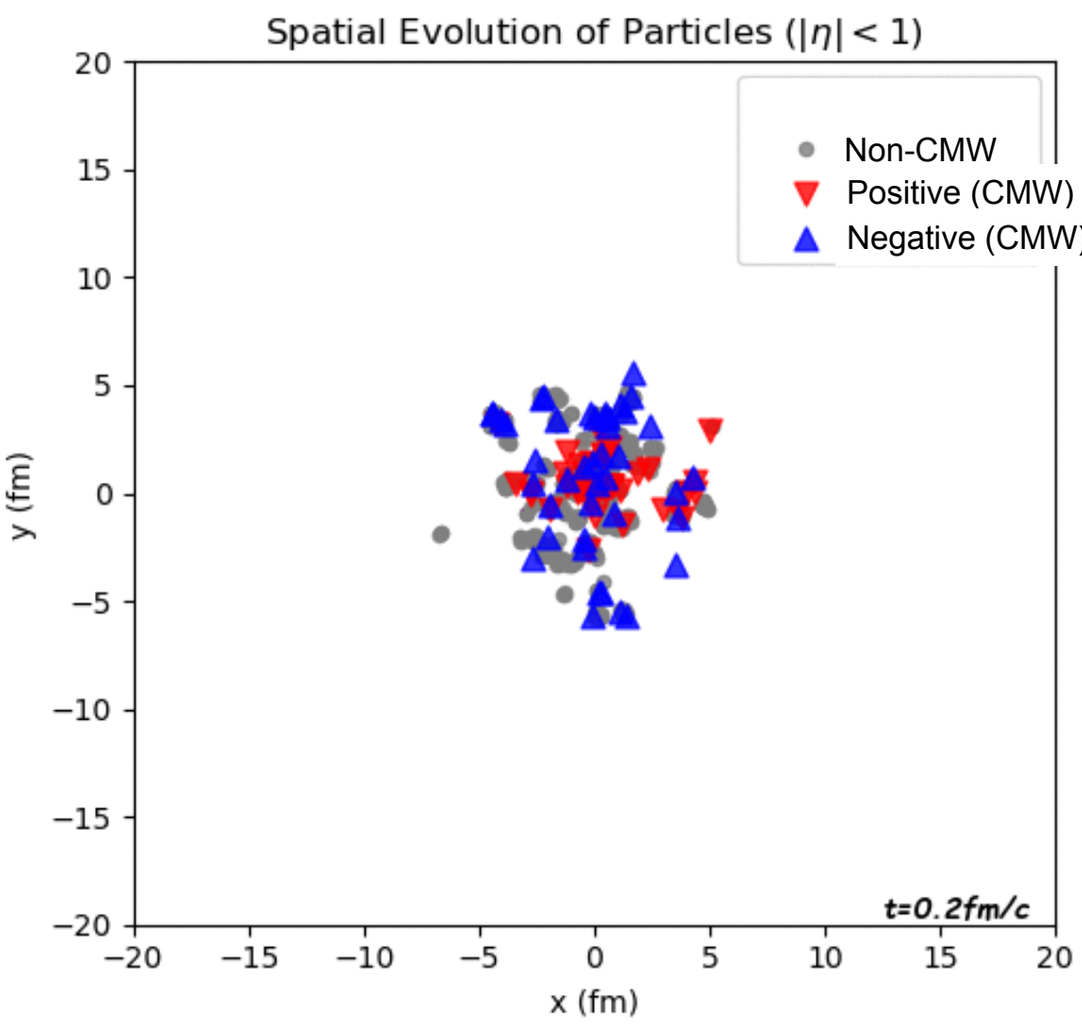


- The slope is zero initially.
- The slope r appears after parton cascade.
- The slope r increases after coalescence.
- The slope r is largely weaken due to resonance decays.

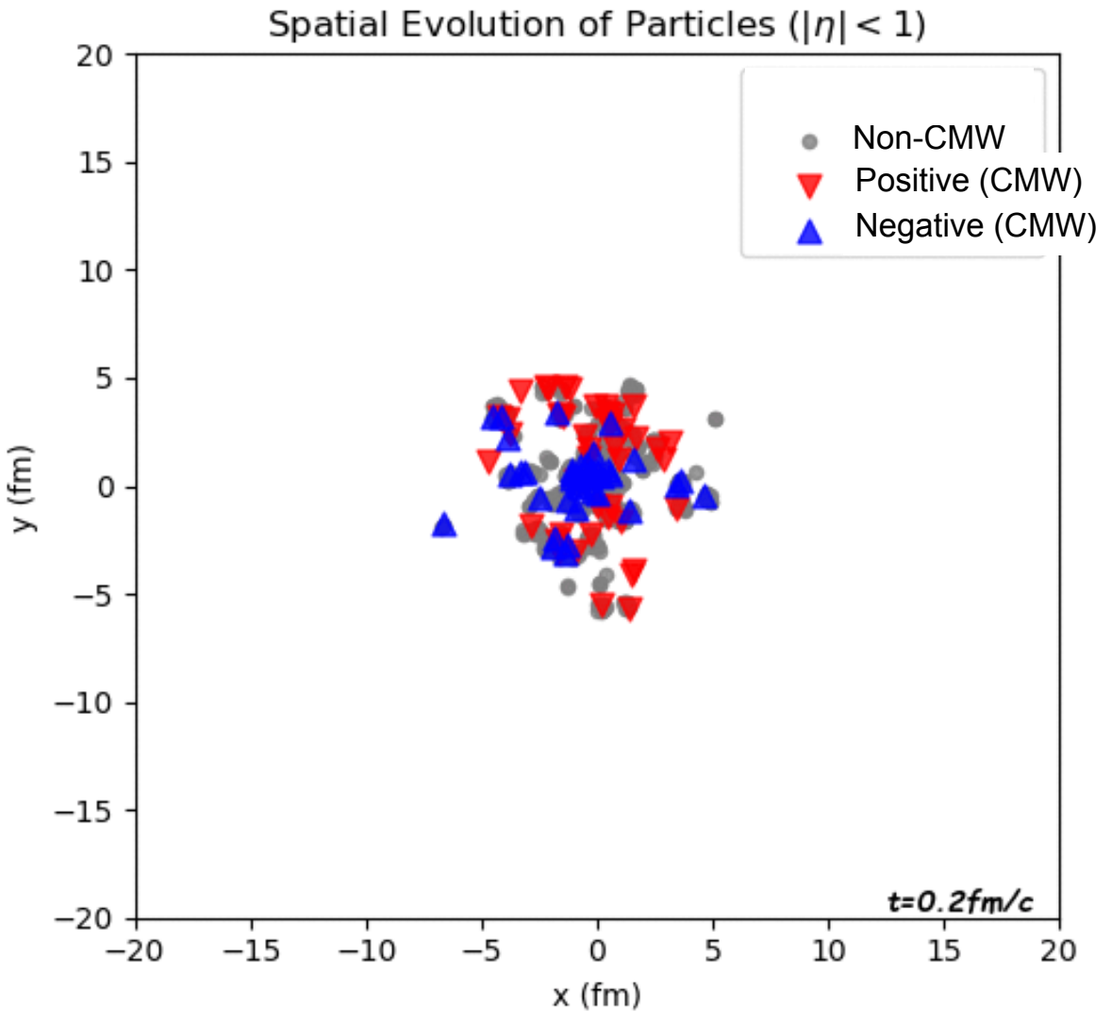
Parton cascade effect on the CMW signal

Au+Au 200 GeV (b=8fm), AMPT+CMW(10%)

Type I (Ach<-0.01)

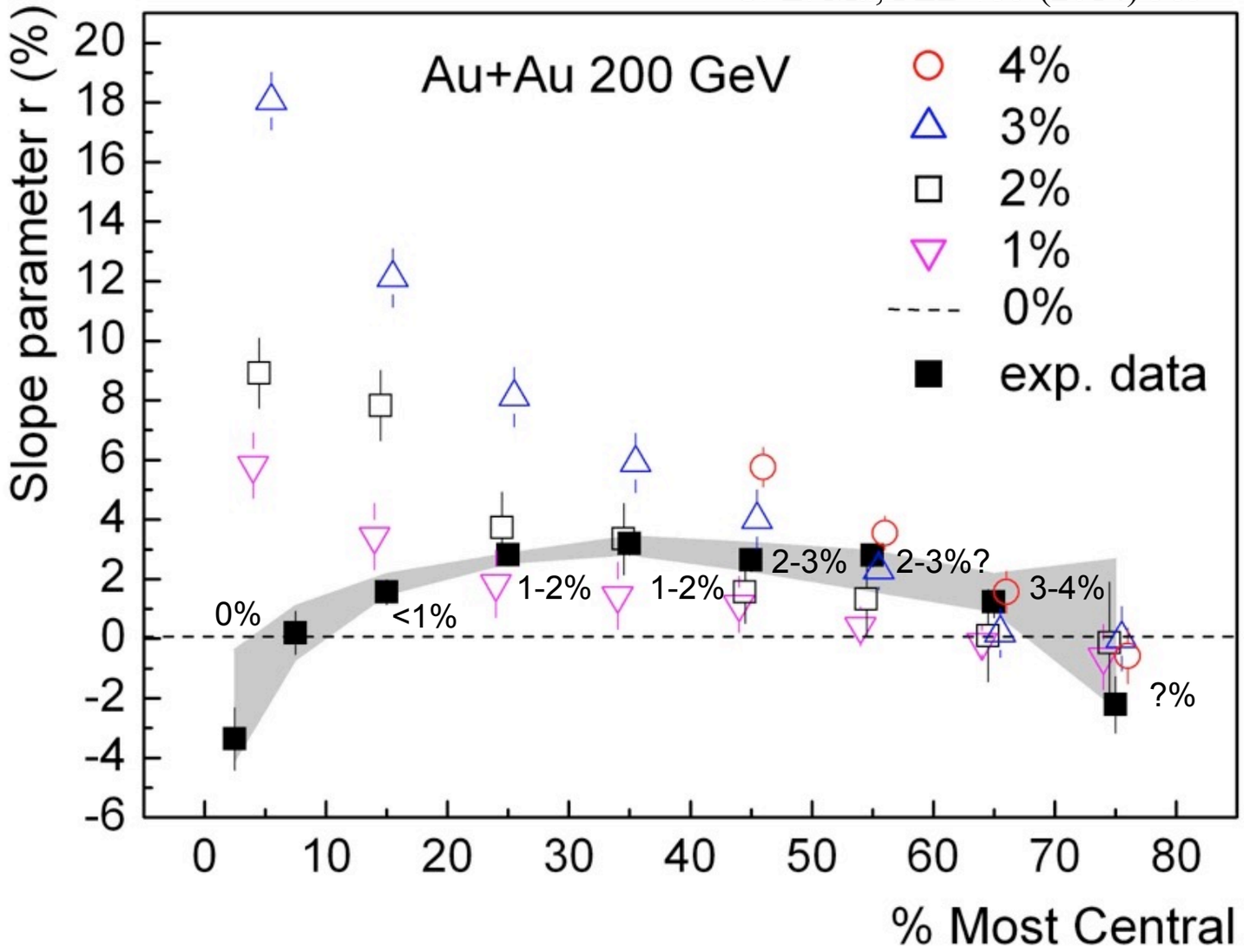


Type II (Ach>-0.01)



A constraint on CMW

G.-L. Ma, PLB 735 (2014) 383



centrality bin	0-10%	10-20%	20-30%	30-40%	40-50%	50-60%	60-70%	70-80%
initial quad. perc.	0%	<1%	1-2%	1-2%	2-3%	2-3%	3-4%	?%

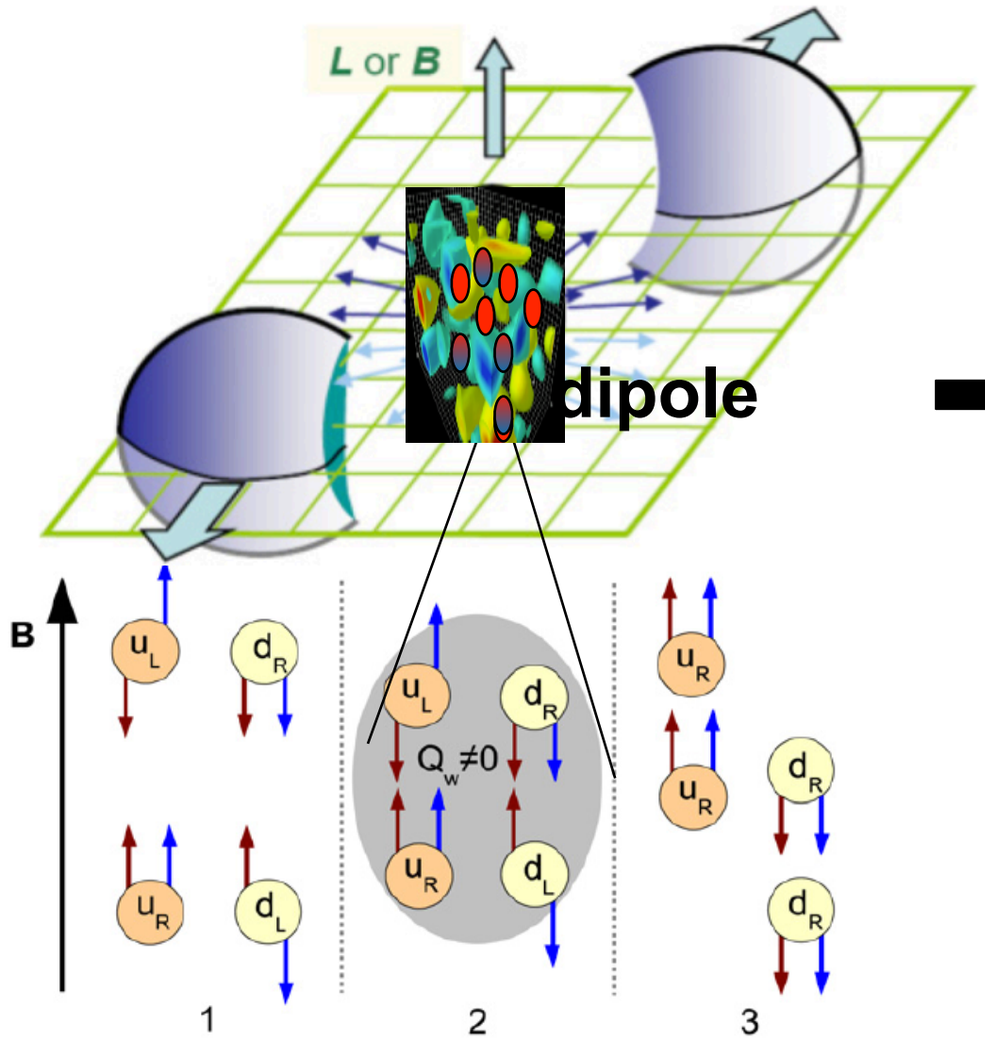
- **A constraint (<4%) to the centrality dependence of initial quadrupole percentage.**

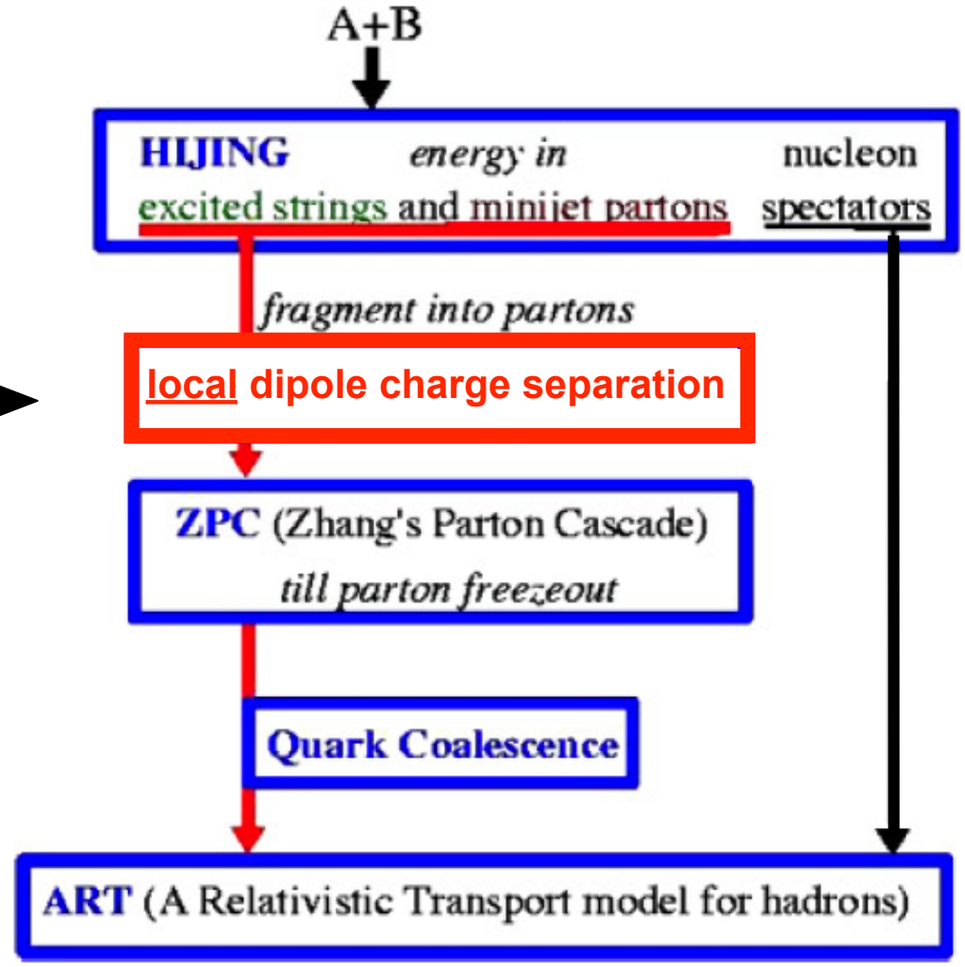
Summary

- **Using AMPT model + CME:**
  - Final state interactions reduce the CME signal significantly.
  - Isobaric collisions could directly observe the CME difference due to different B fields.
- **Using AMPT model + CMW:**
  - A constraint (<4%) to the initial CMW percentage.
- **To search for the chiral anomalous effects:** more observables and detailed studies are needed.

Backup

AMPT model with local charge separation





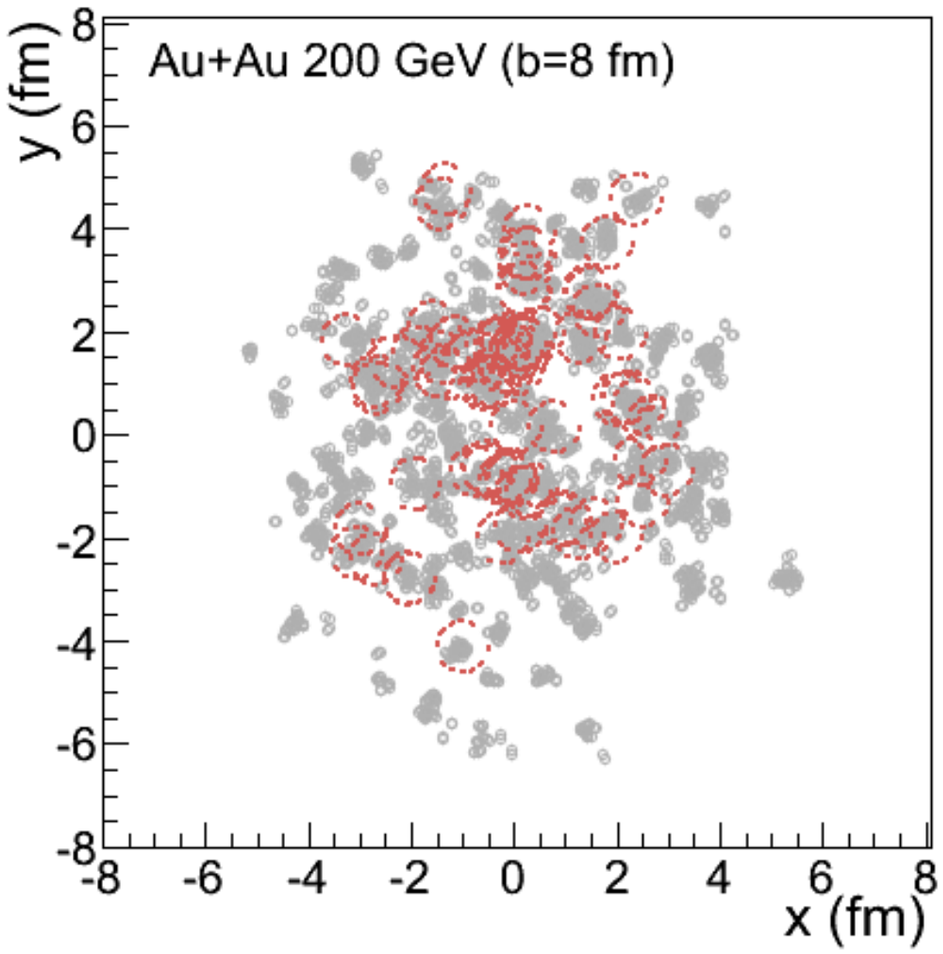
Q. -Y. Shou, G.-L. Ma and Y. -G. Ma, PRC 90 (2014) 047901

- **We include initial local dipole charge separation mechanism into AMPT model.**

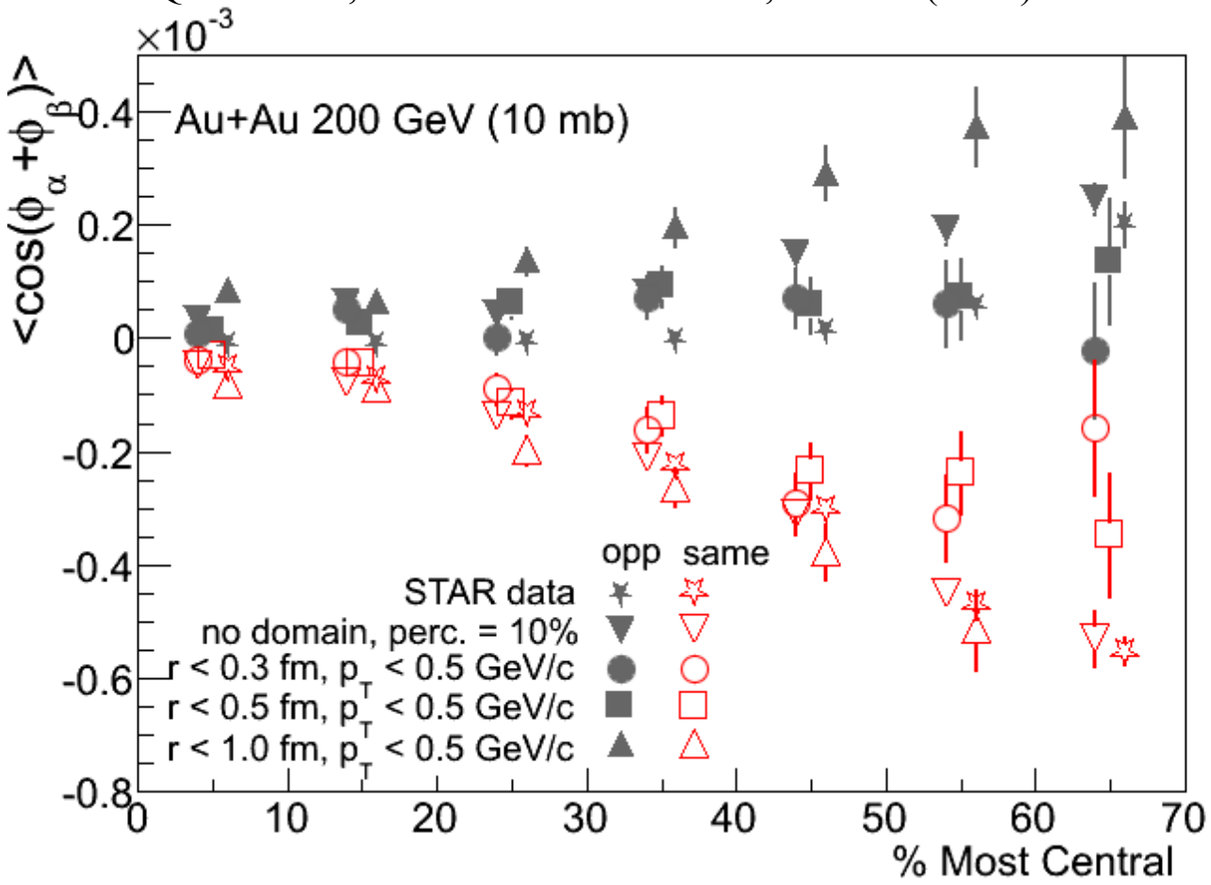
Within a same metastable domain, we switch the p_y values of the downward moving u quarks with those of the upward moving u-bar quarks, and likewise for d-bar and d quarks.

- **We compare the results from local dipole charge separation with the previous global case and exp. data.**
- **We aim to extract the information about the properties of metastable domains, such as number and size of domains.**

<cos(φα+φβ)> from AMPT with local CME

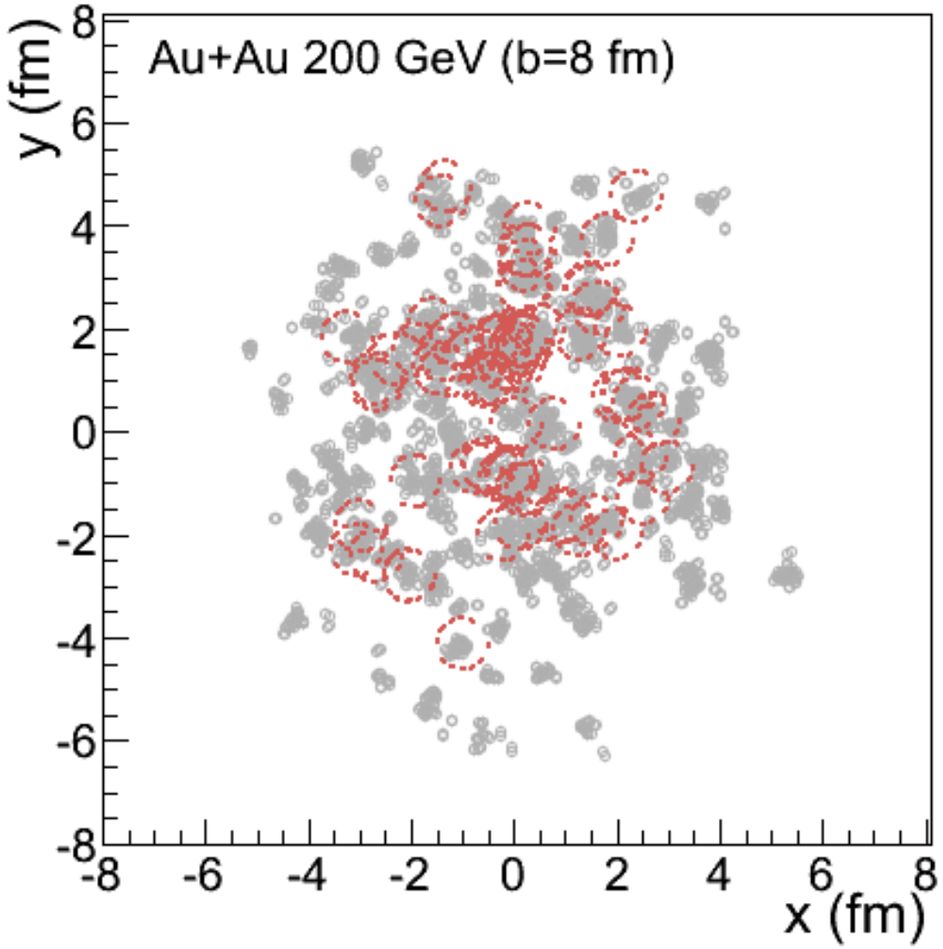


Q. -Y. Shou, G.-L. Ma and Y. -G. Ma, PRC 90 (2014) 047901



- A domain-based charge separation improves the description of opposite-charge correlation.

How many and large are the total domains



Q. -Y. Shou, G.-L. Ma and Y. -G. Ma, PRC 90 (2014) 047901

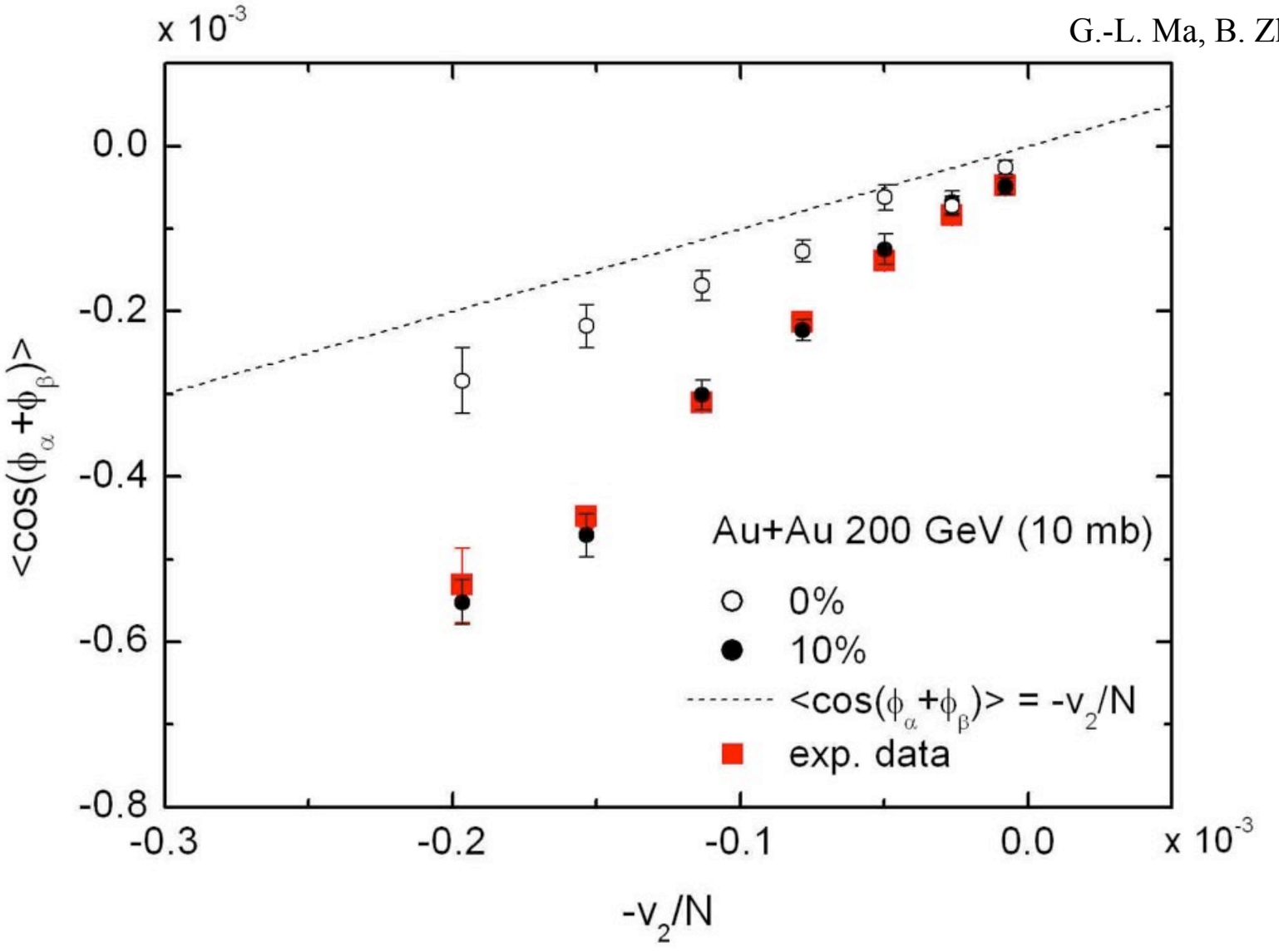
TABLE I: The occupancy factors of the total volume of domains over the fireball volume as functions of centrality bin in Au+Au collisions at $\sqrt{s_{\rm NN}} = 200$ GeV.

% Most Central	$r < 0.3$ fm	$r < 0.5$ fm	$r < 1$ fm
0-10	0.38 %	4.15 %	65.81 %
10-20	0.40 %	4.29 %	70.62 %
20-30	0.36 %	4.00 %	67.31 %
30-40	0.31 %	3.35 %	59.71 %
40-50	0.26 %	2.69 %	48.79 %
50-60	0.19 %	2.20 %	42.33 %
60-70	0.21 %	2.19 %	41.66 %

- Both size and number of metastable domains should be relatively small in the early stage of QGP.

CME && TMC

G.-L. Ma, B. Zhang, PLB 700 (2011) 39



- The original AMPT result (open circles) is close to the expectation of trans. mom. conservation (dash line).

- TMC can partly account for data, and an initial 10% dipole charge separation seems to be needed.